Faculdade de Ciências e Tecnologia da
Universidade de Coimbra

# Exploring the impact of ecstasy on retinal physiology: A pioneer study

Mestrado Integrado em Engenharia Biomédica

**Ana Maria Gonçalves Batista**

**2010**

FACULDADE DE CIÊNCIAS E TECNOLOGIA DA
UNIVERSIDADE DE COIMBRA

# Exploring the impact of ecstasy on retinal physiology: A pioneer study

Dissertação apresentada à Universidade de Coimbra para cumprimento dos requisitos necessários à obtenção do grau de Mestre em Engenharia Biomédica. Este trabalho foi realizado sob orientação do Investigador Doutor António Francisco Rosa Gomes Ambrósio, no Instituto Biomédico de Investigação da Luz e Imagem da Faculdade de Medicina da Universidade de Coimbra.

**Ana Maria Gonçalves Batista**

**2010**

## *Agradecimentos*

Ao Investigador Doutor Francisco Ambrósio, pelo incentivo e apoio prestado durante a realização deste projecto. Ao Professor Doutor Miguel Castelo-Branco e à Professora Bárbara Oliveiros pela colaboração e disponibilidade demonstrada. Ao Professor Miguel Morgado, coordenador da cadeira de projecto do Mestrado integrado em Engenharia Biomédica, pela constante disponibilidade e empenho em prol de todos os alunos deste curso.

Aos colegas com quem tive a oportunidade e o prazer de trabalhar durante este ano e que com o tempo se tornaram bons amigos: Paula, Filipa, Joana L., Célia, Joana G., João, Joana Galvão, Áurea, Ermelindo. O bom ambiente que me proporcionaram dentro e fora do laboratório e ainda a entreajuda que sempre senti conseguiram facilitar esta 'viajem'. Um agradecimento especial à Raquel, pelo apoio, incentivo e por tudo que tive a oportunidade de aprender com ela.

Quero agradecer também aos meus amigos com quem tive a oportunidade de partilhar estes 5 anos de vida académica: Sofia, André, Carlos e Andreia, pelos momentos que passamos juntos, pelo que aprendemos juntos e porque sem vocês nunca seria tão especial. Quero agradecer também ao Pedro que sempre me apoiou e motivou, que sempre esteve ao meu lado durante este período, mesmo nos momentos menos fáceis Sem ti não teria chegado até aqui.

Como não podia deixar de ser quero igualmente agradecer aos meus pais e ao meu irmão, não só pelo carinho, apoio e incentivo, durante o período académico tal como durante toda a minha vida, mas também pelas palavras de repreensão no momento apropriado. Sem vocês não me teria tornado na pessoa que sou hoje.

## *Contents*

## *Abbreviations*

| | |
|---|---|
| AMPA | α-Amino-3-Hydroxy-5-Methyl-4-Isoxazolepropionic Acid |
| BCA | Bicinchoninic Acid |
| BRB | Retinal-Blood Barrier |
| BSA | Bovine Serum Albumin |
| cGMP | Cyclic Guanosine Monophosphate |
| CNS | Central Nervous System |
| DA | Dopamine |
| DAPI | 4',6-Diamidino-2-Phenylindole |
| DA | Dopamine Transporter |
| DOC | Deoxycholic Acid |
| DOPA | 3,4-Dihydroxyphenylalanine |
| DTT | Dithiothreitol |
| EGTA | Ethylene Glycol Tetraacetic Acid |
| ERG | Electroretinogram |
| FFT | Fast Fourier Transform |
| GABA | γ-Aminobutyric Acid |
| GCL | Ganglion Cell Layer |
| GFAP | Glial Fibrillary Acidic Protein |
| GMP | Guanosine Monophosphate |
| GSH | Glutathione |
| HI | Horizontal Cells Type I |
| HII | Horizontal Cells Type III |
| HIII | Horizontal Cells Type III |
| INL | Inner Nuclear Layer |
| IP | I traperitoneal |
| IPL | Inner Plexiform Layer |
| L-DOPA | L-3,4-Dihydroxyphenylalanine |
| MAO | Monoamine Oxidase |
| MDA | 3,4-Methylenedioxyamphetamine |
| MDMA | 3,4-Methylenedioxymethamphetamine |
| mGluR | Metabotropic Glutamate Receptor |

| | |
|---|---|
| mPFC | Medial Prefrontal Cortex |
| NE | Norepinephrine |
| NFL | Nerve Fiber Layer |
| NMDA | N-Methyl-D-Aspartic Acid |
| ONL | Outer Nuclear Layer |
| OPL | Outer Plexiform Layer |
| OPs | Oscillatory Potentials |
| OS | Photoreceptor Outer Segments |
| PBS | Phosphate-Buffered Saline |
| PDE | Phosphodiesterase |
| PFA | Paraformaldehyde |
| PKC | Protein kinase C |
| PLR | Photopic Luminance Response |
| PVDF | Polyvinylidene Fluoride |
| R* | Activated Rhodopsin |
| RIPA | Radio-Immunoprecipitation Assay |
| RPE | Retinal Pigment Epithelium |
| SDS | Sodium Dodecyl Sulfate |
| SDS-PAGE | Sodium Dodecyl Sulfate Polyacrylamide Gel Electrophoresis |
| SEM | Standard Error of the Mean |
| SERT | Serotonin Transpoter |
| SLR | Scotopic Luminance Response |
| TBS | Tris-Buffered Saline |
| TBS-T | Tris-Buffered Saline Tween-20 |
| TPH | Tthyptophan Hydroxylase |
| 2,3-DHBA | 2,3-Dihydroxybenzoic Acid |
| 5-GSyl-α-MeDA | 5-(Glutathione-S-yl)-α-Methyldopamine |
| 5-HIAA | 5-Hydroxyindoleacetic Acid |
| 5-HT | 5-Hydroxytryptamine (Serotonin) |

## *Resumo*

A 3,4-Metilenodioximetanfetamina (MDMA) é um derivado de anfetamina e é o principal componente da droga de abuso 'Ecstasy'. Entre os seus efeitos pode-se incluir sensação de tranquilidade, empatia, diminuição de inibições e redução de pensamentos negativos, mas pode também causar hipertermia, rabdomiólise e em eventualmente pode causar a morte. Pensa-se que os efeitos da MDMA reflectem as suas acções na neurotransmissão serotoninérgica, dopaminérgica e noradrenérgica. Embora algumas evidências indiquem que a MDMA pode induzir neurotoxicidade na retina, poucos estudos foram realizados para avaliar e clarificar esses efeitos. Este estudo é uma continuação de outro estudo iniciado por este grupo no Centro de Oftamologia e Ciências da Visão, no IBILI, Faculdade de Medicina, onde foram detectadas, após uma única administração de MDMA, diferenças significativas em vários parâmetros nos registos de electroretinogramas. No presente estudo, avaliaram-se os efeitos a longo prazo de uma única administração de MDMA (Protocolo 1) e o efeito de múltiplas administrações, mimetizando rotinas de consumo (repetida e esporádica) de consumidores de MDMA (Protocolos 2 e 3). O efeito do MDMA na reactividade glial foi também estudada.

Os animais foram injectados intraperitonealmente com MDMA (15 e 5 mg/kg no caso de uma única ou múltiplas administrações, respectivamente) ou salino (0.9% NaCl). Os electroretinogramas foram obtidos 7 dias antes do tratamento com MDMA ou salino, e 24 h (apenas para administrações repetidas) e 7 dias após o tratamento. A reactividade glial foi avaliada 7 dias após o tratamento por *Western blot* e imunohistoquímica em retinas (*whole-mouted*) e em fatias de retina, usando anticorpos contra três marcadores de células: GFAP, usado como marcador de astrócitos e de células de Müller; vimentina, como marcador de células de Müller; e Cd11-b como marcador de células de microglia.

A administração única de MDMA (Protocolo 1) não alterou significativamente os registos de ERGs. A administração repetida de MDMA durante 7 dias consecutivos causou uma diminuição significativa na amplitude da maioria dos parâmetros escotópicos avaliados nos registos obtidos 24 h após o tratamento, com um posterior aumento deste ponto para registos obtidos 7 dias após administração de MDMA ou salino. Contudo, resultados semelhantes foram observados no grupo Salino. Perante

estes resultados, colocou-se a hipótese de que o stress poderá infuenciar os registos de ERG, mascarando os efeitos de MDMA. Após a administração esporádica de MDMA, duas vezes por semana durante 4 semanas (Protocolo 3), a maioria das alterações significativas nos registos de ERGs foram observadas no grupo Salino. Contudo, uma vez que o número de animais testados foi baixo (4 animais por grupo), ocorreu uma grande variabilidade nos resultados, o que influenciou a análise estatística.

Em relação aos efeitos da MDMA na reactividade glial, não foram observadas diferenças significativas. Contudo, detectou-se uma tendência para o aumento da expressão proteica de GFAP quer no caso de uma única administração quer no caso de administrações repetidas de MDMA.

Em conclusão, embora algumas alterações tenham sido encontradas na fisiologia da retina, quando avaliadas por registos de ERG, e na reactividade glial, após administrações simples ou repetidas de MDMA, não foram detectadas alterações significativas e persistentes. Uma vez que no grupo Salino também se detectaram alterações em vários parâmetros relativos à fisiologia da retina, será necessário realizar estudos futuros para confirmar se o stress pode influenciar os registos de ERG. Adicionalmente, o número de animais testados deve ser aumentado para se poderem tirar conclusões mais definitivas sobre os efeitos prejudiciais da MDMA na retina.

## *Abstract*

3,4-Methylenedioxymethamphetamine (MDMA) is a ring-substituted amphetamine derivative and is the main compound of the recreational drug known as 'ecstasy'. Among its effects, we may include tranquillity, empathy, decreased inhibition and reduction of negative thoughts, but it also may lead to hyperthermia, rabdomiolisis and can ultimately lead to death. The effects of MDMA are thought to reflect its actions on serotonergic, dopaminergic and noradrenergic neurotransmission. Although a few evidences indicate that MDMA might induce retinal neurotoxicity, few attempts have been done to evaluate and clarify those effects. This study followed up another study initiated by this group at Center of Ophthalmology and Vision Sciences, IBILI, Faculty of Medicine, where significant differences in several parameters of electroretinogram recordings were found after a single MDMA administration. In the present study, we assessed the long-term effects of a single MDMA administration (Protocol 1) and the effect of multiple MDMA administration, mimicking the routine consumption (repeated and sporadic) of MDMA consumers (Protocols 2 and 3). The effect of MDMA on glial reactivity was also studied.

Animals were intraperitoneally injected with MDMA (15 and 5 mg/kg for single and multiple administration, respectively) or Saline (0.9% NaCl). Electroretinogram recordings were obtained 7 days before MDMA or saline treatment, 24 h (only after multiple MDMA administration) and 7 days after treatment. The glial reactivity was assessed 7 days after treatment through Western blot analysis and immunohistochemistry in whole-mounted retinas and retinal slices, using antibodies against three cell markers: GFAP, used as a marker of astrocytes and Müller cells; vimentin used to label Müller cells; and Cd11-b as a marker of microglial cells.

A single MDMA administration (Protocol 1) did not affect significantly the ERG response. Repeated MDMA administration for 7 consecutive days (Protocol 2) caused a significant decrease in the amplitude of most of the scotopic parameters evaluated at 24 h time point with an increase from this point to 7 days time point, but similar results were observed in the Saline group. We hypothesized that stress may be influencing ERG recordings, eventually masking MDMA effects. After sporadic MDMA administration, twice a week for 4 weeks (Protocol 3), most of the significant differences observed in ERG responses were in Saline group instead of MDMA group.

However, since the number of animals tested was low (4 animals per group), there was a huge data variability that influenced statistical analysis.

Regarding the effects of MDMA on glial reactivity, no significant changes were observed; however, a tendency for an increase in GFAP expression for both single and multiple MDMA administration was detected.

In conclusion, although some changes have been found in retinal physiology, as assessed by ERG recordings, and in glial reactivity, after single or repeated MDMA administration, no significant and persistent alterations were detected. Since some alterations in several parameters of retinal physiology were also found in the Saline group, further studies will be necessary to confirm if stress has an influence on ERG recordings. In addition, the number of animals must be increased to draw more definitive conclusions about the harmful effects of MDMA in the retina.

# 1. Introduction

## 1.1. The eye

The eye is an important organ that allows gathering information about the surrounding world. This organ is composed by three layers of tissue (Figure 1). The most external one is composed by sclera and cornea. Sclera is a fibrous tissue characterized by its toughness and its white coloration. Cornea it is a transparent tissue, in the front of the eye, that allows the entrance of light rays. The middle layer of tissue is the uveal tract and it is formed by three distinct continuous structures, the choroid, ciliary body and iris. The iris can be seen through the cornea (colored portion) and is composed by two sets of muscles responsible for adjusting pupil diameter, which determines the amount of light that reaches the retina. The ciliary body is a muscular component attached to the lens by zonule fibers allowing it to adjust the refraction power, which is important for image formation. It is also partially responsible for maintaining the eye structure. It has a vascular component which is involved in the aqueous humor production that fills the anterior chamber (between cornea and iris) and posterior chamber (between iris, zonule fibers and lens). The most posterior component of the uveal tract it is the choroid, which is rich in blood vessels and its main function is the nourishment of the outer layers of the retina. The retina is the most internal layer of the eye, and its main function is the conversion of light stimulus into electrical signal that are transmitted to the brain. Besides anterior and posterior chamber, mentioned above, the eye has one more chamber of liquid, the vitreous chamber, localized between the lens and the iris. This chamber is filled with a gelatinous substance mainly composed by collagen fibers: the vitreous humor that is responsible for maintaining the eye integrity. This structure contains phagocytic cells (hyalocytes) that remove blood and other debris that could interfere with light transmission (Forrester et al, 2002; Purves et al, 2004).

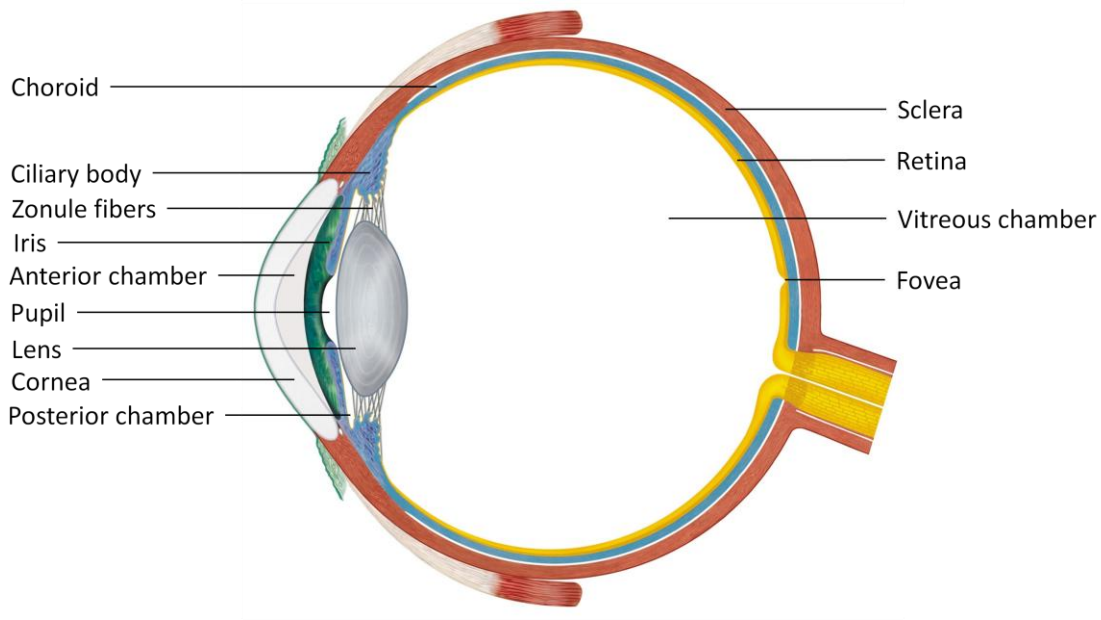


**Figure 1** – The anatomy of the human eye. Adapted from www.angioedupro.com/Sharpoint/anatomy/anatomy_of_the_eye.png, retrieved August 23, 2010.

## *1.2. The retina*

### *1.2.1. Structure of the retina*

The retina, despite its peripheral location, is part of the central nervous system (CNS) and is organized in eight different layers (Figure 2). The first one is the retinal pigment epithelium (RPE), which has an important role on photoreceptors maintenance by renewing photopigments and phagocytosing the photoreceptors disks. It also decreases the backscattering of light that reaches the retina. Following this layer is the photoreceptor outer segments (OS). The cell bodies of photoreceptors are in a layer called outer nuclear layer (ONL). Photoreceptors form synapses with bipolar and horizontal cells composing the outer plexiform layer (OPL). Inner nuclear layer (INL) is constituted by the cell bodies of bipolar, horizontal and amacrine cells. The synaptic zone between bipolar cells, ganglion cells and amacrine cells composes the inner plexiform layer (IPL), while the cell bodies of ganglion cells form the ganglion cell layer (GCL). Finally, the axons of these cells form the nerve fiber layer (NFL), which is responsible to carry the information to the brain (Purves et al, 2004).

The flow of information in the retina occurs in two major ways: the vertical flow and lateral interactions. Vertical path begins in photoreceptors, flows to bipolar cells, then to ganglion cells and finally to the optic nerve where the information is carried to the brain. Horizontal and amacrine cells mediate lateral interactions (Purves et al, 2004).

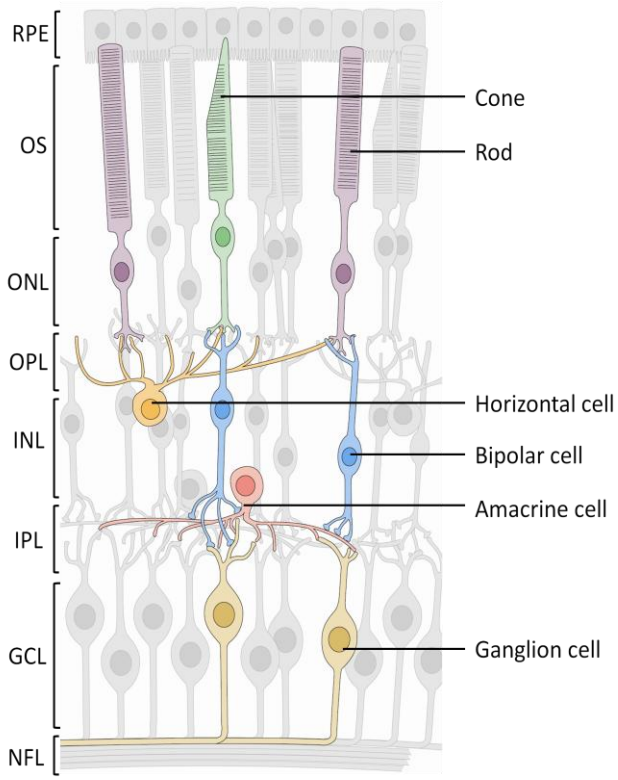


**Figure 2** – The structure of the retina. RPE, retinal pigmented epithelium; OS, photoreceptor outer segments; ONL, outer nuclear layer; OPL, outer plexiform layer; INL, inner nuclear layer; IPL, inner plexiform layer; GCL, ganglion cell layer; NFL, nerve fiber layer. Adapted from Purves et al, 2004.

#### *1.2.1.1. Retinal cell types*

In the retina, like in other CNS regions two types of cells can be discriminated: neurons and glial cells. There are five types of neurons: photoreceptors, bipolar cells, ganglion cells, horizontal cells and amacrine cells, and three types of glial cells: Müller cells, astrocytes and microglia.

##### *1.2.1.1.1. Photoreceptors*

In the vertebrate retina two types of photoreceptors can be distinguished, cones and rods (Figure 3). Their characteristics specializes them for different visual aspects. Cones are responsible for visual acuity and colored vision. They have high spatial resolution but relative low light sensitivity. The human retina has three types of cones, depending on

its photopigment. Since each photopigment is activated by a different wavelength the three types of cones have different sensitivity to light (Purves et al, 2004).

Cones can be classified as "red", "green" and "blue", or more appropriately long, medium and short wavelength cones, which are more sensitive to wavelengths around 560 nm, 530 nm and 420 nm, respectively. Color perception requires the comparison of activity between different types of cones. Unlike cones, there is only one type of rod that is sensitive to wavelengths around 500 nm. They have high light sensitivity but low spatial resolution (Purves et al, 2004).

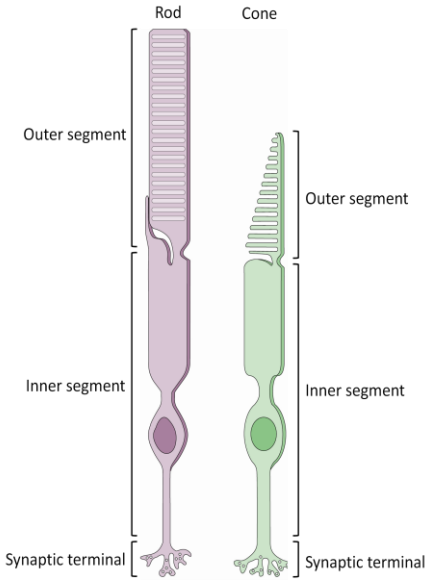


**Figure 3** – The structure of photoreceptors. Adapted from Purves et al, 2004.

Rods and cones are activated at different light intensities. At low levels of light rods are activated (scotopic vision), and visual discriminations are sometimes difficult. As the intensity of light increases, cones are activated. The perception at low lighting conditions where both receptors are activated is called mesopic vision. The response of rods saturates at high intensity of light, and only cones respond, thus only cones contribute to visual perception (photopic vision). The photoreceptors activation by light leads to cell hyperpolarization and consequently to a decrease in glutamate release (Purves *et al*, 2004; Siegel *et al*, 2006).

The photoreceptors distribution across the retina is not symmetric and has important consequences for vision. The total number of rods in the retina is much higher than the

number of cones. However in fovea, a highly specialized region at the centre of retina, rods number is exceeded by cones. The high density of cones in the fovea, as well as the relation one to one with bipolar and ganglion cells in this region, gives cone system the ability to mediate high visual acuity. The acuity is reduced as cones density declines with eccentricity, restricting the highest acuity vision to fovea. The high density of rods outside the fovea gives this region a lower threshold to detect light stimulus, allowing seeing better a dim object by looking away from it (Purves *et al*, 2004).

#### *1.2.1.1.2. Bipolar cells*

Photoreceptors form synapses with bipolar cells. These cells, based on how they react to glutamate release from photoreceptors, can be classified into ON-center and OFF-center bipolar cells, distinguishable by the type of glutamate receptor that they express. The ON-center bipolar cells express G-protein-coupled metabotropic glutamate receptors (mGluR6) that induce the closure of cyclic guanosine monophosphate (cGMP)-gated channels when activated. These cells will hyperpolarize by glutamate activation. In other hand, OFF-center bipolar cells express ionotropic receptors (α-amino-3-hydroxy-5-methyl-4-isoxazolepropionic acid (AMPA) and kainate). Glutamate activation of these receptors leads to cell depolarization (Kolb, 2003; Purves *et al*, 2004).

#### *1.2.1.1.3. Ganglion cells*

The next cells at the vertical information pathway are ganglion cells. Bipolar cells contact with these cells through N-methyl-D-aspartic acid (NMDA), AMPA and kainate glutamate receptors (Kolb, 2003; Purves *et al*, 2004; Manookin *et al*, 2010). The main difference between ganglion cells and bipolar cells is the nature of their electrical response. Unlike bipolar cells, which have graded potentials, ganglion cells have action potentials. These cells have concentric receptive fields and based on how ganglion cells react in the presence of glutamate they can be divided into two types: ON-center and OFF-center. The number of each type in the human retina is approximately the same, and usually the receptive field of neighbor cells is overlapped. This distribution allows the same retinal point to be analyzed by several ganglion cells, of both cell types (Purves *et al*, 2004).

The two types of ganglion cells can be distinguished by the firing rate of the cell when it is stimulated by a small spot of light in the center of its receptive field. Thus, when the

center of an ON-center ganglion cell is exposed to light it depolarizes, increasing their discharge rate. In the other hand, it will hyperpolarize if the surround of the receptive field is exposed to light, decreasing its firing rate. OFF-center ganglion cells have the opposite response. They become activated when the surround is exposed to light and inactive when the center is stimulated (Figure 4) (Purves *et al*, 2004).

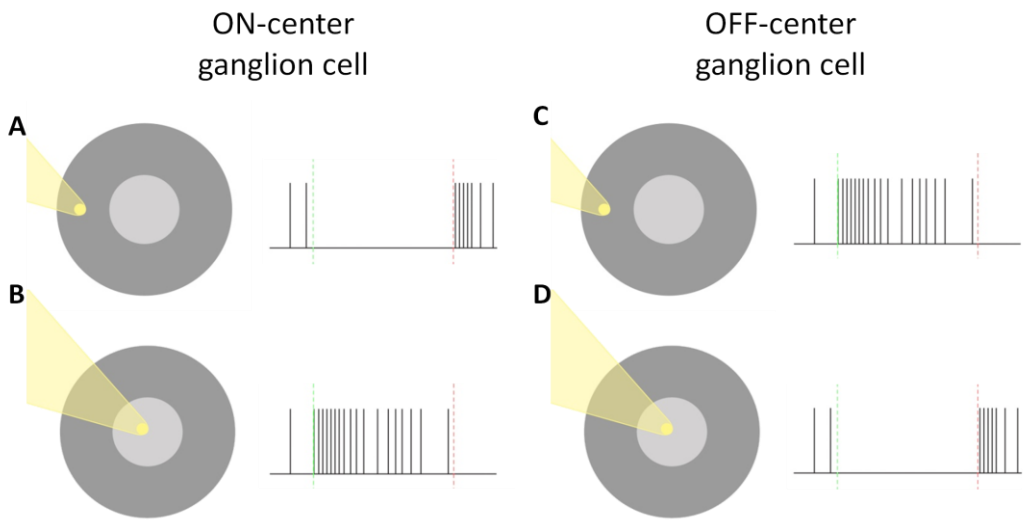


**Figure 4** – The responses of ON- and OFF-center retinal ganglion cells to stimulation of different regions of their receptive fields. A high frequency firing rate is observed when light reaches the center of ON-center cells (B) and the surround of OFF-center ganglion cells (C). The inverse response is observed when the surround of ON-center ganglion cells (A) and the center of OFF-center ganglion cells (D) are stimulated. ▒ – receptive field center; ▒ – receptive field surround. Adapted from Purves *et al*, 2004.

#### *1.2.1.1.4. Interneurons*

In the human retina there are two types of interneurons: horizontal and amacrine cells. In humans, three types of horizontal cells have been identified: Type I, II and III (HI, HII, and HIII, respectively). HI cells have distinct dendritic terminal clusters going to cones and a fan-shaped axon terminal going to rods. Type II cells have abundantly branched and overlapping dendrites, with poorly defined terminals and a short curled axon with small terminals both going to cones. The Type III cells reveal larger diameters and asymmetrically shaped dendritic trees (Kolb *et al*, 1994).

Amacrine cells are localized in the IPL, establishing synapses with bipolar, ganglion and another amacrine cells. A huge variety of amacrine cells can be distinguished depending on its dendritic tree size, neurotransmitter released and its position at the IPL (Koch *et al*, 1997; Purves *et al*, 2004).

#### *1.2.1.1.5. Glial cells*

Like in other CNS regions, retina is also composed by glial cells that have important roles on retinal physiology. There are three types of glial cells in the retina: Müller cells, astrocytes and microglia.

Müller cells are the main glial cell type in the retina and can only be found in this structure (Newman & Reichenbach, 1996; Franze *et al*, 2007). They span the entire retinal thickness and contact with all retinal neurons (Bringman *et al*, 2006). Müller cells have important functions, as retinal homeostatic control by supplying neurons with endproducts of anaerobic metabolism, by removing cellular metabolites, as carbon dioxide and ammonia, and by maintaining extracellular ionic concentrations. They also contribute to neuronal signalling processes by providing neurotransmitter precursors to neurons and by rapidly uptaking and recycling neurotransmitters (Bringman *et al*, 2006).

Astrocytes have important functions related with vessel growth in the retina. As blood vessels are formed, these cells migrate from the optic nerve into the retina, and play an important role in constraining the vessels in the retina. They are also important to regulate the integrity and function of the vessels (Zhang & Stone, 1997).

Microglial cells have an important role maintaining the retinal homeostasis and are required to immune response cascade initiation (Langmann, 2007). These cells are also important during development, since they are involved in the phagocytosis of cellular debris resultant from apoptotic neurons (Langmann, 2007).

### *1.2.1.2. Retinal blood supply*

Blood supply of retinal cells has two components: choroidal blood vessels and central retinal artery from the optic nerve head. The first one is responsible for outer retina (essentially photoreceptors) nourishment. In the human eye, central retinal artery has four main branches and is responsible for inner retinal cells maintenance.

An important structure concerning retinal blood supply is the blood-retinal barrier (BRB). This structure regulates the molecular transport to retinal tissue due to the presence of tight junctions, defending the retina against toxins. BRB can be divided into two barriers: outer BRB and inner BRB. The outer BRB is formed by tight junctions

between endothelial cells in RPE, while tight junctions between endothelial cells of the retinal capillaries form the inner BRB (Forrester *et al*, 2002).

### *1.2.2. Phototransduction*

Phototransduction is the process by which light is converted into electrical signs by cones and rods. The presence of photopigments is essential and although they are different in cones and rods, this process is similar in both. The process is better characterized in rods than cones and most of what is known about phototransduction results from experiences on them (Siegel *et al*, 2006). In this section, phototransduction process in rods will be described.

Photopigments are composed by a light-absorbing chromophore named retinal (vitamin A aldehyde) attached to one of several proteins called opsins. In rods there is only one kind of photopigment, rhodopsin. When rhodopsin retinal absorbs light photons its conformation changes from the *11-cis* form to *all-trans*-retinal, leading to its activation. Activated rhodopsin (R*) causes the dissociation of γ and β subunits from α subunit of an intracellular messenger called transducin. This molecule, when active (α subunit bound to GTP), activates phosphodiesterase (PDE), which is responsible for cGMP hydrolyzation to GMP, ultimately resulting in intracellular cGMP concentration decrease. This molecule binds to cGMP-gated channels present at the outer segment membrane, keeping them opened and allowing the entrance of $Na^+$ and $Ca^{2+}$. Its decrease leads to cGMP-gated channels closure, decreasing the influx of cations and consequently to photoreceptor hyperpolarization (Figure 5) (Purves *et al*, 2004; Siegel *et al*, 2006).

As mentioned above, cGMP-gated channels are permeable to $Ca^{2+}$, and thus its closure results in a decrease of intracellular $Ca^{2+}$ concentration, triggering a series of changes on phototransduction cascade. An increase of guanylate cyclase activity (enzyme responsible for cGMP synthesis) is observed at low $Ca^{2+}$ concentrations, increasing cGMP intracellular concentration. It has also been reported that cGMP affinity to cGMP-gated channels is increased when $Ca^{2+}$ concentration decreases. Both the alterations induced by intracellular $Ca^{2+}$ concentration decrease results on a decrease of the sensitivity of the receptor to light, which is important for light adaptation (Purves *et al*, 2004).

Another mechanism involved in light adaptation involves a protein called arrestin that has the capacity to block transducin activation by R* and facilitates R* degradation. After degradation, rhodopsin undergoes a process of recycling that involves the isomerisation of *all-trans* to *11-cis*-retinal, which is highly important to keep photoreceptors sensitivity (Purves *et al*, 2004; Siegel *et al*, 2006).

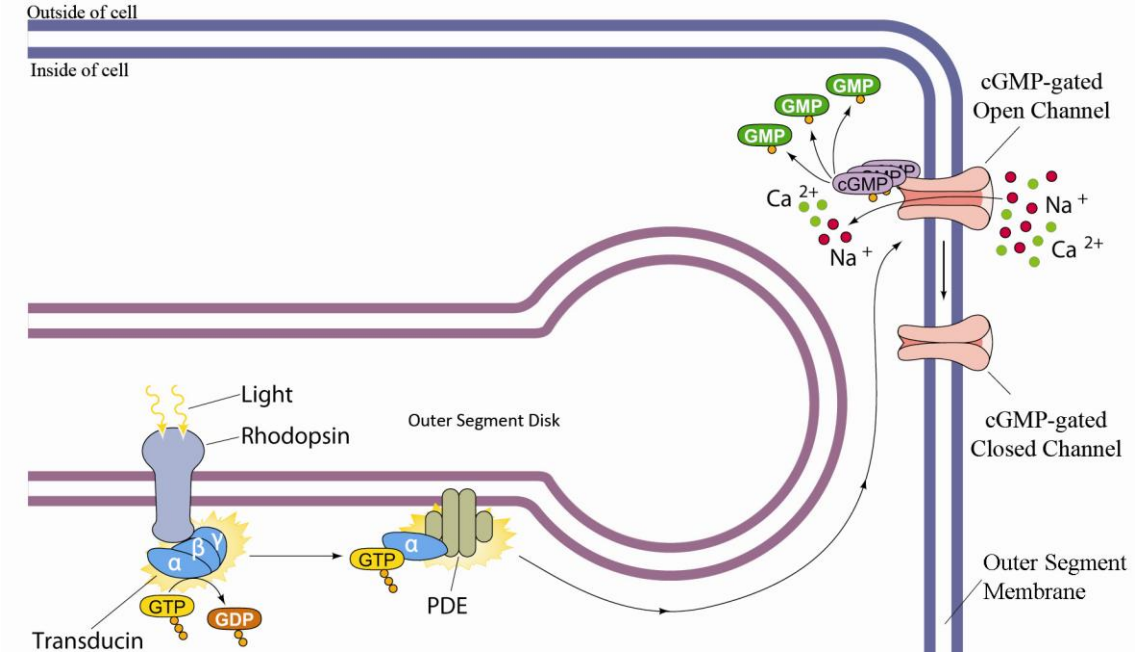


**Figure 5** – Phototransduction in rod photoreceptors. Rhodopsin activation by light leads to transducin activation and consequently to PDE activation triggering the hydrolysis of cGMP. This causes the closure of cGMP-gated channels resulting in membrane hyperpolarization. cGMP, cyclic guanosine monophosphate; PDE, phosphodiesterase. Adapted from Purves *et al*, 2004.

### *1.2.3. Retinal circuits*

The electrical signs resulting from phototransduction are interpreted by bipolar and horizontal cells. Photoreceptors stimulation leads to glutamate release decrease, thus resulting on OFF-center bipolar cells hyperpolarization and depolarization of ON-center bipolar cells. ON- center bipolar cells depolarization will cause an increase of glutamate release into IPL, leading to the activation of ON-center ganglion cells, increasing its firing rate (Figure 6). The detection of luminance contrasts is only possible because ganglion cells are sensitive to differences between light intensity on the center and surround of its receptive fields (Purves *et al*, 2004).

#### *1.2.3.1. Importance of lateral interactions*

As mentioned above, in the retina there are two types of interneurons, the horizontal and amacrine cells that can have excitatory or inhibitory effects. Horizontal cells are located at the OPL and their actions regulate the amount of neurotransmitter released by photoreceptors. They have AMPA and kainate receptors at their membrane, and since the activation of photoreceptors by light reduces the release of glutamate, this leads to horizontal cells hyperpolarization. Horizontal cells release an inhibitory neurotransmitter, γ-aminobutyric acid (GABA), causing a negative feedback on photoreceptors. These cells are believed to have an important role on light adaptation mechanisms (Purves *et al*, 2004).

Amacrine cells modulate signal processing between bipolar and ganglion cells. These cells are mainly inhibitory (release GABA and glycine) and are thought to have an important role in determining the receptive field size of ganglion cells. Through glycine release they inhibit the transmission of peripheral signals to the ganglion cell defining its ON-center (Forrester *et al*, 2002).

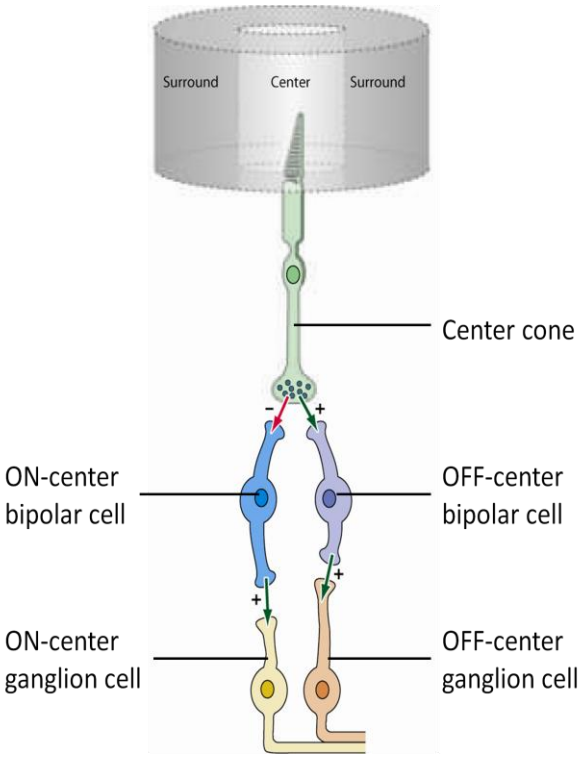


**Figure 6** – Retinal circuits responsible for generating receptive field responses in retinal ganglion cells. Photoreceptors stimulation leads to glutamate release decrease, thus resulting on OFF-center bipolar cells hyperpolarization and depolarization of ON-center bipolar cells. Consequently ON-center ganglion cell depolarizes, increasing its firing rate. The firing rate of OFF-center ganglion cells decreases. Sign-conserving synapse is indicated with a '+' and sign-inverting synapse is represented by a '-'. Adapted from Purves *et al*, 2004.

### *1.3. Electroretinogram (ERG)*

The electrical response from all retinal elements to light stimulus can be measured by electroretinography (Forrester *et al*, 2002). This technique allows an efficient assessment of the status of the visual pathways (Rosolen *et al*, 2005; Creel, 2010), and it is helpful to diagnose and evaluate some ocular diseases (Wali & Leguire, 1991). The toxicity of chemical agents to the retina can also be assessed by this method (Rosolen *et al*, 2005). Besides the standard ERG, additional information about the function of the retina can also be provided by specialized types of ERG, like multifocal ERG, pattern ERG or direct-current ERG (Marmor *et al*, 2004).

Recording an electroretinogram requires the use of electrodes, while the eye is stimulated by light flashes. Skin electrodes are thought to be effective, although corneal electrodes are still the most often used (Wali & Leguire, 1991). Several components can be distinguished in an ERG waveform (Figure 7), but a- and b-waves are the ones usually measured (Creel, 2010). An electroretinogram waveform pattern can be affected by several factors, like the intensity and duration of the stimulus, and the status of light/dark retinal adaptation (Forrester *et al*, 2002; Barraco *et al*, 2006).

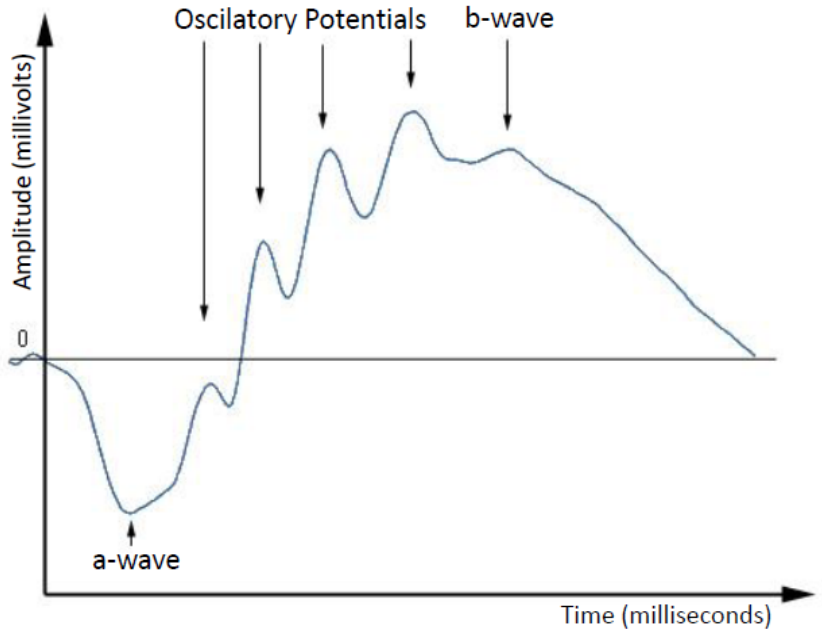


**Figure 7** – Flash scotopic electroretinogram in nocturnal species. The initial depletion (a-wave) is followed by the b-wave. In the rising phase of b-wave, oscillatory potentials (OPs) are detected. Adapted from Rosolen *et al*, 2005.

A-wave is thought to be generated by photoreceptors (Nixon *et al*, 2001; Forrester *et al*, 2002; Barraco *et al*, 2006; Perlman, 2010). It is believed that it reflects the decrease on cell potential after light photons absorption by photoreceptors, due to cGMP-gated channels closure (Perlman, 2010). Cone and rod contribution to this wave formation is thought to depend on the anatomo-physiological specificities of each species, whether it is a diurnal or nocturnal animal. Through different stimulation protocols it is possible to assess the status of scotopic and photopic systems, thus determining the contribution of each type of photoreceptor to a-wave formation (Rosolen *et al*, 2005). It has been reported that for nocturnal species a-wave results mainly from rods activation (Nixon *et al*, 2001).

The mechanisms leading to b-wave formation are more complex. It is believed that b-wave reflects the activity of ON-center bipolar cells that are depolarized by light. However, Müller cells and cones also seem to be implicated (Stockton & Slaughter, 1989; Wen & Oakley, 1990; Nixon *et al*, 2001; Alexander *et al*, 2006; Perlman, 2010).

In the rising phase of b-wave, high-frequency wavelets can be identified, called oscillatory potentials (OPs) (Li *et al*, 1991). These low amplitude oscillating waves are believed to reflect the inhibitory feedback circuits in the inner part of the retina initiated by amacrine cells (Wanger & Persson, 1984; Li *et al*, 1991; Creel, 2010).

### *1.4. 3, 4-methylenedioxymethaphemtamine (MDMA)*

3,4-methylenedioxymethamphetamine (MDMA) is a ring-substituted amphetamine derivative (Figure 8) (Kay *et al*, 2010). As an amphetamine derivative, MDMA can be considered a stimulant drug, but it is also structurally related to the hallucinogenic compound mescaline, thus exhibiting both stimulant and hallucinogenic proprieties (Schwartz *et al*, 1997; Green *et al*, 2003; Gudelsky *et al*, 2008; Xavier *et al*, 2008; Kay *et al*, 2010).

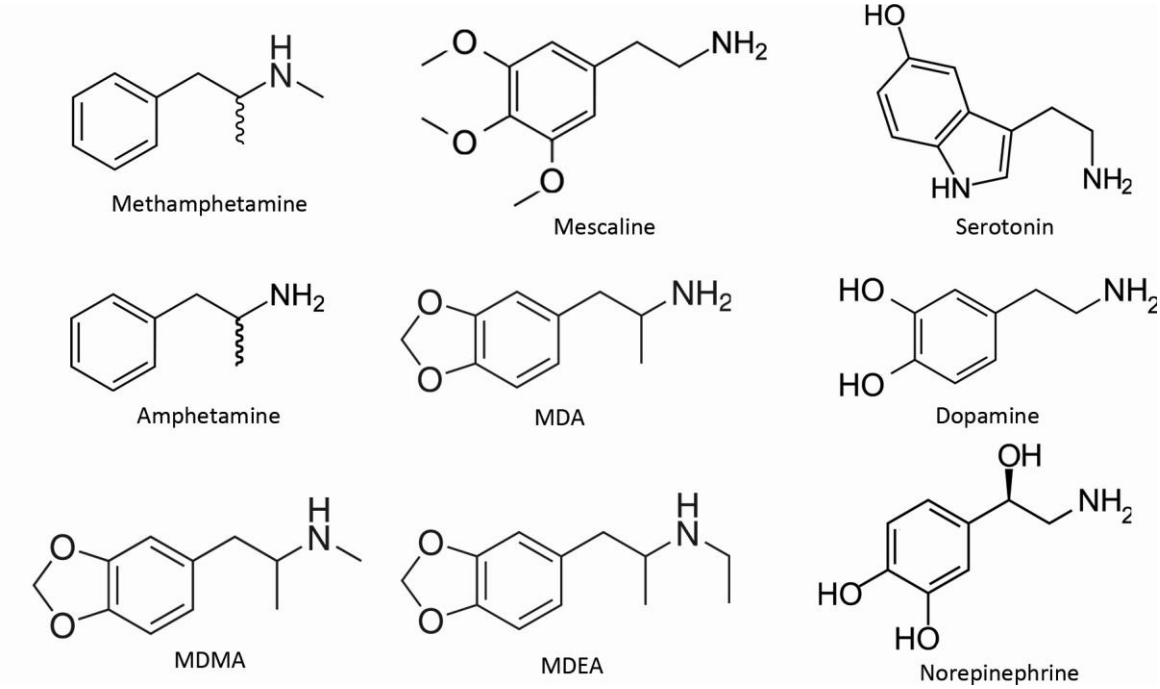


**Figure 8** – Chemical structure of amphetamine, some of its derivates including MDMA. The chemical structure of some neurotransmitters is also represented.. MDMA, 3,4-methylenedioxymethamphetamine; MDA, 3,4-methylenedioxyamphetamine; MDEA, 3,4-methylenedioxy-*N*-ethylamphetamine; Mescaline, 3,4,5-trimethoxyphenethylamine. Adapted from Green *et al*, 2003 and Xavier *et al*, 2008.

#### *1.4.1. Brief history*

MDMA is the main compound of the recreational drug known as 'ecstasy' and has been one of the most popular illegal drugs since the mid-1980s (Freudenmann *et al*, 2006). It was first synthesized in 1912 by the German pharmaceutical company Merck (Cole & Sumnall, 2003). MDMA is often described as an 'anorectic drug' or an 'appetite suppressor' (Kay *et al*, 2010), however it was patented by Merck in 1914 as an

important intermediate for therapeutically effective compounds (Freudenmann *et al*, 2006; Kay *et al*, 2010). It has been suggested that the incorrect association of MDMA with an appetite suppressor might be related with some studies carried out between 1949 and 1957 on MDMA's metabolite, 3,4-methylenedioxyamphetamine (MDA), to evaluate its potential role as an 'anorectic drug' (Freudenmann *et al*, 2006).

In 1978 the first MDMA's psychoactive effects were reported in humans, revealing the drug's ability to reduce defensiveness and anxiety. MDMA was then recognized as a potential tool for the treatment of psychosis, and served that purpose until the mid-1980s (Valentine, 2002).

In 1985, MDMA was classified as an illegal drug, but one year later its use was considered to be safe under medical supervision. In 1988, it was permanently reclassified as an illegal drug (Valentine, 2002; Green *et al*, 2003). This classification had no influence on its recreational use (Valentine, 2002). Nowadays, MDMA is one of the most popular recreational drugs being "rave" and "techno" parties the places of highest consumption (Schwartz *et al*, 1997; Green *et al*, 2003; Diller *et al*, 2007).

In Portugal, the consumption of MDMA has gained more relevance over the years. According to "Inquérito Nacional ao Consumo de Substâncias Psicoactivas na População Geral", in 2007 MDMA was the third most used drug. In six years, it was observed an increase of MDMA consumption of 0.6% among the total population (15-64 years) and of 1.2% in the youngest population (15-34 years).

### *1.4.2. Acute MDMA effects*

The onset effects of MDMA occur 30 to 60 minutes after ingestion. Peak effects are attained after 90 min and can persist for 3 to 5 hours. Effects may include tranquillity, relaxation, reduction of negative thoughts, empathy, decreased inhibitions, feelings of intimacy, and euphoric state, among others (Valentine, 2002; Green *et al*, 2003). Because of these initial effects, MDMA was thought to be safe for most recreational (Valentine, 2002).

Despite this, a single MDMA administration can cause a series of adverse effects. It has been reported that it can lead to hyperthermia, hyponatremia, multiorganic failure, rabdmiolisis, disseminated intravascular coagulation, serotonin syndrome and in ultimate cases may even cause death (Farré *et al*, 2004).

#### *1.4.2.1. MDMA effects on serotonergic neurotransmission*

The actions of MDMA on neurotransmission are not well understood. It is known that MDMA acts by increasing extracellular concentrations of monoamine neurotransmitters such as serotonin (5-HT), dopamine (DA) and norepinephrine (NE) (Bogena *et al*, 2003; Green *et al*, 2003; Gudelsky *et al*, 2008; Xavier *et al*, 2008).

The neurotoxic effects of this drug on serotonergic system in animals are well characterized (Gyongyosi *et al*, 2010). It was observed that MDMA administration leads to an acute and rapid release of 5-HT in the brain. The release is apparently due to MDMA actions on 5-HT transporter (SERT) and on 5-HT metabolism (Green *et al*, 2003; Gudelsky *et al*, 2008; Xavier *et al*, 2008).

It has been reported that 5-HT release can be markedly attenuated with pre-treatment with a serotonin uptake inhibitor (Green *et al*, 2003), indicating that the MDMA-induced 5-HT release is somehow related with interactions at SERT level. This effect has also been observed in humans, since pre-treatment with citalopram, an inhibitor of SERT activity, a decrease in the effects induced by MDMA administration was reported (Liechti *et al*, 2000). Thus, it is likely that the 5-HT transporter is involved in the MDMA induced release of serotonin (Green *et al*, 2003, Gudelsky *et al*, 2008).

MDMA, like other amphetamine analogs, inhibits the catabolic enzyme monoamine oxidase (MAO), which degrades 5-HT and dopamine, thus resulting in an increase of extracellular concentration of both neurotransmitters (Leonardi *et al*, 1994).

It is also proclaimed that MDMA can interfere with 5-HT metabolism (Green *et al*, 2003, Gudelsky *et al*, 2008). MDMA causes short-term and long-term decrease on the activity of the enzyme required for 5-HT synthesis, tryptophan hydroxylase (TPH). The inhibitory effect of MDMA on the enzyme is still detectable two weeks after a single administration (Che *et al*, 1995; Green *et al*, 2003) and is thought to have a role on long-term depletion of 5-HT. MDMA hyperthermic response, which may be influenced by room temperature (Green *et al*, 2003; Colado *et al*, 2004), was also showed to be correlated to the MDMA-induced reduction of TPH activity. At an ambient temperature of 6ºC, MDMA causes a hypothermic response instead of a hyperthermic response (Green *et al*, 2003; Colado *et al*, 2004). A decrease in TPH activity was not observed when its activity was analyzed in hypothermic conditions (Green *et al*, 2003; Colado *et al*, 2004). A decreased on TPH activity was not observed when its activity was

analyzed in hypotermic conditions (Green *et al*, 2003; Colado *et al*, 2004). It is believed that MDMA-induced hyperthermic response enhance free radical formation leading to TPH activity decrease (Green *et al*, 2003). Calcium influx has also been implicated on TPH activity decrease (Johnson *et al*, 1992; Green *et al*, 2003). Reports suggested that pre-treatment with a non-selective blocker of T-type calcium channels, flunarizine, in rats that received multiple MDMA administrations can markedly attenuate MDMA-induced decrease on TPH activity (Johnson *et al*, 1992).

#### *1.4.2.2. MDMA effects on dopaminergic neurotransmission*

Similar to what is observed for serotonin, several studies showed a rapid release of dopamine (DA) in several brain sections after MDMA administration (Green *et al*, 2003; Colado *et al*, 2004; Gudelsky *et al*, 2008). Moreover, a decrease in DA metabolism was also found after MDMA administration (Green *et al*, 2003; Colado *et al*, 2004,).

It was reported that MDMA-induced DA release in the striatum involves transport-dependent and exocytose processes (Nair *et al*, 2004). In rats, the administration of mazidol, an inhibitor of the DA transporter (DAT), attenuates the increase of extracellular DA concentration induced by MDMA, indicating that transport dependent mechanisms are involved (Shankaran *et al*, 1999). The exocytose process is thought to involve 5-$HT_2$ activation (Nair *et al*, 2004). These receptors are known to utilize protein kinase C (PKC) for intracellular signalling and PKC apparently has a modulatory effect on MDMA-induced release of DA (Nair *et al*, 2004). Nair and Gudelsky found that the administration of PKC inhibitors (BIM and chelerythrine) reduce the DA release elicited by MDMA. PKC activator (PDBu) administration enhanced the efflux of DA produced by MDMA systemic administration (Nair *et al*, 2004). The involvement of 5-$HT_2$ activation in DA release induced by MDMA was also showed by Koch and Galloway. Pre-treatment with the serotonin reuptake inhibitor, fluoxetine, significantly decreases MDMA-induced DA release (Koch *et al*, 1997). A potentiating effect was observed by pre-treatment with a 5-HT receptor agonist or a non-selective agonist, once again re-enforcing the possible involvement of serotonin on MDMA-induced DA release (Green *et al*, 2003). 5-HT receptors effect on MDMA interaction with DA release is thought to be related with the decrease in GABA release dependent of 5-$HT_2$ receptor. Thus, activation of 5-HT receptors leads to a decrease on GABA release which

represents an increase on striatal DA release (Gudelsky *et al*, 2008). Because of MDMA effect on striatal DA concentration, this drug has wrongly reported as a possible therapeutic drug for Parkinson's patients. But, in fact, its consumption is most likely to increase the incidence of the disease (Colado *et al*, 2004).

Like in the striatum, MDMA promotes DA release in nucleus accumbens, which also seems to be modulated by interactions between 5-HT and GABA. The ambient temperature plays an important role on MDMA-induced release of DA, being this release greater at 30 ºC than at 20 ºC. These effects where not observed in the striatum (Gudelsky *et al*, 2008).

MDMA also promotes the release of DA in medial prefrontal cortex (mPFC) where PKC activity also seems to have a modulatory effect. However, contrary to what is observed in the striatum, in mPFC, an enhancement of MDMA-induced DA release after inhibition of PKC was reported (Nair *et al*, 2004; Gudelsky *et al*, 2008). An increase in extracellular DA is also observed in rat hippocampus after MDMA ingestion, despite the sparsely innervations on dopaminergic neurons (Shankaran *et al*, 1998). Evidences suggest that MDMA-induced release of DA in hippocampus is modulated by noradrenergic neurons. Treatment with desipramine, an inhibitor of norepinephrine reuptake, results in a decrease of hippocampal DA induced by MDMA (Shankaran *et al*, 1998). The same result was observed in animals after damage of noradrenergic neurons (Gudelsky *et al*, 2008). The MDMA-induced release of DA in hippocampus is also thought to be related with an increase of tyrosine that undergoes a non-enzymatic hydroxylation originating 3,4-dihydroxyphenylalanine (DOPA) caused by the increase of free radical formation. This compound can later be converted to DA via aromatic amino acid descarboxylase into serotonergic neurons (Gudelsky *et al*, 2008).

#### *1.4.2.3. MDMA effects on noradenergic neurotransmission*

MDMA administration appears to influence norepinephrine neurotransmission, however in opposition to what has been observed in serotonergic and dopaminergic systems, evidences are not so well documented. MDMA leads to an increase of extracellular concentration of NE (Green *et al*, 2003). The inhibition of NE reuptake with desipramine blocks its release (Green *et al*, 2003). This result suggests that NE release is due to MDMA actions on NE transporter. However, there are no evidences

suggesting that MDMA leads to long-term effects on NE neurotransmission (Green *et al*, 2003).

### *1.4.3. MDMA metabolism and metabolites neurotoxicity*

The metabolism of MDMA seems to have an important role on MDMA-induced neurotoxicity. It has been reported that central administration of MDMA do not cause neurotoxic effects suggesting that its peripheral metabolization is important (Colado *et al*, 2004).

MDMA can be metabolized, in rat, by three major pathways: hydroxylation, demethylenation and N-demethylation (Green *et al*, 2003; Colado *et al*, 2004), leading to different metabolites that may also have neurotoxic actions (Figure 9) (Colado *et al*, 2004). The major MDMA metabolite is MDA and its plasma levels in rat increase rapidly after MDMA administration (Green *et al*, 2003). Administration of MDA can also produce an acute release of 5-HT, but MDA was reported to be less potent than MDMA (Green *et al*, 2003).

The demethylenation of both MDMA and MDA leads to catechol formation, which can rapidly form *ortho*-quinones. These molecules are redox-active and able to originate reactive oxygen and nitrogen species. In the presence of glutathione (GSH), *ortho*-quinones may conjugate with GSH to form molecules such as 5-(glutathione-S-yl)-α-methyldopamine (5-GSyl-α-MeDA) and 5-(glutathione-S-yl)-N-methyl-α-methyldopamine that can easily cross the blood-brain barrier using GSH transport (Colado *et al*, 2004). These GSH conjugates are still redox-active and may undergo further GSH addition yielding the di-conjugate 2,5-bis-(glutathione-S-yl)-α-methyldopamine (2,5-bis-(glutathione-S-yl)-α-MeDA) (Green *et al*, 2003; Colado *et al*, 2004).

Results demonstrate this possible involvement of GSH conjugation to reactive MDMA catechol metabolites in the neurotoxic effects of MDMA. GSH administration seemed to decrease the brain uptake index of 5-GSyl-α-MeDA, demonstrating a competitive uptake mechanism (Colado *et al*, 2004).

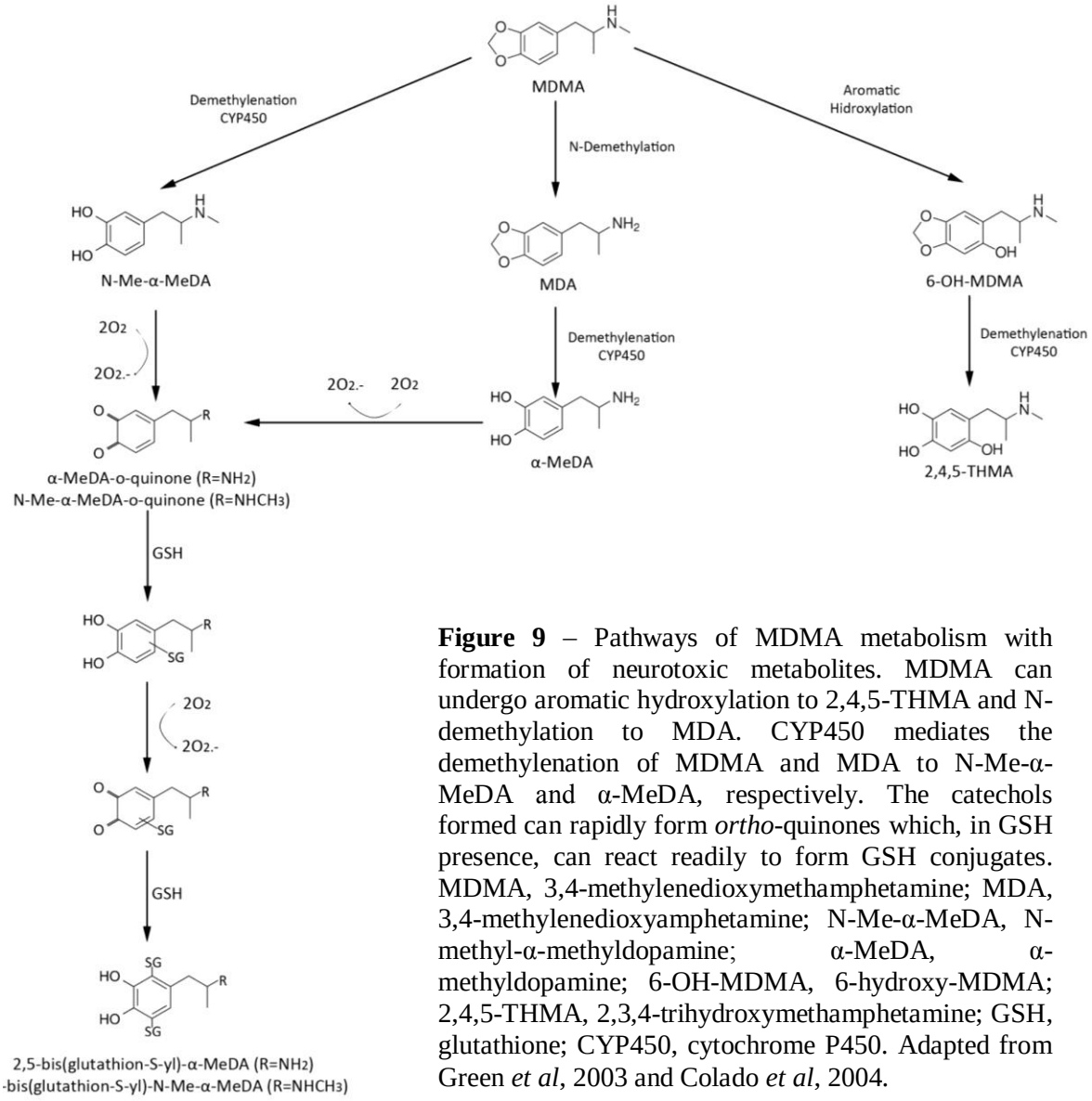


**Figure 9** – Pathways of MDMA metabolism with formation of neurotoxic metabolites. MDMA can undergo aromatic hydroxylation to 2,4,5-THMA and N-demethylation to MDA. CYP450 mediates the demethylenation of MDMA and MDA to N-Me-α-MeDA and α-MeDA, respectively. The catechols formed can rapidly form *ortho*-quinones which, in GSH presence, can react readily to form GSH conjugates. MDMA, 3,4-methylenedioxymethamphetamine; MDA, 3,4-methylenedioxyamphetamine; N-Me-α-MeDA, N-methyl-α-methyldopamine; α-MeDA, α-methyldopamine; 6-OH-MDMA, 6-hydroxy-MDMA; 2,4,5-THMA, 2,3,4-trihydroxymethamphetamine; GSH, glutathione; CYP450, cytochrome P450. Adapted from Green *et al*, 2003 and Colado *et al*, 2004.

### *1.4.4. MDMA and oxidative stress*

Evidences suggest that MDMA administration leads to an augment of free radical formation, which can be an indicator of neurotoxic damage. It was reported an increase in lipid peroxidation, as well as a decrease in endogenous antioxidant defences, like ascorbic acid and vitamin E as a result of MDMA ingestion (Sprague & Nichols, 1995; Colado *et al*, 1997). Also, the formation of 2,3-dihydroxybenzoic acid (2,3-DHBA) from salicylic acid that only occurs in the presence of free radicals is another sign of this effect (Colado *et al*, 1997). In fact, the neurotoxic damage induced by MDMA is due to

oxidative stress. The administration of metabolic antioxidants, like α-lipoic acid or α-phenyl-N-*tert*-butyl nitrone, a free radical scavenger, protects 5-HT terminal nerve endings against the drug administration, probably due to a reduction in the production of free radicals (Colado & Green, 1995). Moreover, hyperthermia may have an important role on free radical formation, since by inhibiting MDMA-induced hyperthermia a decrease of free radical formation is observed (Colado *et al*, 1999).

### *1.4.5. Long-term effects*

MDMA is considered a selective neurotoxic drug for 5-HT neurons. It has been demonstrated that this drug leads to long-term decrease of 5-HT and 5-Hydroxyindoleacetic acid (5-HIAA, 5-HT main metabolite) concentrations (Colado *et al*, 1997; Green *et al*, 2003; O'Shea *et al*, 2006; Gudelsky *et al*, 2008).

As mentioned before, administration of high MDMA doses can cause inhibition of TPH, consequently inhibiting 5-HT synthesis, which can lead to a decrease in 5-HT concentration (Baumann *et al*, 2006). After MDMA administration there is decreased binding of [$^3$H]-paroxetine to 5-HT endings, which can be seen as a sign of degenerating neurons (Green *et al*, 2003; Colado *et al*, 2004). A decrease on [$^3$H]-5-HT uptake into synaptossomes was also observed which is an indicator of decreased 5-HT uptake sites (Colado *et al*, 2004).

It is thought that 5-HT depletion is mainly caused by oxidative stress (Colado *et al*, 1997; Gudelsky *et al*, 2008), but the mechanisms are not completely understood. Some authors stand that the depletion of 5-HT neurons caused by MDMA was due to an excessive acute release of DA (Shankaran *et al*, 1998; Green *et al*, 2003; Colado *et al*, 2004; Gudelsky *et al*, 2008). Others believe that it is a reflex of the MDMA-induced hyperthermic response (Green *et al*, 2003; Colado *et al*, 2004; O'Shea *et al*, 2006; Gudelsky *et al*, 2008). As mentioned above, pre-treatment with ascorbic acid has protective effects against MDMA neurotoxicity, by preventing the depletion of 5-HT neurons, suggesting that oxidative stress plays a role in the neurotoxic effect of this drug (Gudelsky *et al*, 2008). There are evidences suggesting that acute stimulation of DA release and 5-HT receptor activation by MDMA or some MDMA metabolites is required for free radical formation leading to the long-term effects of the drug

(Gudelsky *et al*, 2008). MDMA can increase extracellular DA concentration by converting (L-3,4-Dihydroxyphenylalanine) L-DOPA into DA within 5-HT neurons. This process is believed to contribute to the DA-derived oxidative damage to 5-HT terminals (Gudelsky *et al*, 2008), since L-DOPA administration potentiates the depletion of 5-HT induced by MDMA (Shankaran *et al*, 1998; Colado *et al*, 2004). The inhibition of DA synthesis has been effective in preventing the loss of 5-HT terminals (Green *et al*, 2003). Thus, it is generally believed that enhanced DA release due to MDMA administration leads to an increase in free radical formation and consequently to a neurotoxic effect on 5-HT neurons (Green *et al*, 2003).

However, some authors defend that what seems to be an influence of DA is actually an influence of the hyperthermic response (Green *et al*, 2003). In fact there are studies reporting that L-DOPA, although it results in an increase of DA release, does not lead to an augment of free radical formation. Instead, it was observed an increase in the hyperthermia response period. Agents who seemed to be protective against neurotoxicity induced by MDMA, like haloperidol, had no effect when animal's temperature was kept elevated. Opposing to these results, a protective effect against neurodegenerative loss of 5-HT was achieved when hyperthermic response induced by MDMA was prevented (Green *et al*, 2003; O'Shea *et al*, 2006). As mentioned before, the ambient temperature plays an important role in the effect of MDMA on body temperature. At low ambient temperatures, it was observed a hypothermic response in animals, and in this case it was observed a protective effect against MDMA-induced neurotoxicity (Colado *et al*, 2004). These evidences and the fact that MDMA-induced increase of free radical formation is augmented in hyperthermic conditions indicates that the long-term neurotoxic effects of MDMA are due to the acute hyperthermic response (Green *et al*, 2003).

### *1.5. Visual problems induced by MDMA*

MDMA actions, as well as the mechanisms underlying those actions, have been largely studied in several brain regions. Despite retina being part of CNS the toxic effects of MDMA in this structure are barely known.

Significant drug levels, as well as of its metabolite MDA, were found in the vitreous humor after a fatal overdose (De Letter *et al*, 2002). Small changes in light perception have also been observed in humans after repeated MDMA consumption (Farré *et al*, 2004). Moreover, a MDMA consumer had visual problems, possibly induced by this drug, since its abstinence resulted in visual improvement (Michael *et al*, 2003). Another study showed that repeated MDMA administration can induce retinal cell apoptosis, especially in ganglion cell layer and inner nuclear layer. This result seemed to be correlated with an increase in oxidative stress since the antioxidant CR-6 had a protective effect (Miranda *et al*, 2007). The cell viability in retinal cell cultures is also affected by MDMA (Álvaro *et al*, 2008), once more supporting its possible neurotoxic effect in the retina.

The study of the potential physiological alterations in the retina after MDMA administration was initiated at Center of Ophthalmology of Coimbra recently. In scotopic tests, it was found that 3 hours after MDMA administration (15 mg/kg) that implicit times of all parameters evaluated were significantly decreased in both scotopic and photopic conditions. A significant increase in the amplitude of a-wave, photopic b-wave and photopic OP4 at this time point was also observed. Since hyperthermia is an acute effect of the drug, a third group was formed where the animal body temperature was elevated. This group showed similar results, indicating that these effects can be due to hyperthermia. For a longer period after the drug administration, 24 h, only the a-wave amplitude remained elevated.

Regarding photopic tests, during light adaptation process it was observed an increase in b-wave amplitude and a decrease on its implicit time for MDMA group, 24 hours after administration, compared to hyperthermic and control groups. In the remaining tests to evaluate the photopic system, no significant differences were found between groups at 24 h time point.

## *1.6. Objectives*

Despite some evidences of visual problems induced by MDMA, little attention has been given to the possible toxic effects of MDMA to the retina. The impact of MDMA on retinal physiology is an important issue that we tried to clarify using electroretinography, a non-invasive technique that allows *in vivo* evaluation of physiological retinal responses to light. MDMA effect on glial reactivity is another issue that we tried to clarify, since glial reactivity may reflect neurotoxic damages induced by this drug.

Regarding the MDMA administration, three administration protocols were used. In the first one, a single MDMA injection was administrated (15 mg/kg) to evaluate its long-term effects in retinal physiology. The second and third MDMA administration protocols mimic two routines of consumption of MDMA users: the consumption during a vacation week and weekend consumption. These MDMA administration protocols were used to determine its acute and long-term effects after multiple administrations.

# 2. Methods

## 2.1. Animals

Male Wistar rats aged 8 weeks, weighing about 265g were used. The animals were placed three per cage and maintained at 22 ± 2ºC, with 12 h light/dark (reverse light cycle). The access to water and food was free. The animals were randomly divided in two groups: saline and MDMA.

## 2.2. Animal Treatment

MDMA was dissolved in saline solution (0.9% NaCl) and administered through an intraperitoneal (IP) injection to MDMA group. The vehicle was administered the same way to saline group. The injection periodicity and dose are described below.

### 2.2.1. Experimental design

#### 2.2.1.1. Protocol 1

This protocol allowed the evaluation of long-term effects of MDMA (7 days after MDMA injection) in the retinal physiology. Rats received a single MDMA (15 mg/kg) IP injection. A total of twelve animals per group was used.

#### 2.2.1.2. Protocol 2

Animals received MDMA (5 mg/kg) or saline injection, once a day during 7 days. This protocol was used to determine the acute and long-term effects of MDMA repeated consumption in the retina, mimicking "one week vacation" consumption. In this protocol nine animals per group were used.

#### 2.2.1.3. Protocol 3

To evaluate the effects of MDMA sporadic use on retinal physiology, "weekend consumption" was mimicked. Four animals per group were injected with MDMA (5 mg/kg) or saline once a day, twice a week, at two following days, during 4 weeks, totalling 10 injections.

### *2.3. Electroretinograms*

The ERGs were performed at different time points: 7 days before treatment, which was considered the baseline recording; 24 h after treatment (for protocols 2 and 3); and 7 days after treatment (Figure 10). ERG recordings were performed after, at least, 12 h (720 min) of dark adaptation. To avoid the influence of circadian rhythm all ERGs were performed in the morning.

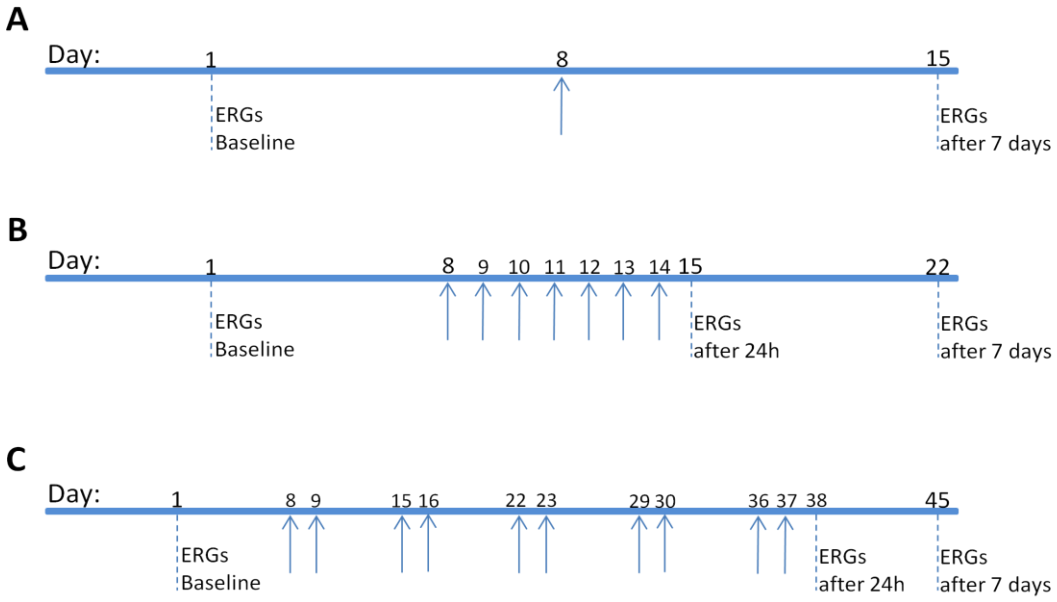


**Figure 10 –** Schematic representation of MDMA administration protocols 1, 2 and 3 (A, B and C, respectively). Arrows indicate MDMA or Saline administration.

Animals were anesthetized with an IP injection of ketamine (75 mg/kg) and xylazine (50 mg/kg) under dim red light illumination. Isolated clips were used to avoid the eye closure and pupil was fully dilated with topical tropicamide (1%). The body temperature was maintained at 37ºC using a heating pad (Figure 11).

The electrical responses were recorded using gold wire electrodes placed at the cornea, two reference electrodes placed at the head and a ground electrode in the tail (Figure 11). Corneal electrode potential was stable. The impedance was maintained below 5 kOhm during the entire record with saline solution application.

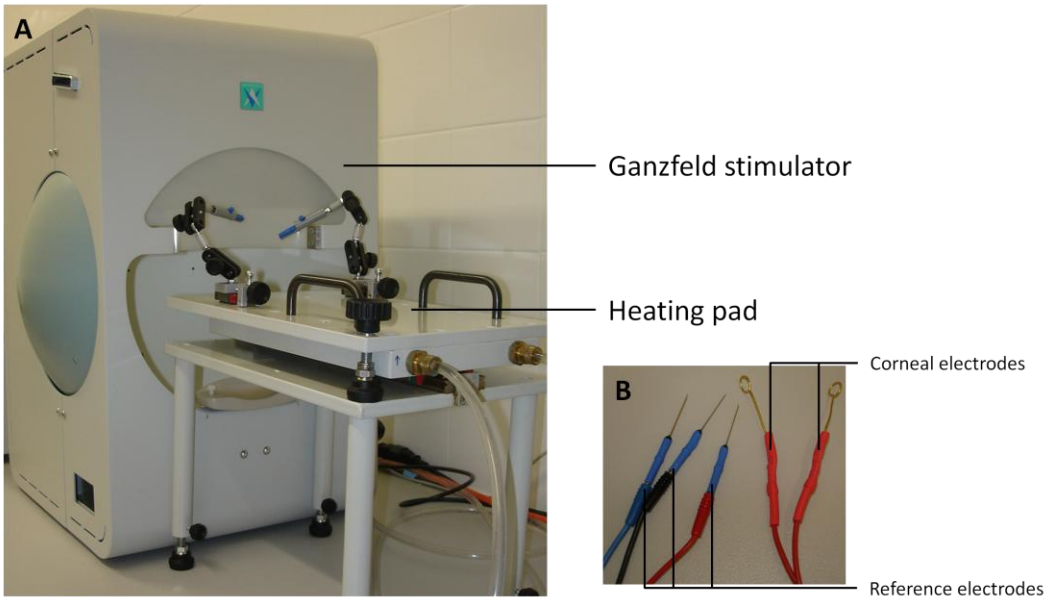


**Figure 11 – (A)** Image showing the apparatus used to perform ERGs in small animals. Light stimulation by the Ganzfeld stimulator (Roland Consult GmbH, Brandenburg, Germany) is computer-controlled. The heating pad to keep animal temperature around 37ºC is also shown. **(B)** Corneal and reference

Data were recorded with a band width of 1 to 300 Hz, sampled at 3.4 kHz (0.65 Hz to Photopic Flicker test) by a digital acquisition system (Roland Consult GmbH, Brandenburg, Germany) (Figure 11) and analyzed with the RETIport software (Roland Consult GmbH, Brandenburg, Germany).

After dark adaptation each animal was exposed to four different light stimulation protocols delivered by a Ganzfeld stimulator (Roland Consult GmbH, Brandenburg, Germany). Following Rosolen and co-workers recommendations the four tests performed were: *Scotopic Luminance Response* (SLR), *Photopic adaptometry*, *Photopic luminance response* (PLR) and *Photopic Flicker* (Figure 12).

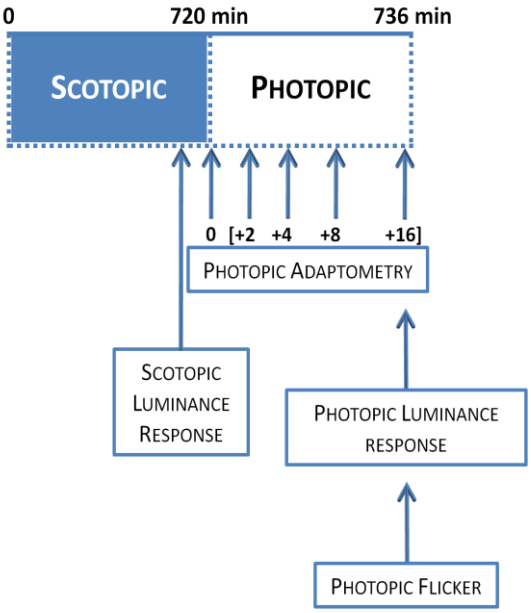


**Figure 11** – Schematic representation of the sequential ERG tests performed. Adapted from Rosolen *et al*, 2005.

In SLR test, animals were exposed to a series of white light flashes with different intensities (0.0095 to 9.49 cd-s/m$^2$) delivered three times at 0.1 Hz. During *Photopic adaptometry* animals received bright white flashes (9.49 cd-s/m$^2$) delivered three times at 1.3 Hz in five different time points (0 min (onset), 2, 4, 8, 16 min) on a white background (25 cd/m$^2$). In PLR, also with a white background (25 cd/m$^2$), animals were exposed to white flashes, delivered three times at 1.3 Hz for seven intensities (0.0095 to 9.49 cd-s/m$^2$). In *Photopic Flicker* test ten bright flashes (3.00 and 9.49 cd-s/m$^2$) at 6.3 Hz were delivered with a white background (25 cd/m$^2$).

### *2.4. Data handling*

From each ERG waveform several components were obtained: a-wave, b-wave and OPs (four in scotopic ERG and three in photopic ERG). For each one two measures were extracted: the amplitude and the implicit time values.

The a-wave amplitude was measured from the baseline to the first negative trough. The b-wave amplitude (maximum positive signal) was measured relatively to the maximum negative signal (a-wave). The implicit time of a-wave and b-wave were measured from the flash onset to a-wave trough and to b-wave peak, respectively (Figure 13). To obtain b-wave amplitude and implicit time values a high frequency cut-off of 50Hz digital filter was used. Since OPs are high-frequency wavelets (Li *et al*, 1991) they were eliminated by this digital filtering (Figure 13). Amplitude and implicit time values of OPs were obtained using digital filters of low frequency cut-off of 60 Hz and 55 Hz for

scotopic and photopic ERG, respectively (Figure 13). A Fast Fourier Transform (FFT) was used to determine the flicker responses. The amplitude and phase values for the first (6,3 Hz) and second (12,7 Hz) harmonics were considered.

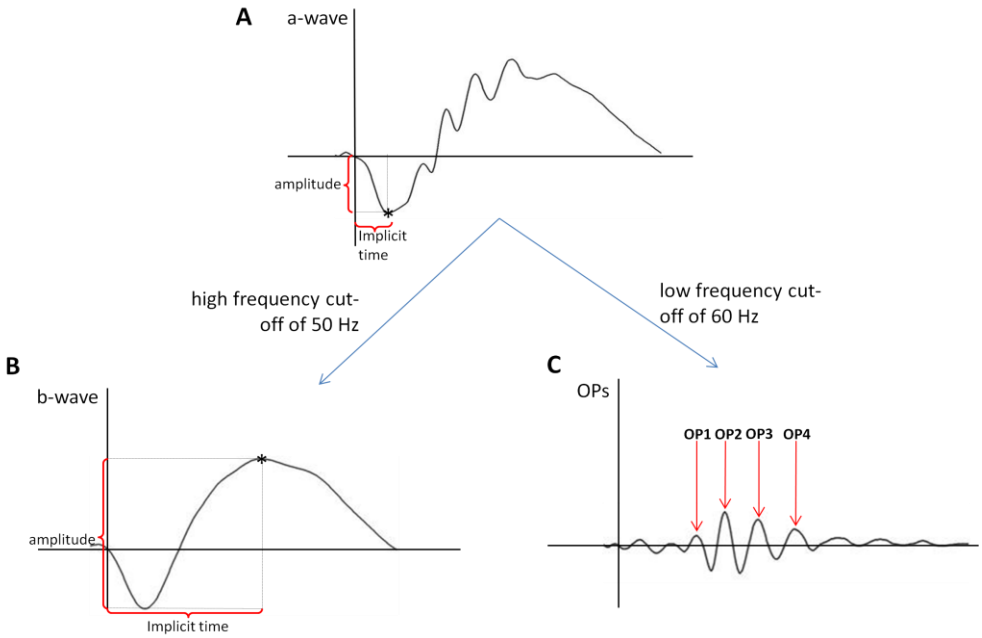


**Figure 13** – Example of ERG waveforms before and after digital filtering. **A** – Original scotopic ERG waveform. **B** – Scotopic ERG waveform after the use of a high frequency cut-off of 50 Hz to extract b-wave. **C** – Scotopic ERG waveform after applying a low frequency cut-off of 60 Hz.

### *2.5. Western Blot Analysis*

The animals were sacrificed, and the retinas were dissected, rinsed in ice-cold phosphate-buffered saline (PBS; 1.37 M NaCl, 27 mM KCl, 18 mM $KH_2PO_4$, 100 mM $Na_2HPO_4.2H_2O$), and lysed in radio-immunoprecipitation assay (RIPA) buffer (150 mM NaCl, 50 mM Tris, 5 mM EGTA, 1% Triton, 0.5% DOC, 0.1% SDS supplemented with 1 mM dithiothreitol (DTT) and complete miniprotease inhibitor cocktail tablets. Protein was quantified by the bicinchoninic acid (BCA) method, and 10 µg protein from each sample were used for immunoblots, after adding 6x concentrated sample buffer (0.5 M Tris, 30% glycerol, 10% SDS, 0.6 M DTT, 0.012% bromophenol blue) and heating the samples for 5 min at 95ºC. Proteins were separated by 8% sodium dodecyl sulfate polyacrylamide gel electrophoresis (SDS-PAGE) and transferred to polyvinylidene fluoride (PVDF) membranes. The membranes were blocked for 1 h at room temperature in Tris-buffered saline (TBS) containing 1% Tween-20 (TBS-T) and 5% skim milk. Then, membranes were incubated with the primary antibody (mouse anti-GFAP,

1:5,000 or mouse anti-vimentin, 1:1,000) in TBS-T with 1% skim milk overnight at 4ºC. Membranes were washed for 1 h with TBS-T with 0.5% skim milk and then incubated with a secondary antibody (goat anti-mouse IgG, 1:20,000) for 1 h at room temperature. The membranes were processed using the Enhanced Chemi-Fluorescence system (GE Healthcare) on a gel imager (Thypoon FLA 9000), and digital quantification of bands intensity was performed (Image Quant, IQ Solutions). Membranes were re-probed with an antibody, mouse anti-α-actin, as described above. Incubation with different primary antibodies required, in some cases, the membrane stripping. For that, membranes were placed in 100% methanol during 15 min under agitation, washed in water and placed into stripping solution (100 mM 2-mercaptoethanol, 2% SDS, 62.4 mM Tris-HCl) at 60ºC. The membranes were washed in TBS-T, blocked and incubated with the secondary antibody to confirm the antibody removal. After membrane stripping membranes the procedure described above was repeated. Data is presented as ratio between the immunoreactivity of GFAP and α-actin or vimentin and α-actin, and is expressed as percentage of control.

### *2.6. Immunohistochemistry*

#### *2.6.1. Whole Mounts*

The animals were anesthetized with an IP injection of ketamine (75 mg/kg) and xylazine (50 mg/kg) and then perfused using saline solution (0.9% NaCl) followed by 4% paraformaldehyde (PFA). The eyes were removed and the retinas were dissected in cold PBS. Retinas were immersed in 2% (wt/vol) PFA for 10 min at room temperature and then washed twice in PBS. The retinas were blocked in 10% goat serum in PBS with 0.3% Triton at room temperature and then incubated with the primary antibody (mouse anti-Cd11-b, 1:100) in blocking solution for 72 h at 4ºC. Retinas were washed with PBS for 6 to 7 h, until a final wash overnight at 4ºC and incubated with a secondary antibody (goat anti-mouse IgG, 1:100) in blocking solution overnight at 4ºC. Before mounting, retinas were, once more, washed with PBS for 6 to 7 h, before a final wash overnight at 4ºC. The preparations were visualized under a Zeiss Confocal Microscope LSM 510 Meta. For each retina, 5 random images were taken and qualitative analyses were performed.

### *2.6.2. Retinal Slices*

Animals were sacrificed, the eyes were dissected and placed in 4% PFA for about 10 min at room temperature and then the cornea, lens and vitreous humor were removed. The eye cup was placed in 4% PFA for a total fixation time of 30 min. After washing for at least for 5 min the eye cup was cryoprotected for 1 h with 15% sucrose in PBS followed for 1 h with 30% sucrose in PBS. The eye cups were placed in Tissue-Tek O.C.T - 30% sucrose in PBS (1:1) for 10 min, and then frozen and stored at -80ºC. Retinal slices (10 µm tick) were cut using Shandon SME cryotome cryostat (GMI). The mixing of Tissue-Tek O.C.T with equal volume of 30% sucrose in PBS allows a better incorporation of the eye cup and a better cutting of the sample (Barthel & Raymond, 1990). The cryosections were dried for 45 min at room temperature and then fixed for 10 min with acetone (-20ºC). Before blocking for 30 min with 10% goat serum in PBS with 1% bovine serum albumin (BSA) in a humidified environment, cryosections were hydrated twice with PBS and permeabilized for 30 min using PBS with 0.25% Triton. The cryosections were incubated with the primary antibody (mouse anti-GFAP, 1:500; mouse anti-Vimentin, 1:750; mouse anti-Cd11-b, 1:100) in a humidified environment overnight at 4ºC. To analyze Cd11-b immunoreactivity, the animals were perfused as described above. After washing three times for 10 min with PBS, the cryosections were incubated with the secondary antibody (goat anti-mouse IgG, 1:250). At the same time, the nuclei were stained with 4',6-diamidino-2-phenylindole (DAPI, 1:5.000). For each cryosection, three random images were taken using a Zeiss Confocal Microscope LSM 510 Meta. The densitometry analyses were performed with ImageJ software and results are expressed as a percentage of control.

## *2.7. Statistical Analysis*

Due to the high variability of the collected data, those that did not fit into the interval mean ± 3 SD were excluded. Data was analyzed with SPSS (SPSS Inc.). For Protocol 1, P*aired-Samples t-test* was used. However, when Gaussian distribution was not verified, the non-parametric equivalent (*Wilcoxon test*) was used. Protocols 2 and 3 were analyzed using R*epeated Measures ANOVA* followed by *Paired-Samples t-test*, or *Friedman test* followed by *Wilcoxon test*, if samples did not have a Gaussian distribution, as indicated in the figure legends. Data from Western Blots and retinal slices immunohistochemistry were analyzed with Prisma 5 (GraphPad Software) using

the non-parametric test, *Mann-Whitney test*. P values less than 0.05 were taken as significant.

# 3. Results

## 3.1. Protocol 1

In this protocol, 24 animals were randomly divided into two groups: MDMA group (n = 12) received an intraperitoneal injection of MDMA (15 mg/kg); Saline group (n = 12) received 0.9% NaCl. Electroretinogram recordings were performed 7 days before treatment, which was considered the baseline recording, and 7 days after MDMA or Saline administration. Within each group 7 days time point mean values were statistically compared to baseline mean values using *Paired-Samples t-test* or *Wilcoxon test* when Gaussian distribution was not observed. The effects of MDMA administration on glial reactivity were also analyzed.

### 3.1.1. Effect of MDMA administration on rat scotopic ERG

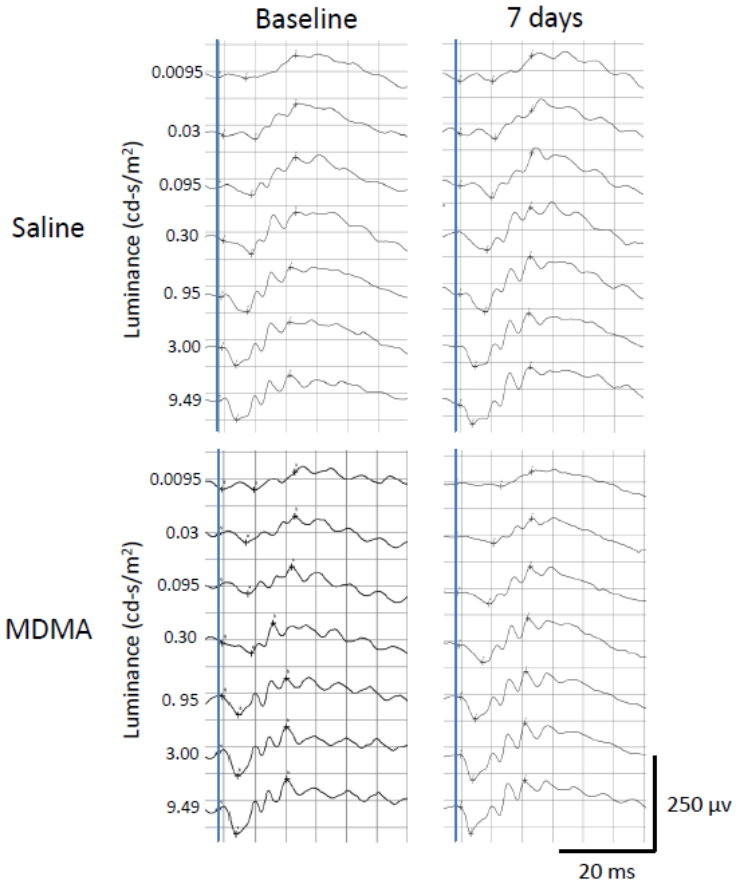


**Figure 14** – Representative recordings of scotopic ERGs performed 7 days before (baseline recording) and 7 days after MDMA (MDMA group) or Saline administration (Saline group). ERG responses were elicited by seven different light intensity (0.0095 – 9.49 cd-s/$m^2$) stimuli. Each trace represents an average of three responses to light stimulus with the same intensity. Solid blue vertical line indicates the light stimulus onset.

Scotopic ERGs were elicited by seven different light intensity stimuli ranging from 0.0095 to 9.49 cd-s/$m^2$ (Figure 14). The a-wave was only identifiable for light stimuli higher than 0.03 cd-s/$m^2$ and its amplitude increased with luminance increase. Regarding the amplitude and implicit time of a-wave, no significant differences were obtained between 7 days time point and baseline, for either MDMA or Saline groups (Figures 15A and B). Regarding the amplitude of b-wave, no significant differences were detected between 7 days time point and baseline for both groups as well (Figure 15C). However, in MDMA group, the implicit time of b-wave was significantly increased at 7 days time point when compared to baseline ($p < 0.05$) (Figure 15D).

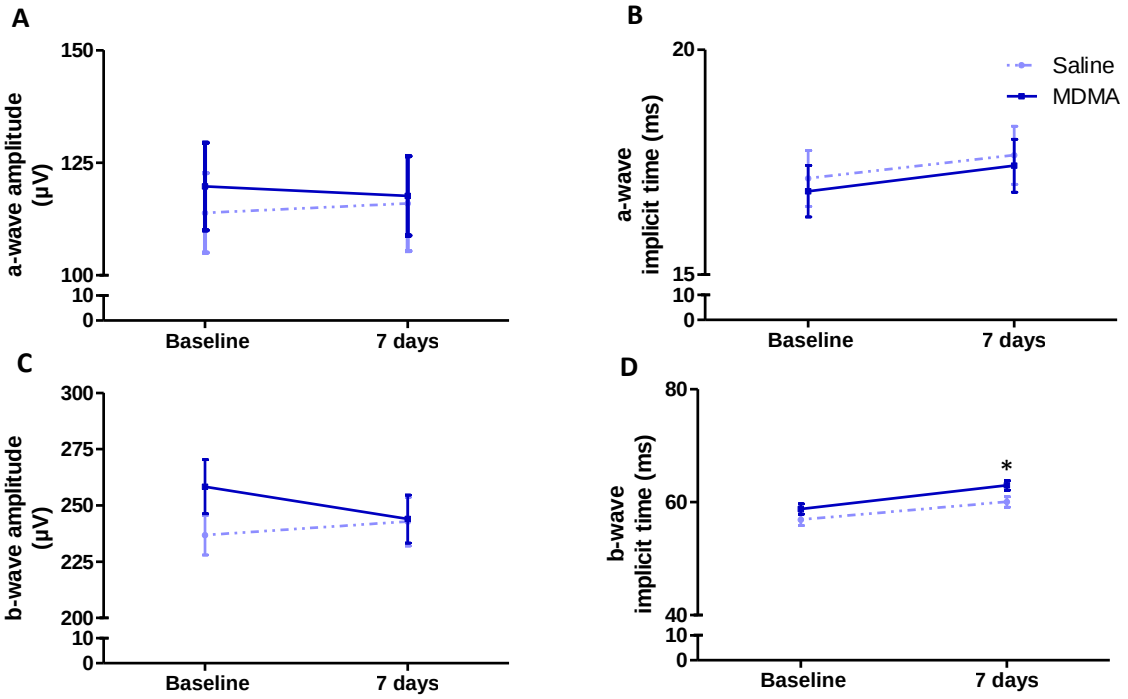


**Figure 15 –** Effect of a single MDMA administration on **A** – a-wave amplitude; **B** – b-wave amplitude; **C** – a-wave implicit time; **D** – b-wave implicit time of rat scotopic ERG. The ERGs were recorded 7 days before (baseline recording) and 7 days after MDMA or Saline administration. Scotopic ERGs were elicited by seven different light intensities (0.0095 – 9.49 cd-s/$m^2$). The four parameters were analyzed using *Wilcoxon test*. Data is presented as mean±SEM. Twelve animals were used for each group. * $\rho<0.05$ – Comparing with baseline for MDMA group.

To evaluate differences in b-wave amplitude relatively to a-wave amplitude, the ratio between b-wave and a-wave amplitudes (b/a ratio) was calculated. Significant changes

were noticed between 7 days time point and baseline for Saline group ($p < 0.01$). The ratio values decreased at 7 days time point for this group (Table 1).

**Table 1 –** b/a ratio for Saline and MDMA.

| | **Group** | *Saline* | | *MDMA* | |
|---|---|---|---|---|---|
| | **Time Point** | *Baseline* | *7 days* | *Baseline* | *7 days* |
| **Ratio b/a** | *Mean* | 3.56 | 2.60¤¤ | 3.21 | 2.91 |
| | *SEM* | 0.83 | 0.27 | 0.83 | 0.43 |

¤¤ $p<0.01$ – Comparing with baseline for Saline group

The analysis of the oscillatory potentials allowed an evaluation of the potential effects of MDMA in the inner retina. A single MDMA administration did not induce significant changes in OP1 amplitude 7 days after the injection comparing to the baseline time point (Figure 16A). In contrast, OP1 implicit time was significantly higher for both MDMA and Saline groups at 7 day time point comparing to baseline ($p < 0.001$ in both groups). Regarding OP2 and OP3 amplitudes a significant decrease was observed between 7 days time point and baseline for MDMA group ($p < 0.05$ in both parameters) (Figures 16C and 16E). OP2 and OP3 implicit times were significantly higher in 7 days time point comparing to baseline values for both MDMA ($p < 0.001$ in both parameters) and Saline groups ($p < 0.01$ and $p < 0.001$ in OP2 and OP3 respectively) (Figures 16D and 16F). The amplitude of OP4 was significantly higher in 7 days time point when compared to baseline values for Saline group ($p < 0.05$) (Figure 16G). The implicit time of this oscillatory potential did not present significant differences between 7 days time point and baseline (Figure 16H).

The sum of all oscillatory potentials amplitude was determined (Table 2), and no significant differences were observed between 7 days time point values and baseline values for MDMA or Saline groups.

**Table 2 -** Scotopic OPs amplitude sum for Saline and MDMA groups.

| | **Group** | *Saline* | | *MDMA* | |
|---|---|---|---|---|---|
| | **Time Point** | *Baseline* | *7 days* | *Baseline* | *7 days* |
| **Sum OPs** | *Mean* | 319.12 | 306.63 | 362.56 | 318.07 |
| | *SEM* | 11.28 | 11.87 | 24.84 | 16.86 |

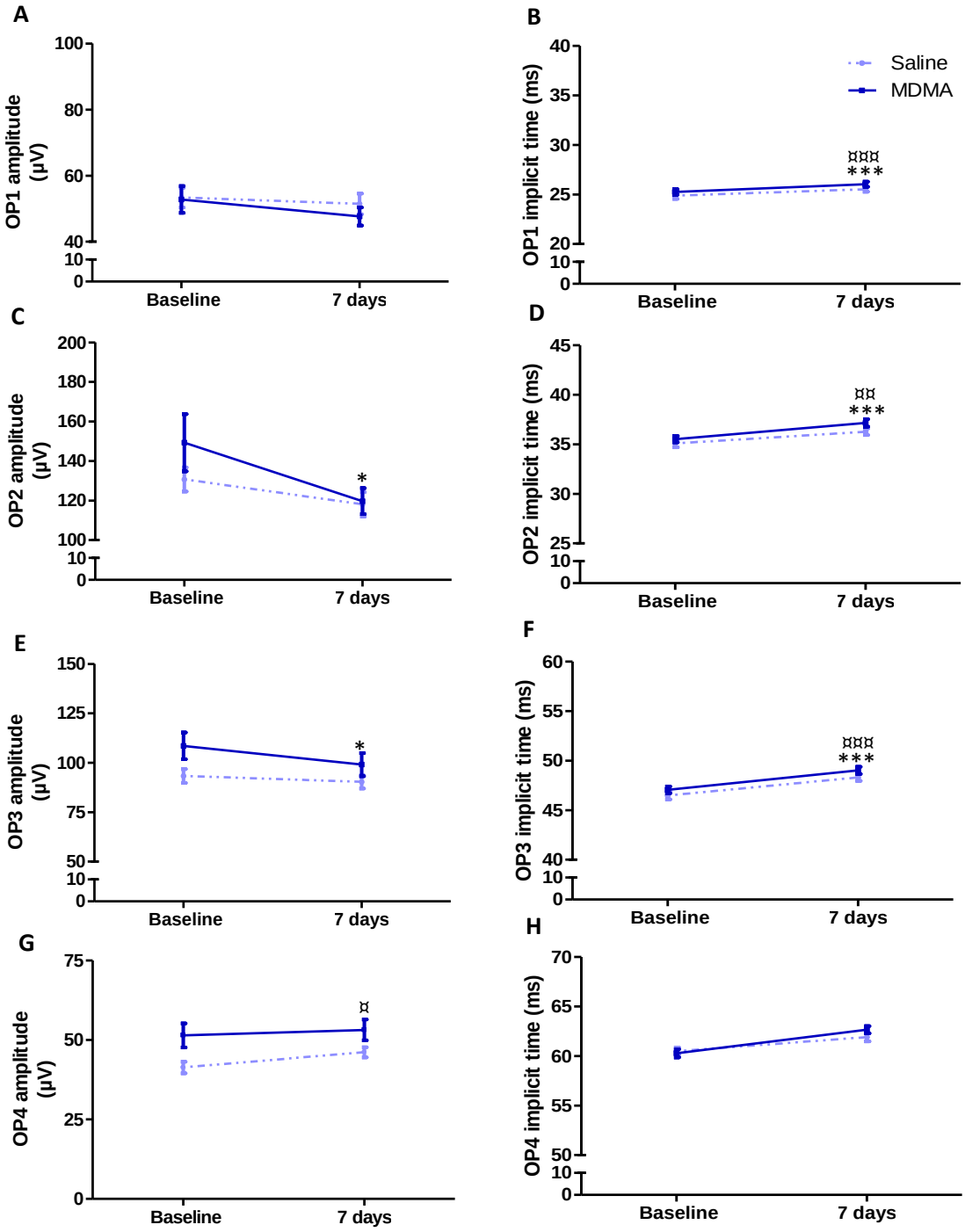


**Figure 16 –** Effect of MDMA administration on the amplitude and implicit time of rat scotopic Oscillatory Potentials (OPs). The ERG recordings were performed 7 days before (baseline recording) and 7 days after MDMA or Saline intraperitoneal injection and were elicited by seven different light intensities (0.0095 – 9.49 cd-s/m$^2$). Except for OP1 and OP4 implicit times, the analysis was performed using *Wilcoxon test*. In these parameters Gaussian distribution was observed, so a *Paired-Sample t-test* was used. **(A, C, E, G)** – OP1, OP2, OP3 and OP4 amplitudes, respectively. **(B, D, F, H)** – OP1, OP2, OP3 and OP4 implicit times, respectively. Data is presented as mean±SEM. Twelve animals were used for each group. * $\rho<0.05$, *** $\rho<0.001$ – Comparing with baseline for MDMA group; ¤ $\rho<0.05$, ¤¤ $\rho<0.01$, ¤¤¤ $\rho<0.001$ – Comparing with baseline for Saline group.

### *3.1.2. Effect of MDMA administration on rat photopic ERG*

#### *3.1.2.1. Light adaptation*

To evaluate MDMA effects on photopic ERGs, animals were exposed to a light adaptation period. Animals were exposed to bright white flashes (9.49 cd-s/$m^2$) delivered at 0 min (onset), 2, 4, 8 and 16 min with a white background (25 cd/$m^2$). ERGs were recorded 7 days before and 7 days after MDMA administration (Figure 17). The number of cones in rats is low (nocturnal animals) and a lack of a-wave in photopic ERGs is observed, since these photoreceptors are responsible for a-wave formation in photopic conditions.

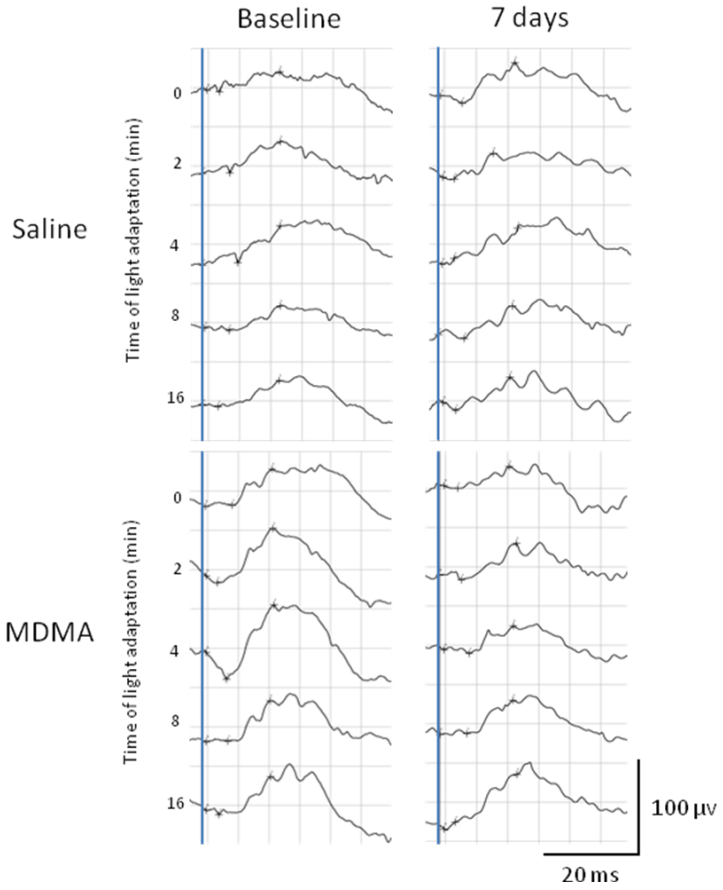


**Figure 17** – Representative recordings of light adaptation ERG performed 7 days before (baseline recording) and 7 days after treatment (MDMA or Saline injection). ERGs were elicited by bright white flashes (9.49 cd-s/$m^2$) delivered at 0 min (onset), 2, 4, 8 and 16 min with a white background light (25 cd/$m^2$). Each trace represents an average of three responses to light stimulus of the same intensity. Solid blue vertical line indicates de light stimulus onset.

From light adaptation ERGs b-wave was extracted and the mean value for all times of adaptation was analyzed. Regarding the amplitude and implicit time of b-wave, no significant differences were found between 7 days time point and baseline for both groups (Figures 18A and 18B).

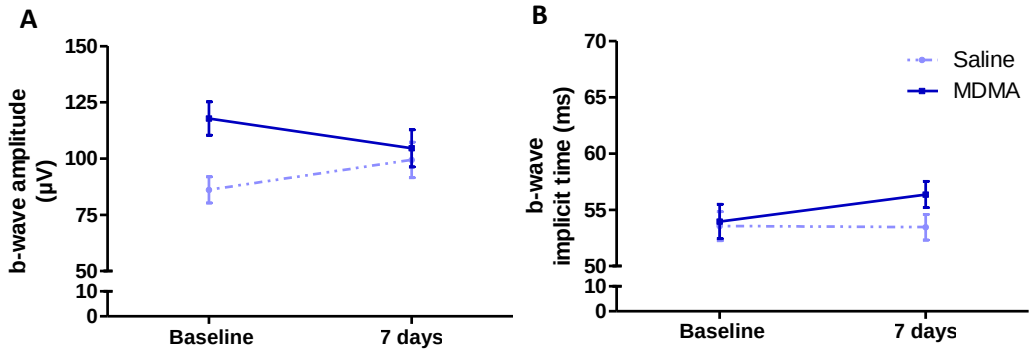


**Figure 18** – Effect of MDMA administration on rat b-wave amplitude **(A)** and b-wave implicit time **(B)** during light adaptation ERG. ERGs were recorded during light adaptation, 7 days before (baseline recording) and 7 days after a single MDMA or Saline intraperitoneal injection, and were elicited by bright white flashes (9.49 cd-s/$m^2$) delivered at 0 min (onset), 2, 4, 8 and 16 min with a white background (25 cd/$m^2$). Analysis was performed using the non-parametric test *Wilcoxon test*. Data is presented as mean±SEM (n = 12 for each group).

#### *3.1.2.2. Photopic b-wave and oscillatory potentials*

After the light adaptation period, photopic ERGs were recorded (Figure 19). Waveforms were elicited by seven different light intensities (0.0095 to 9.49 cd-s/$m^2$) with a white background. As in light adaption ERG, a-wave was not identifiable and b-wave was only detectable for bright light stimuli (3.00 and 9.49 cd-s/$m^2$).

MDMA administration did not cause significant differences in b-wave amplitude between the two time points in both groups (Figure 20A). Regarding b-wave implicit time, a statistical significant decrease was detected in MDMA group ($p < 0.05$) (Figure 20B).

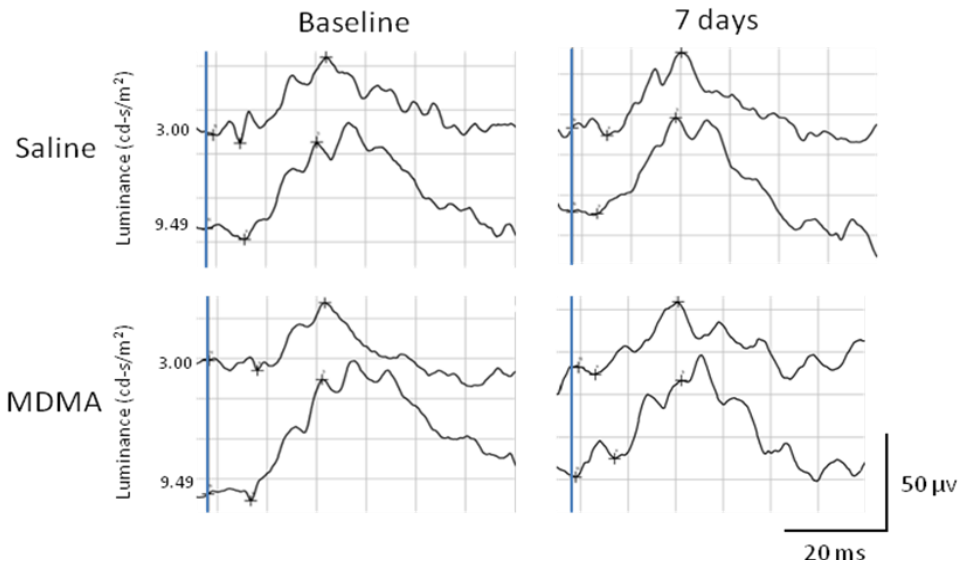


**Figure 19** – Representative ERG recordings of photopic luminance response for Saline (n = 12) and MDMA injected animals (n = 12). ERGs were recorded 7 days before (baseline recording) and 7 days after treatment and were elicited by seven different light intensities (0.0095 to 9.49 cd-s/m$^2$) with a white background. Responses to bright light flashes with intensities of 3.00 and 9.49 cd-s/m$^2$ are represented. An average of three responses to light stimulus with the same intensity is represented in each trace. Solid blue vertical line indicates the onset of light stimulus.

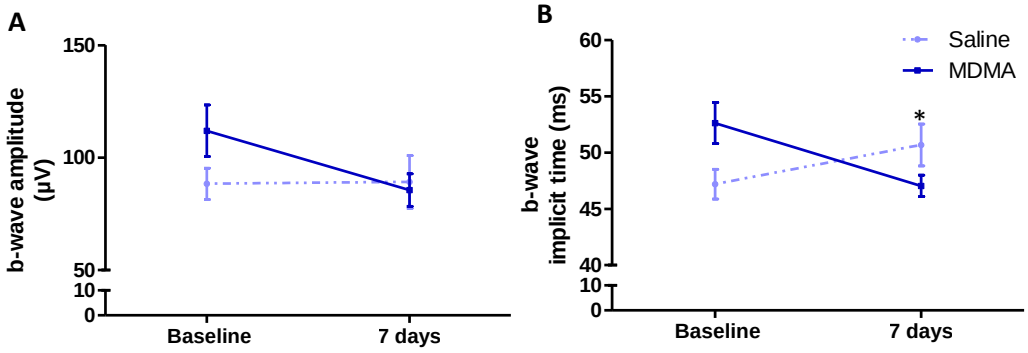


**Figure 20** – Effect of MDMA administration on rat photopic b-wave amplitude **(A)** and b-wave implicit time **(B)**. Photopic ERGs were performed, after light adaptation, 7 days before (baseline recording) and 7 days after a single MDMA or Saline intraperitoneal injection. The recordings were obtained by exposing the animals to seven different light intensities (0.0095 to 9.49 cd-s/m$^2$) with a white background. Data was analyzed using the *Wilcoxon test*. Data is presented as mean±SEM (n = 12 for each group). * $\rho<0.05$ – Comparing with baseline for MDMA group.

In photopic ERG only three oscillatory potentials (OPs) can be detected: OP2, OP3 and OP4, and their amplitudes are much smaller than those registered in scotopic ERGs. MDMA administration did not induce any significant difference in the amplitude or implicit time of any OP (Figure 21).

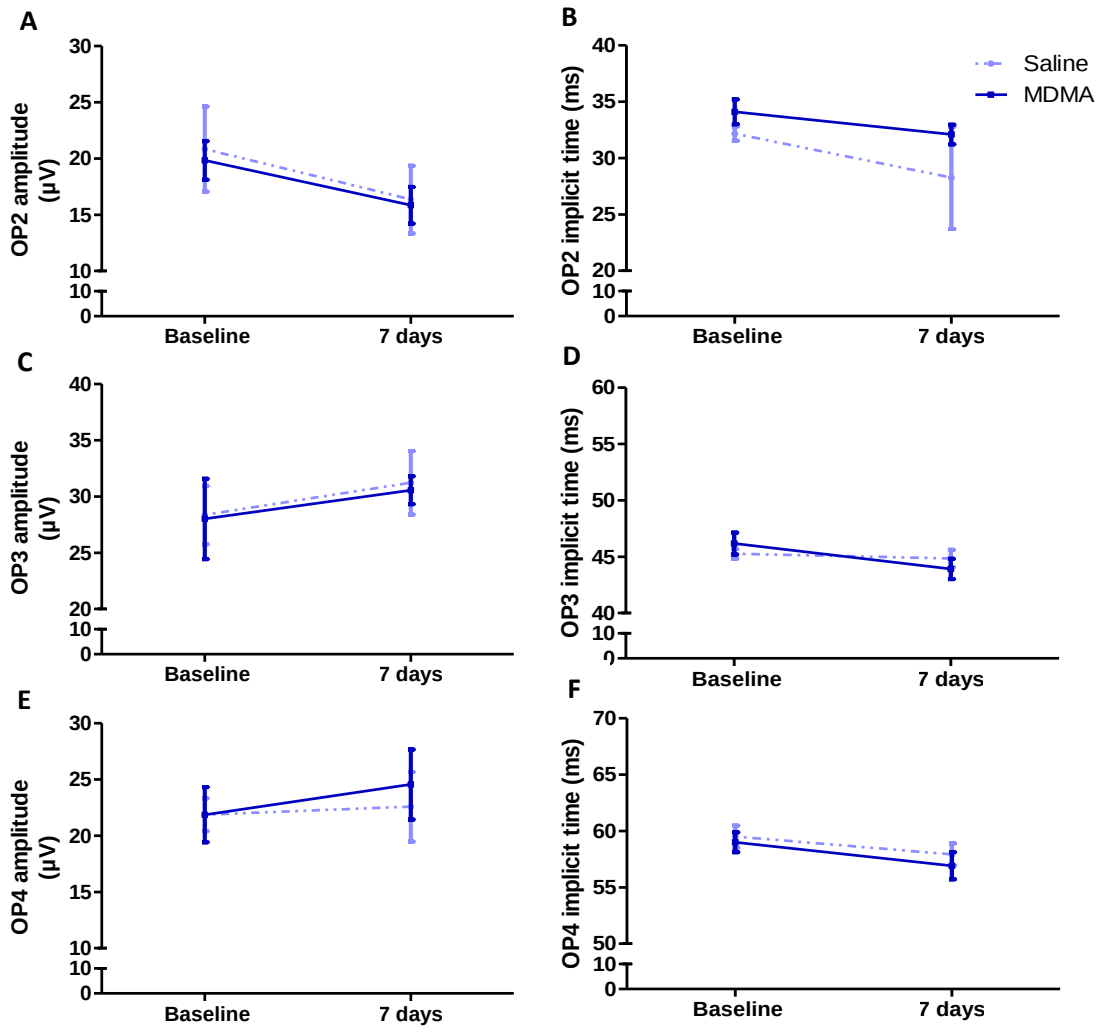


**Figure 21** – MDMA influence on rat photopic oscillatory potentials (OPs). ERGs were recorded 7 days before (baseline recording) and 7 days after MDMA or Saline administration and were elicited by seven different light intensities (0.0095 to 9.49 cd-s/m$^2$) with a white background, but only responses to bright light flashes with intensities of 3.00 and 9.49 cd-s/m$^2$ were analyzed. Data were analyzed using the *Wilcoxon test*. **(A, C, E)** – OP2, OP3 and OP4 amplitudes, respectively. **(B, D, F)** – OP2, OP3 and OP4 implicit times, respectively. Data is presented as mean±SEM. Twelve animals were used for each group.

The sum of the amplitudes of photopic oscillatory potentials was also calculated (Table 3), and as expected, no significant changes were detected for either MDMA or Saline groups.

**Table 3 –** Photopic OPs amplitude sum for Saline and MDMA group.

| | **Group** | *Saline* | | *MDMA* | |
|---|---|---|---|---|---|
| | **Time Point** | *Baseline* | *7 days* | *Baseline* | *7 days* |
| **Sum OPs** | *Mean* | 99.05 | 88.18 | 101.60 | 91.70 |
| | *SEM* | 10.73 | 19.05 | 13.66 | 19.78 |

### *3.1.3. Effect of MDMA administration on rat photopic flicker ERG*

A pure cone response was evaluated using high temporal frequency stimuli, the photopic flicker ERG. Photopic flicker responses were elicited by flashes with two different light intensities (3.00 and 9.49 cd-s/m$^2$) with a white background (Figure 22).

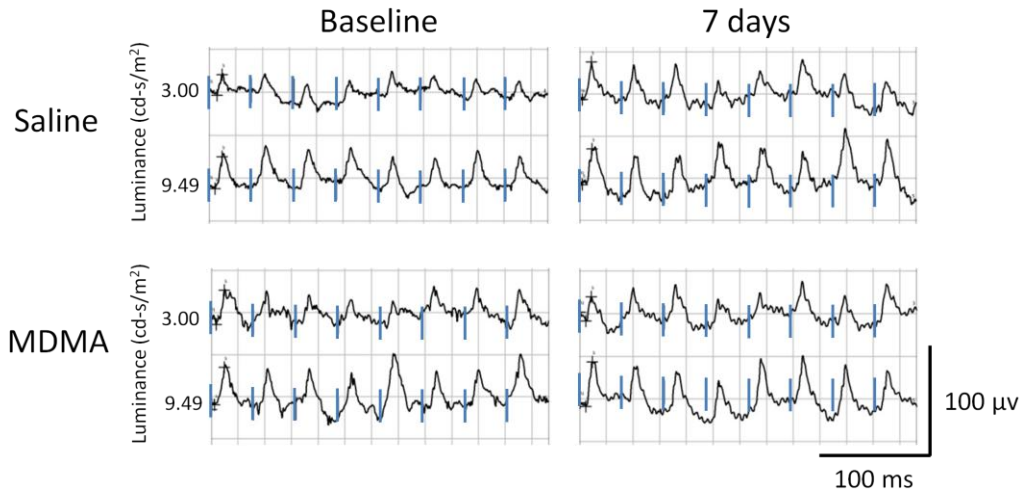


**Figure 22** – Representative recordings of photopic flicker ERG recorded 7 days before (baseline recording) and 7 days after MDMA or Saline administration elicited by two different light intensities (3.00 and 9.49 cd-s/m$^2$) with a white background. Each trace represents an average of ten responses to light stimulus of the same intensity. The onset of light stimulus is indicated by the small solid blue vertical lines.

The Fast Fourier Transform (FFT) first and second harmonic amplitude and implicit times of the original ERG waveforms were determined. Both first and second harmonic amplitudes did not show significant differences between 7 days time point values and baseline values (Figure 23A and 23C). For first harmonic implicit time no significant changes were detected as well (Figure 23B). The second harmonic implicit time showed a significant increase in MDMA group at 7 days time point comparing to baseline ($p < 0.01$) (Figure 23D).

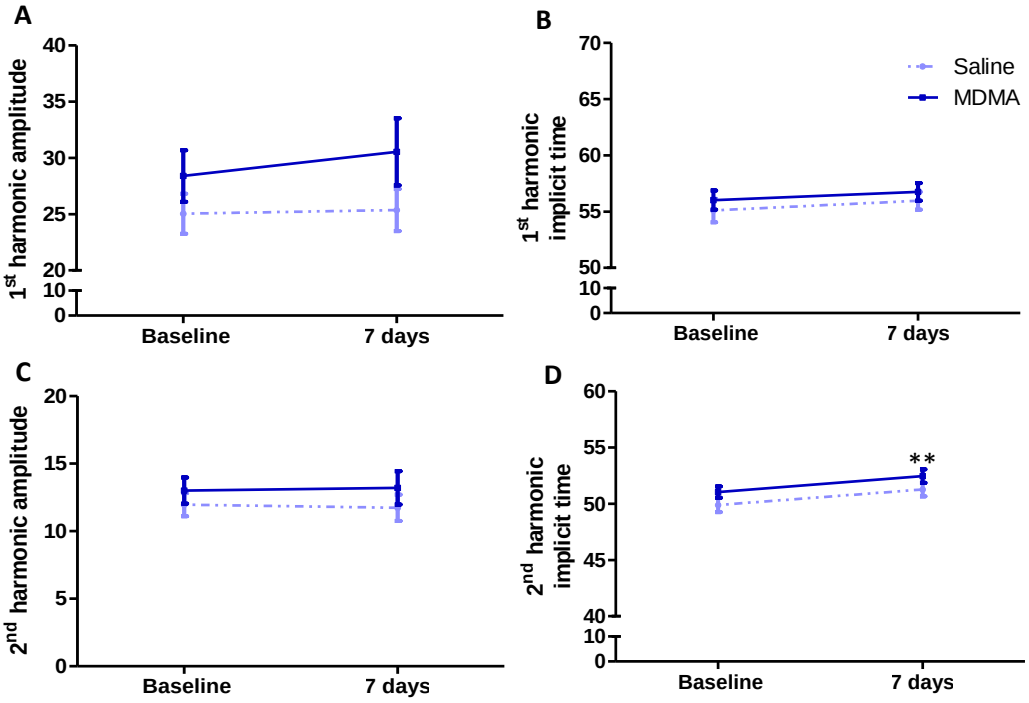


**Figure 23** – Effect of MDMA administration on rat photopic flicker ERG. ERGs were performed 7 days before (baseline recording) and 7 days after MDMA or Saline administration and were elicited by two different light intensities (3.00 and 9.49 cd-s/m$^2$) with a white background. Statistical analysis was performed using the *Wilcoxon test*. (**A, C)** – FFT first and second harmonic amplitudes, respectively. **(B, D)** – FFT first and second harmonic implicit times, respectively. Data is presented as mean±SEM. Twelve animals were used for each group. ** $\rho<0.01$ – Comparing with baseline for MDMA group.

### *3.1.4. Effect of MDMA administration on glial reactivity*

Glial reactivity was also analyzed in order to evaluate the MDMA effect on glial cells. The expression of glial fibrillary acidic protein (GFAP), an intermediate filament protein, that is used to identify astrocytes and Müller cells, and the expression of vimentin, which is used as a marker for Müller cells, were analyzed by Western blot and immunohistochemistry in retinal slices. Although a slight increase in GFAP immunoreactivity in MDMA group was observed, statistical significance was not reached (Figure 24A, 25A and 25B). Similarly, no significant differences were observed between MDMA and Saline groups for vimentin immunoreactivity by Western blotting. However, by immunohistochemistry, a significant increase in vimentin immunoreactivity was detected in the retina of MDMA-injected animals (Figure 24B, 25C and 25D).

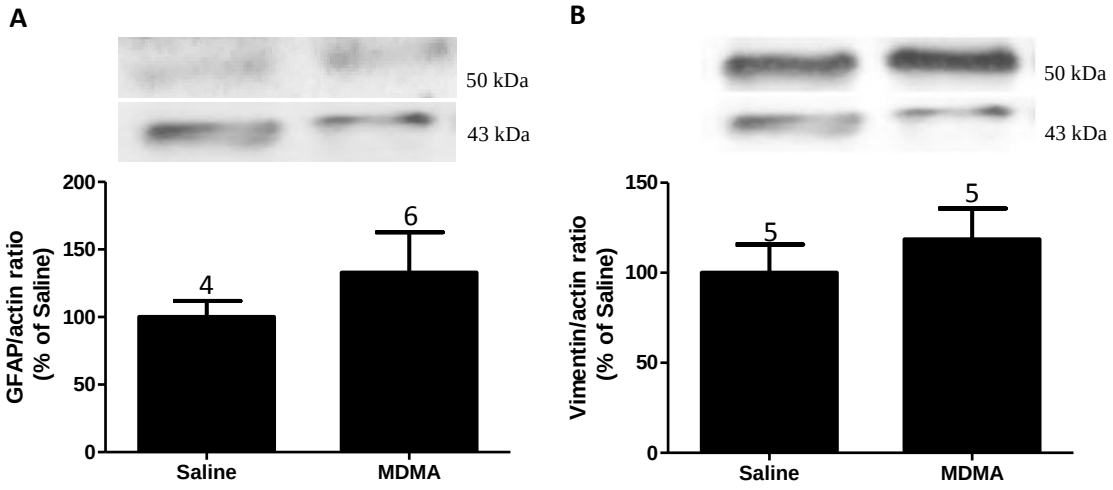


**Figure 24** – Effect of MDMA on the protein levels of GFAP **(A)** and vimentin **(B)**. Total number of retinal extracts of Saline- and MDMA-injected animals is presented above each graphic bar. The densitometric measurements were performed and the ratio between GFAP or vimentin and β-actin immunoreactivities was calculated. Statistical analysis was performed using *Mann Whitney test*. Data is presented as mean±SEM.

The effect of MDMA on Cd11-b (used as a microglia marker) protein expression was analyzed by immunohistochemistry in whole-mounted retinas and in retinal slices. From each retinal slice three random pictures were acquired and densitometric measurements were performed. No evident differences were observed between the two groups relatively to Cd11-b immunoreactivity (Figures 25E, 25F and 26).

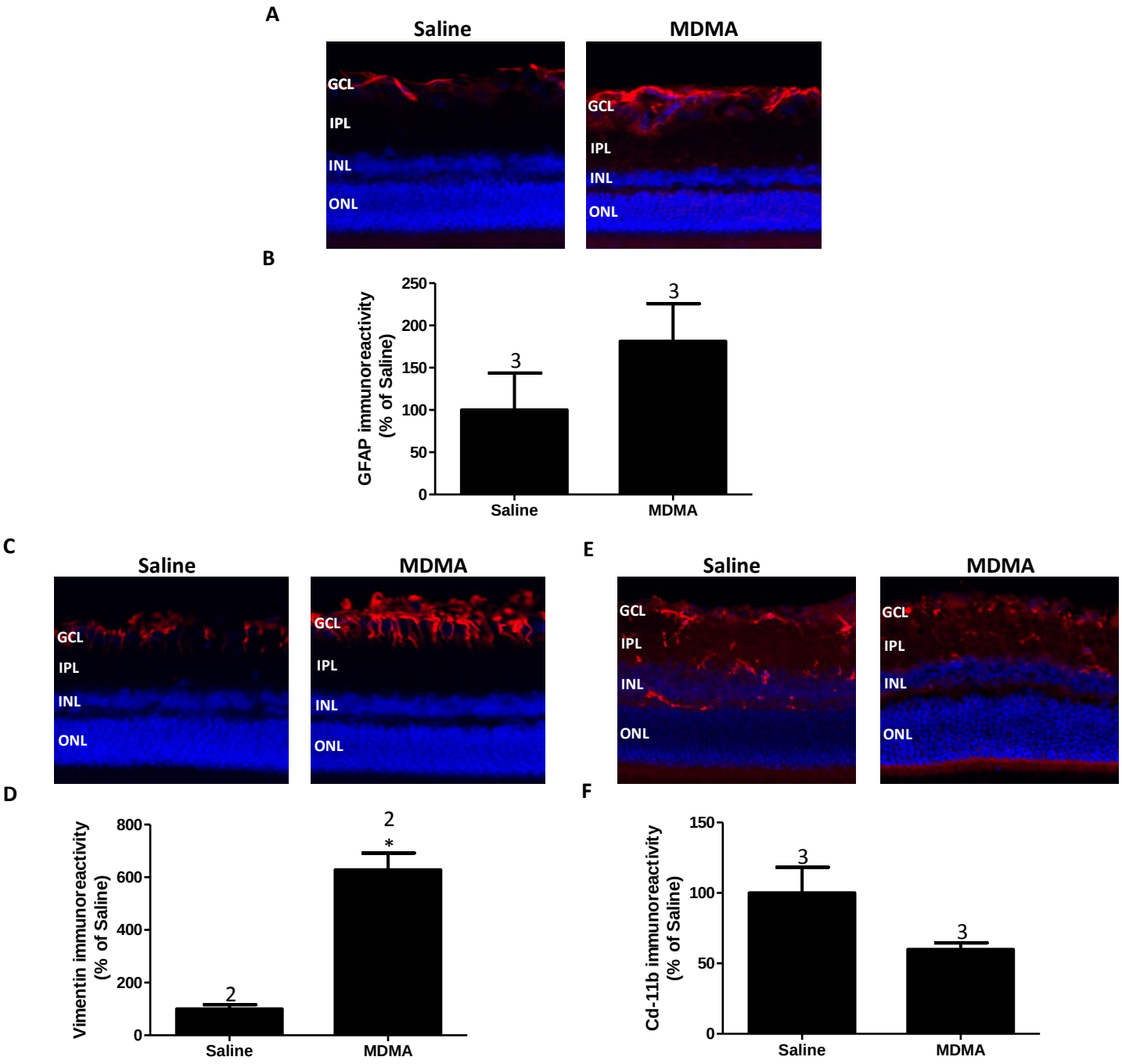


**Figure 25** – Effect of MDMA on glial reactivity in the retina. The immunoreactivity of GFAP, vimentin and Cd11-b was analyzed in retinal slices. The total number of animals used is presented above each graphic bar. Densitometric measurements were performed using ImageJ and statistical significance was analyzed using *Mann Whitney test*. The average pixel gray values were expressed as percentage of control. **(A, C, E)** – Representative images of GFAP, vimentin and Cd11-b immunoreactivity, respectively, for both MDMA and Saline groups. **(B, D, F)** – Quantification of GFAP, vimentin and Cd11-b immunoreactivity, respectively. Data is presented as mean±SEM. GCL, ganglion cell layer; IPL, inner plexiform layer; INL, inner nuclear layer; ONL, outer nuclear layer.

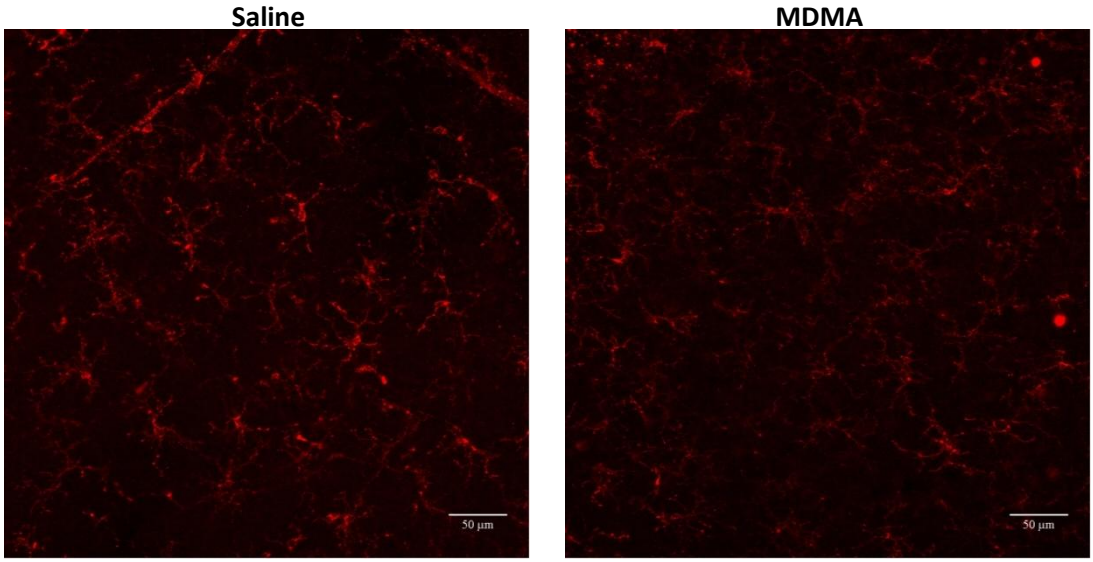


**Figure 26** – Effect of a single MDMA injection on Cd11-b immunoreactivity in whole-mounted retinas. Cd11-b immunoreactivity was analyzed 7 days after Saline or MDMA injection. For each retina, five random images were acquired. Four animals were used for each group.

### *3.2. Protocol 2*

In this protocol, nine animals received an intraperitoneal injection of MDMA (5 mg/kg) or Saline during seven consecutive days. ERG recordings were performed 7 days before MDMA or Saline administration (baseline record), and 24 h and 7 days after treatment. For both groups, the mean value of each ERG parameter was determined and the influence of MDMA or Saline administration was analyzed using *Friedman test*. Each time point was also compared with the others, in other words, 24 h and 7 days time point values were compared with baseline values, and 7 days time point was compared with 24 h time point, using *Wilcoxon test*. The effects of MDMA administration on glial reactivity were also analyzed 7 days after the last injection.

### *3.2.1. Effect of repeated MDMA administration on rat scotopic ERG*

Scotopic ERG was performed in dark adapted animals and elicited by seven light stimuli with intensities ranging from 0.0095 to 9.49 cd-s/$m^2$ (Figure 27). From each recording, a-wave, b-wave and four oscillatory potentials (OPs) were analyzed. Similarly to Protocol 1, a-wave amplitude was only detectable for luminance values higher than 0.03 cd-s/$m^2$, and its amplitude increased with luminance increase.

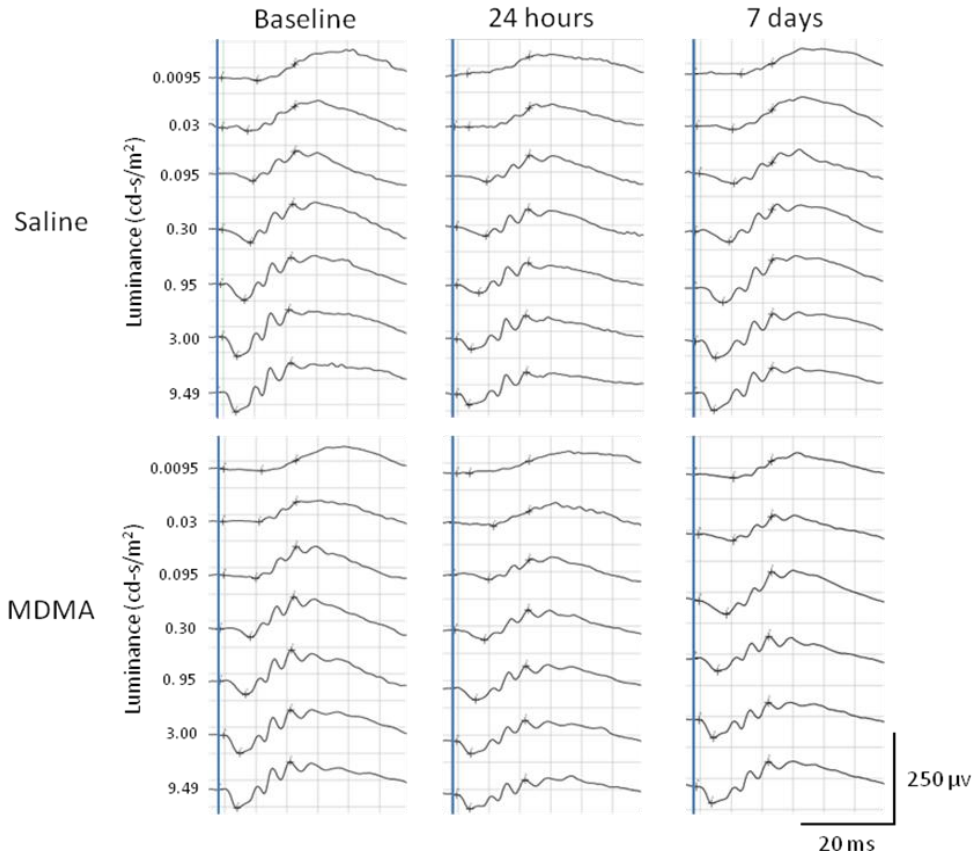


**Figure 27** – Representative ERG recordings of scotopic luminance response test for Saline- (n = 9) and MDMA-injected animals (n = 9). ERGs were performed 7 days before (baseline recording) MDMA or Saline intraperitoneal injection and 24 h and 7 days after treatment. Waveforms were elicited by seven light stimuli with intensities ranging from 0.0095 to 9.49 cd-s/$m^2$. Each trace represents the average of three responses to light stimulus of the same intensity. Solid blue vertical line indicates the light stimulus onset.

For a-wave amplitude, significant differences were detected for both MDMA and Saline groups between the three time points ($p < 0.001$ in both groups). Comparing the time points with each other in pairs of two it was notice that a-wave amplitude decreased significantly in both groups at 24h time point comparing to baseline ($p < 0.001$ in both groups), and that 7 days time point values were significantly increased when compared to 24 h time point values ($p < 0.001$ and $p < 0.05$ in MDMA and Saline group,

respectively). Significant differences were also observed between 7 days time point and baseline for Saline group ($p < 0.05$) (Figure 28A). The a-wave implicit time was significantly decreased at 7 days time point when compared to baseline for MDMA group (Figure 28B).

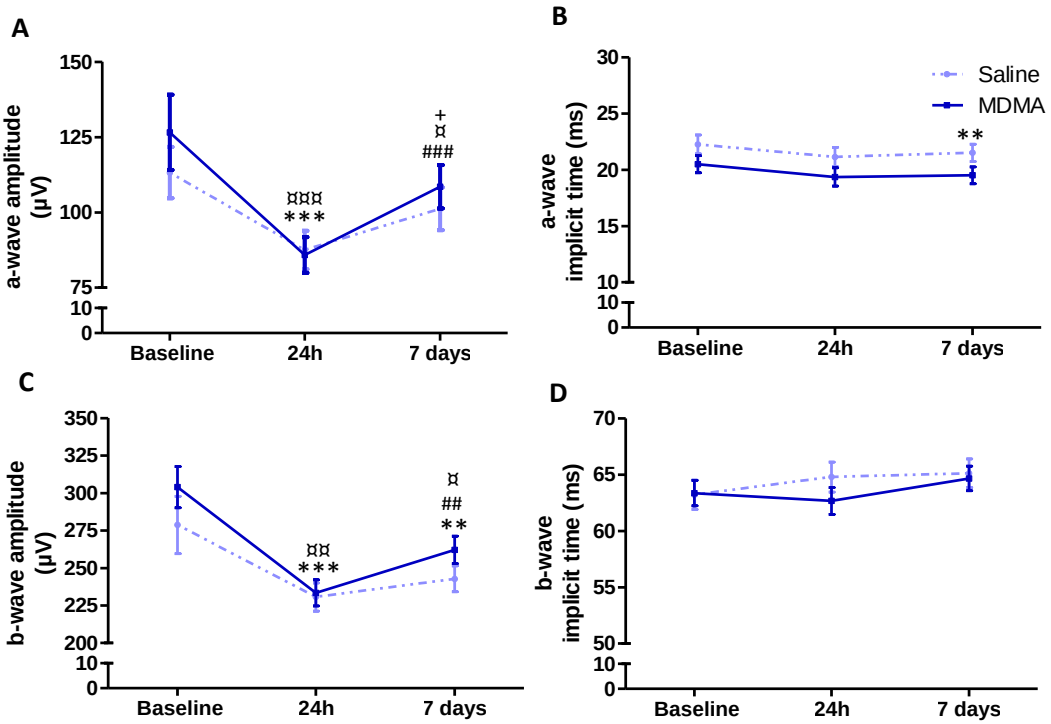


**Figure 28** – Effect of repeated MDMA administration on rat scotopic a-wave and b-wave. The ERGs were recorded 7 days before (baseline recording), and 24 h and 7 days after Saline or MDMA administration. Waveforms were elicited by seven different light intensities (0.0095 – 9.49 cd-s/m$^2$). Data were analyzed using *Friedman test* followed by *Wilcoxon test*. **(A, B) –** Scotopic a-wave amplitude and implicit time, respectively. **(C, D)** – Scotopic b-wave amplitude and implicit time, respectively. Data is presented as mean±SEM. ** $\rho<0.01$, *** $\rho<0.001$ – Comparing with baseline for MDMA group; ## $\rho<0.01$, ### $\rho<0.001$ – Comparing with 24 h time point for MDMA group; ¤ $\rho<0.05$, ¤¤ $\rho<0.01$, ¤¤¤ $\rho<0.001$ – Comparing with baseline for Saline group; + $\rho<0.05$ – Comparing with 24 h time point for Saline group.

Regarding b-wave amplitude, in MDMA group significant differences were detected between the three time points ($p < 0.001$). The b-wave amplitude values decreased significantly from baseline to 24 h time point ($p < 0.001$), and an increase from this point to 7 days time point ($p < 0.01$) was noticed. A significant decrease also occurred at 7 days time point when compared to baseline ($p < 0.01$). In Saline group, a significant decrease from baseline to 24 h ($p < 0.01$) and 7 days time points ($p < 0.05$) was detected (Figure 28C). For b-wave implicit time no significant changes were observed (Figure 28D).

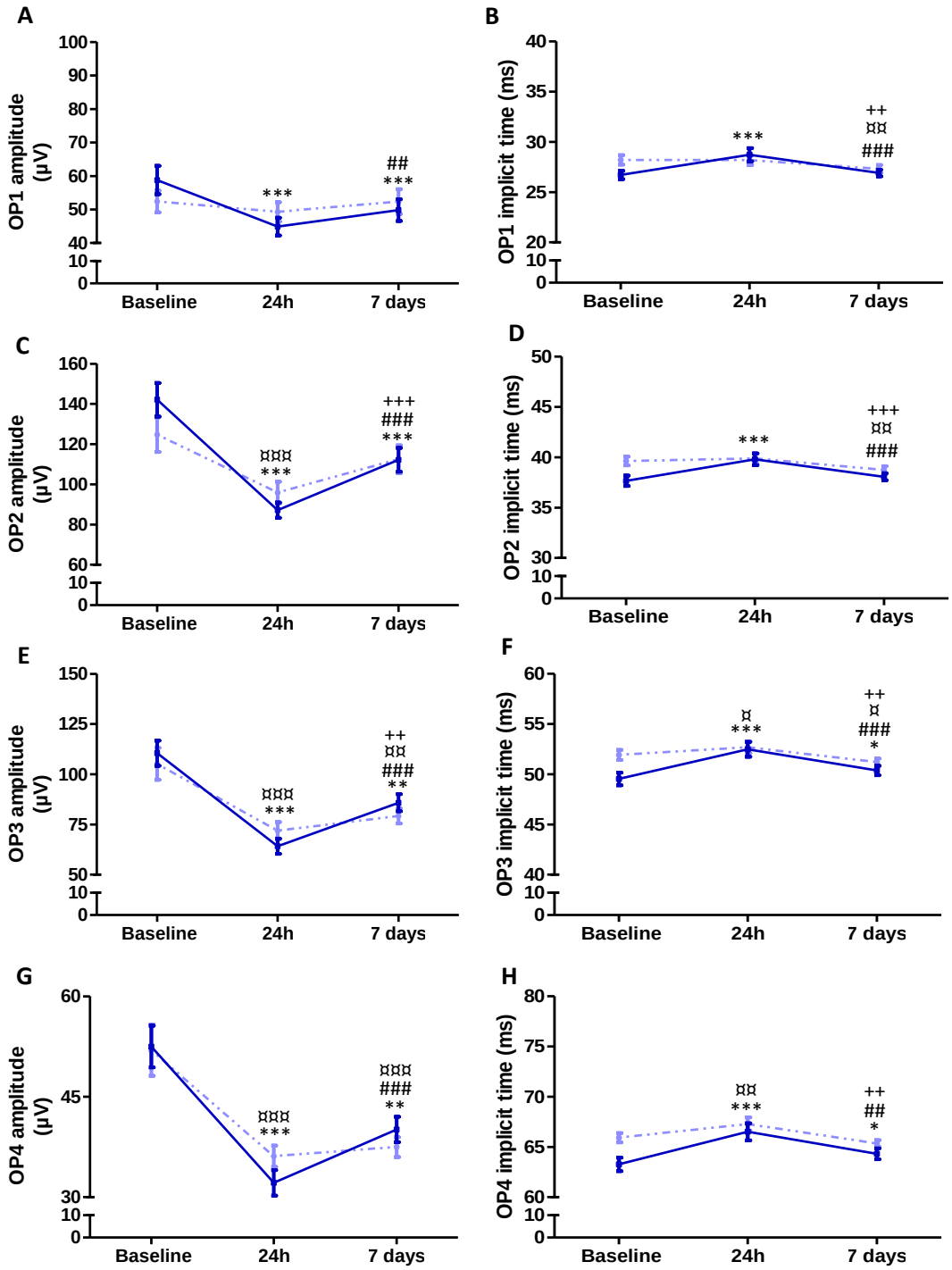


**Figure 29** – MDMA effect on rat scotopic oscillatory potentials (OPs). ERGs were performed 7 days before (baseline recording), and 24 h and 7 days after Saline or MDMA intraperitoneal injection, and were elicited by light stimulus with intensities ranging from 0.0095 to 9.49 cd-s/m$^2$. Data were analyzed with *Friedman test* followed by *Wilcoxon test*. **(A, C, E, G)** – OP1, OP2, OP3 and OP4 amplitudes, respectively. **(B, D, F, H)** – OP1, OP2, OP3 and OP4 implicit times, respectively. Data is presented as mean±SEM. Nine animals for each group were used. * $\rho<0.05$, ** $\rho<0.01$, *** $\rho<0.001$ – Comparing with baseline for MDMA group; ## $\rho<0.01$, ### $\rho<0.001$ – Comparing with 24 h time point for MDMA group; ¤ $\rho<0.05$, ¤¤ $\rho<0.01$, ¤¤¤ $\rho<0.001$ – Comparing with baseline for Saline group; ++ $\rho<0.01$, +++ $\rho<0.001$ – Comparing with 24 h time point for Saline group.

As in the previous protocol, the ratio between b-wave amplitude and a-wave amplitude was determined (Table 4) to analyze the differences in b-wave amplitude relatively to a-wave amplitude. No significant differences were observed for either MDMA or Saline groups.

**Table 4** – b/a ratio for Saline and MDMA groups.

| | **Group** | *Saline* | | | *MDMA* | | |
|---|---|---|---|---|---|---|---|
| | **Time Point** | *Baseline* | *24 h* | *7 days* | *Baseline* | *24 h* | *7 days* |
| **Ratio b/a** | *Mean* | 11.60 | 7.60 | 7.00 | 11.50 | 11.63 | 6.75 |
| | *SEM* | 4.59 | 1.89 | 2.02 | 9.58 | 4.40 | 1.26 |

Regarding the MDMA effect on OPs, it was observed a significant influence in their amplitudes by this drug ($p < 0.001$ for all OPs). However, OP2, OP3 and OP4 amplitudes were also influenced by Saline administration ($p < 0.001$ for all OPs) (Figure 29A, 29C, 29E and 29G). Similar results were observed when each time point was compared with the others in pairs of two (24 h and 7 days time points with baseline; 7 days time point with 24 h time point). In addition, the implicit time of the OPs also showed significant differences between the three time points for both MDMA ($p < 0.001$ for all parameters) and Saline groups ($p < 0.05$ for OP1 and $p < 0.01$ for the remaining OPs) (Figure 29B, 29D, 29F and 29H).

The sum of all OPs amplitude was calculated in Saline and MDMA groups (Table 5). Significant differences were observed overtime ($p < 0.001$ for both groups). Time points were compared with the others in pairs of two and significant differences were observed for all combinations.

**Table 5** – OPs amplitudes for Saline and MDMA groups.

| | **Group** | *Saline* | | | *MDMA* | | |
|---|---|---|---|---|---|---|---|
| | **Time Point** | *Baseline* | *24 h* | *7 days* | *Baseline* | *24 h* | *7 days* |
| **Sum Ops** | *Mean* | 335.60 | 254.50¤¤¤ | 254.54+++¤¤ | 365.11 | 229.87*** | 289.59###** |
| | *SEM* | 22.22 | 12.47 | 15.13 | 20.54 | 10.10 | 9.61 |

** $\rho<0.01$, *** $\rho<0.001$ – Comparing with baseline for MDMA group; ### $\rho<0.001$ – Comparing with 24 h time point for MDMA group; ¤¤ $\rho<0.01$, ¤¤¤ $\rho<0.001$ – Comparing with baseline for Saline group; +++ $\rho<0.001$ – Comparing with 24 h time point for Saline group.

### *3.2.2. Effect of repeated MDMA administration on rat photopic ERG*

#### *3.2.2.1. Light adaptation*

To evaluate the effects of MDMA administration on photopic ERGs, animals were light adapted by eliciting bright white flashes (9.49 cd-s/$m^2$) delivered at 0 min (onset), 2, 4, 8 and 16 min with a white background (25 cd/$m^2$). The representative recordings of light adaptation ERG are illustrated in Figure 30.

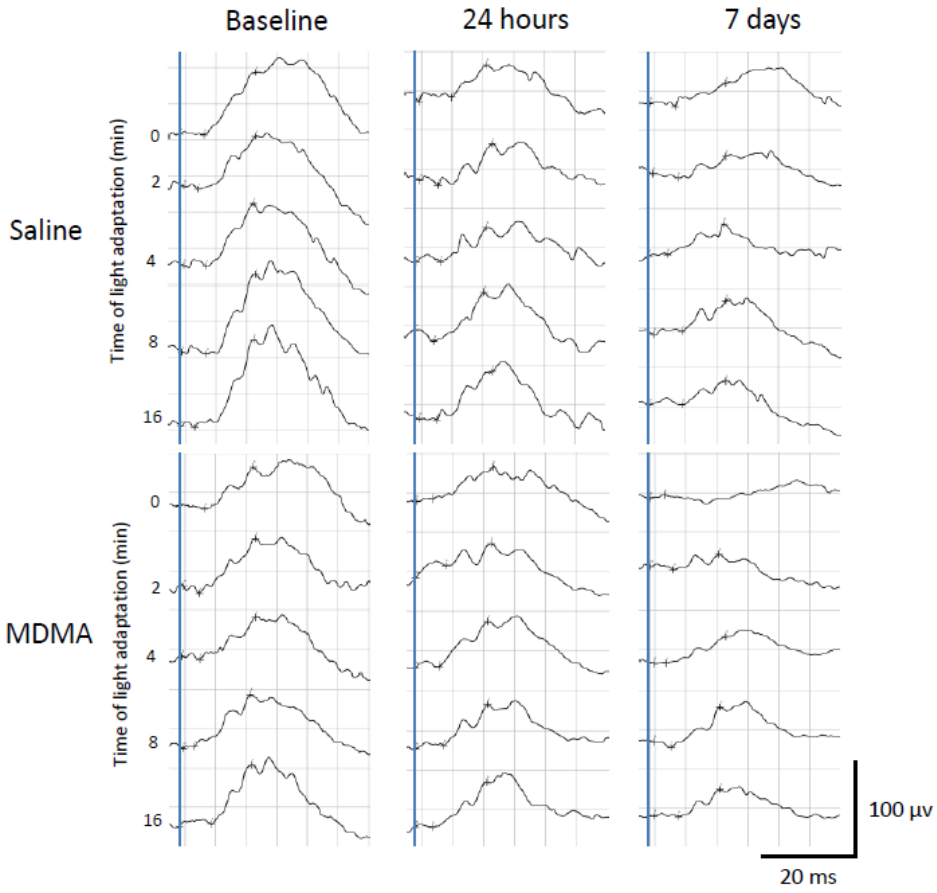


**Figure 30** – Representative recordings of light adaptation ERG recorded at baseline (7 days before treatment), and 24 h and 7 days after Saline or MDMA administration. ERGs were elicited with bright white flashes (9.49 cd-s/$m^2$) delivered at 0 min (onset), 2, 4, 8 and 16 min with a white background (25 cd/$m^2$). Each trace represents an average of three responses to light stimulus of the same intensity. Solid blue vertical line indicates the onset of light stimulus.

From light adaptation ERGs b-wave was extracted and the mean value of all times of adaptation was analyzed. In Saline group, the amplitude of b-wave of light adaptation ERG was significantly decreased at 24 h ($p < 0.05$) and 7 days ($p < 0.01$) time points

when compared to baseline. For MDMA group, a similar profile was observed, but no significant differences were observed. Regarding b-wave implicit time, significant differences were detected for both MDMA and Saline groups ($p < 0.05$ and $p < 0.01$, respectively). For Saline group, 24 h and 7 days time points were significantly increased when compared to baseline ($p < 0.01$ for both groups). In MDMA group, only the 24 h time point was significantly increased when compared to baseline ($p < 0.01$).

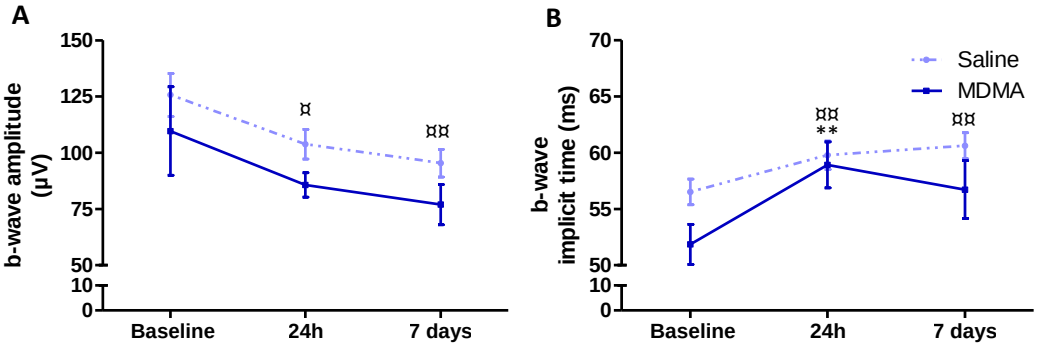


**Figure 31** – Effect of MDMA administration on light adaptation ERG. ERGs were recorded during light adaptation, 7 days before (baseline record), and 24 h and 7 days after Saline or MDMA treatment, and were elicited by bright white flashes (9.49 cd-s/m$^2$) delivered at 0 min (onset), 2, 4, 8 and 16 min with a white background (25 cd/m$^2$). Data were analyzed using *Friedman test* followed by *Wilcoxon test*. **(A, B)** – Light adaptation b-wave amplitude and implicit time, respectively. Data is presented as mean±SEM. Nine animals were used for each group. ** $\rho<0.01$ – Comparing with baseline for MDMA group; ¤ $\rho<0.05$, ¤¤ $\rho<0.01$ – Comparing with baseline for Saline group.

### *3.2.3. Photopic b-wave and oscillatory potentials*

After light adaptation period, photopic ERG was obtained by exposing animals to seven different light intensities (0.0095 to 9.49 cd-s/m$^2$) with a white background (Figure 32). As in the previous protocol, b-wave was only detected for bright light stimuli (3.00 and 9.49 cd-s/m$^2$). MDMA or Saline administration did not affected b-wave amplitude. However, comparing the time points in pairs of two, for Saline group, a significant decrease at 24 h time point when compared to baseline ($p < 0.05$) was observed, and for MDMA group a significant decrease at 7 days time point when compared to baseline ($p < 0.05$) was detected (Figure 33A). For b-wave implicit time no significant differences were observed between the three time points. However, in MDMA group, analyzing the

time points in pairs of two, the implicit time of b-wave at 24 h time point was significantly increased when compared to baseline ($p < 0.05$) (Figure 33B).

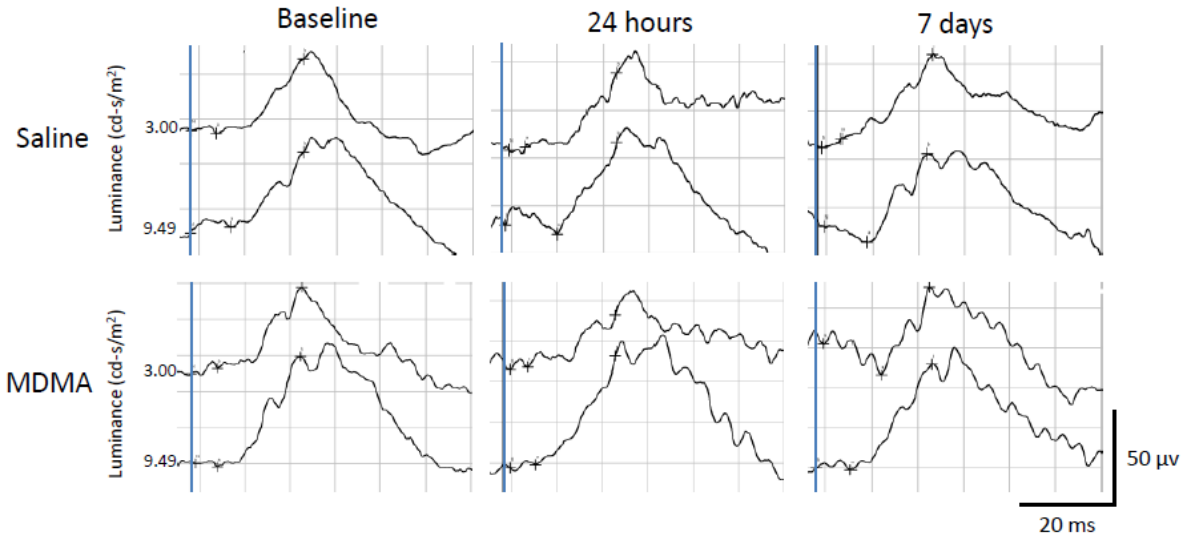


**Figure 32** – Representative recordings of photopic ERGs. Photopic ERGs were performed after light adaptation 7 days before (baseline recording), and 24 h and 7 days after Saline and MDMA administration, and were elicited by seven different light intensities (0.0095 to 9.49 cd-s/$m^2$) with a white background. Responses to bright light flashes with intensities of 3.00 and 9.49 cd-s/$m^2$ are presented. An average of three responses to light stimulus with the same intensity is represented in each trace. The onset of light stimulus is represented by the solid blue vertical line. Nine animals were used for each group.

From photopic ERG, three oscillatory potentials (OPs) were extracted and the amplitudes and implicit times were analyzed. Comparing the three time points, no significant differences were noticed for OP2 amplitude, but a significant decrease was found between 7 days time point and baseline for MDMA group ($p < 0.05$) (Figure 34A).

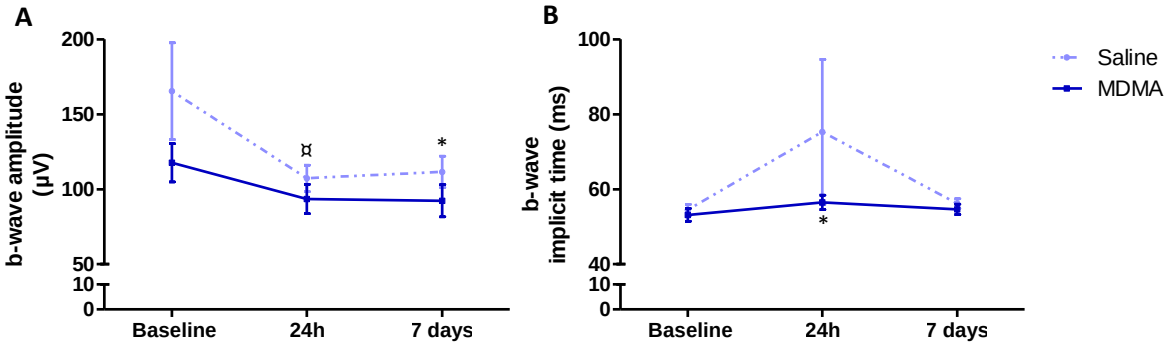


**Figure 33** – Effect of MDMA on rat photopic b-wave amplitude **(A)** and b-wave implicit time **(B)**. Photopic ERGs were performed 7 days before (baseline recording), and 24 h and 7 days after Saline or MDMA administration, and were elicited by seven different light intensities (0.0095 to 9.49 cd-s/$m^2$) with a white background. Only the responses to bright light flashes (3.00 and 9.49 cd-s/$m^2$) were analyzed using *Friedman test* followed by *Wilcoxon test*. Data is presented as mean±SEM (n = 9 for each group). * $\rho<0.05$ – Comparing with baseline for MDMA group; ¤ $\rho<0.05$ – Comparing with baseline for Saline group.

MDMA or Saline did not significantly influence OP2 implicit time overtime (Figure 34B). However, 24 h time point was significantly increased when compared to baseline ($p < 0.05$), but only for Saline group. In OP3 amplitude no significant differences were observed (Figure 34C). The implicit time also did not show significant changes between the three time points. However, analyzing the time points in pairs of two it was noticed that 24 h and 7 days time points were significantly increased when compared to baseline values ($p < 0.05$ for both), but only for MDMA group (Figure 34D). OP4 amplitude revealed significant differences overtime for MDMA group. A significant decrease was observed between baseline and 24 h time point ($p < 0.05$). A significant increase was detected at 7 days time point when compared to 24 h time point ($p < 0.05$), but no significant differences were observed between 7 days time point and baseline (Figure 34E). MDMA significantly affected OP4 implicit time. A significant increase at 24 h time point compared to baseline ($p < 0.05$) was noticed (Figure 34F).

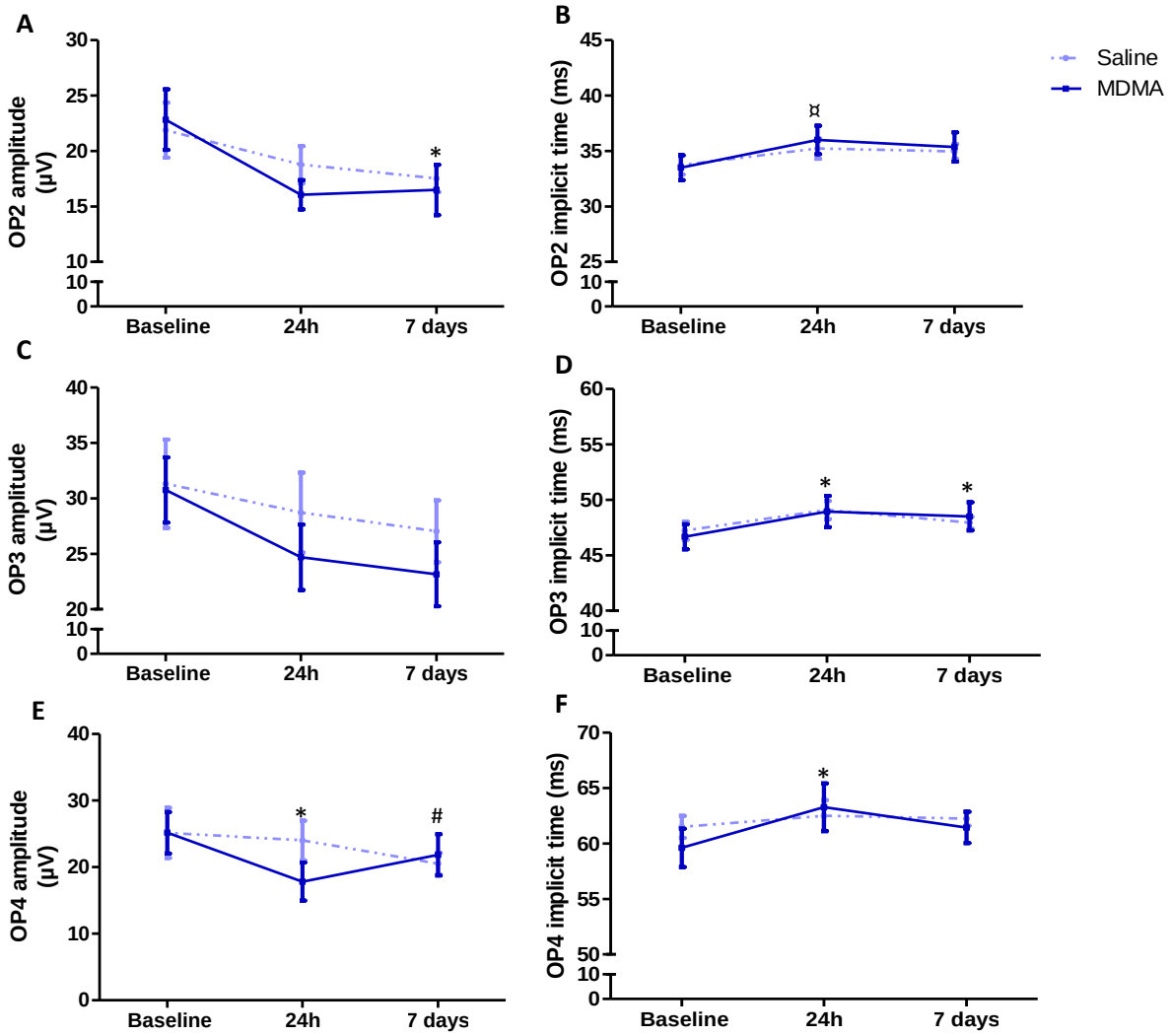


**Figure 34** – Effect of MDMA on photopic oscillatory potentials (OPs). ERGs were recorded 7 days before (baseline recording), and 24 h and 7 days after Saline or MDMA administration, and were elicited by seven different light intensities (0.0095 to 9.49 cd-s/m$^2$) with a white background. Data was analyzed using *Friedman test* followed by *Wilcoxon test*. **(A, C, E)** – Photopic OP2, OP3 and OP4 amplitudes respectively. **(B, D, F)** – Photopic OP1, OP2, OP3 and OP4 implicit times, respectively. Data is presented as mean±SEM (n = 9 for each group). * $\rho<0.05$ – Comparing with baseline for MDMA group; # $\rho<0.05$ – Comparing with 24 h time point for MDMA group; ¤ $\rho<0.05$ – Comparing with baseline for Saline group.

The sum of photopic oscillatory potentials was calculated (Table 6), but no significant differences were observed in both groups for this parameter.

**Table 6** – Photopic OPs amplitudes for Saline and MDMA groups.

| | **Group** | *Saline* | | | *MDMA* | | |
|---|---|---|---|---|---|---|---|
| | **Time Point** | *Baseline* | *24 h* | *7 days* | *Baseline* | *24 h* | *7 days* |
| **Sum Ops** | *Mean* | 78.35 | 59.91 | 64.22 | 72.39 | 57.28 | 57.59 |
| | *SEM* | 9.97 | 7.91 | 4.27 | 8.52 | 7.68 | 9.61 |

### *3.2.4. Effect of repeated MDMA administration on rat photopic flicker ERG*

Photopic flicker responses allowed gather information about pure cone responses (Figure 35). FFT first and second harmonic amplitude and implicit time values were analyzed. For first harmonic amplitude no significant changes were found between the three time points. However, the amplitude at baseline was significantly higher than the amplitude at 24 h ($p < 0.01$) and 7 days ($p < 0.05$) time points for both MDMA and Saline groups (Figure 36A). First harmonic implicit time was significantly different in both groups overtime ($p < 0.05$ in both groups). Comparing the time points in groups of two it was noticed that 24 h time point was significantly increased compared to baseline for Saline group ($p < 0.05$). MDMA group also showed a significant increase from baseline to both 24 h ($p < 0.01$) and 7 days ($p < 0.01$) time points (Figure 36B). Differences for MDMA and Saline groups were also found in the second harmonic amplitude between the three time points ($p < 0.05$ for both groups). Analyzing time points in pairs of two, for MDMA and Saline groups a significant decrease was observed between baseline and both 24 h ($p < 0.01$ and $p < 0.05$, respectively) and 7 days ($p < 0.05$ and $p < 0.01$, respectively) time points (Figure 36C).

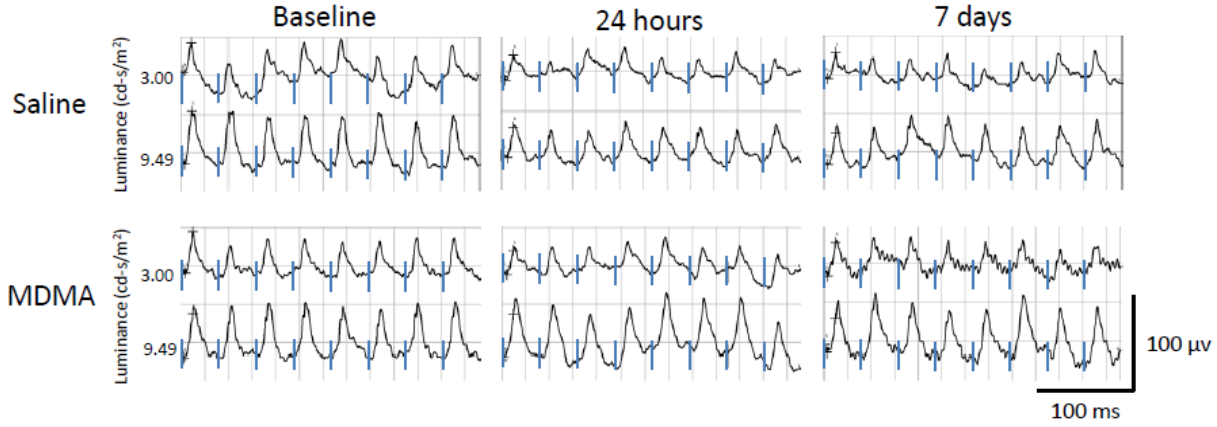


**Figure 35** – Representative recordings of photopic flicker ERG. ERGs were performed 7 days before treatment (baseline), and 24 h and 7 days after Saline or MDMA administration, and were elicited by different light intensities (3.00 and 9.49 cd-s/$m^2$) with a white background. Each trace represents an average of ten responses to light stimulus with the same intensity. Solid blue vertical lines indicate the onset of light stimulus. Nine animals were used for each group.

Second harmonic implicit time revealed a significant increase at 24 h time point when compared to baseline, for Saline group ($p < 0.05$). For MDMA group, 7 days time point was significantly increased when compared to baseline ($p < 0.05$). However, no significant differences were found for both groups overtime (Figure 36D).

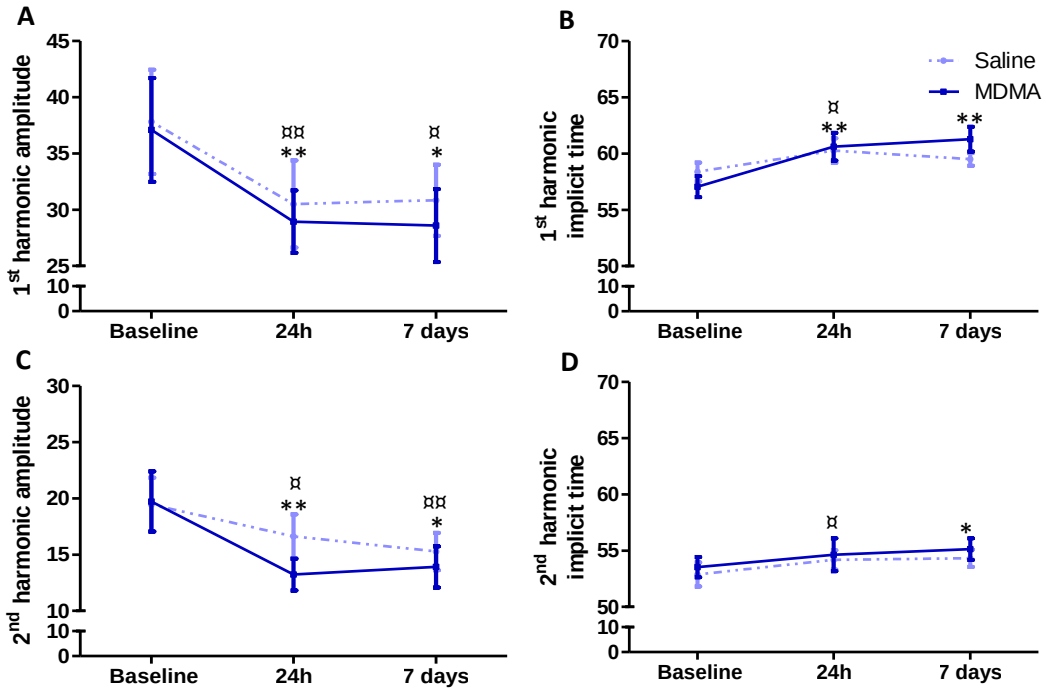


**Figure 36** – Effect of repeated MDMA administration on rat photopic flicker ERG. ERGs were recorded 7 days before (baseline recording), and 24 h and 7 days after Saline or MDMA treatment. Animals were exposed to two different light intensities (3.00 and 9.49 cd-s/$m^2$) with a white background. Data was analyzed using *Friedman test* followed by *Wilcoxon test*. **(A, C)** – First harmonic amplitude and implicit time, respectively. **(B, D) –** Second harmonic amplitude and implicit time, respectively. Data is presented as mean±SEM. Nine animals were used for each group. * $\rho<0.05$, ** $\rho<0.01$ – Comparing with baseline for MDMA group; ¤ $\rho<0.05$, ¤¤ $\rho<0.01$ – Comparing with baseline for Saline group.

### *3.2.6. Effect of repeated MDMA administration on glial reactivity*

The MDMA effects on glial reactivity in the retina were analyzed 7 days after the last MDMA injection. The GFAP and vimentin protein content (immunoreactivity) was determined by Western blot and by immunohistochemistry in retinal slices. The results show no significant differences in GFAP immunoreactivity between MDMA and Saline groups (Figures 37A, 38A and 38B). MDMA also did not affect vimentin protein content in the retina (Figures 37B, 38C and 38D).

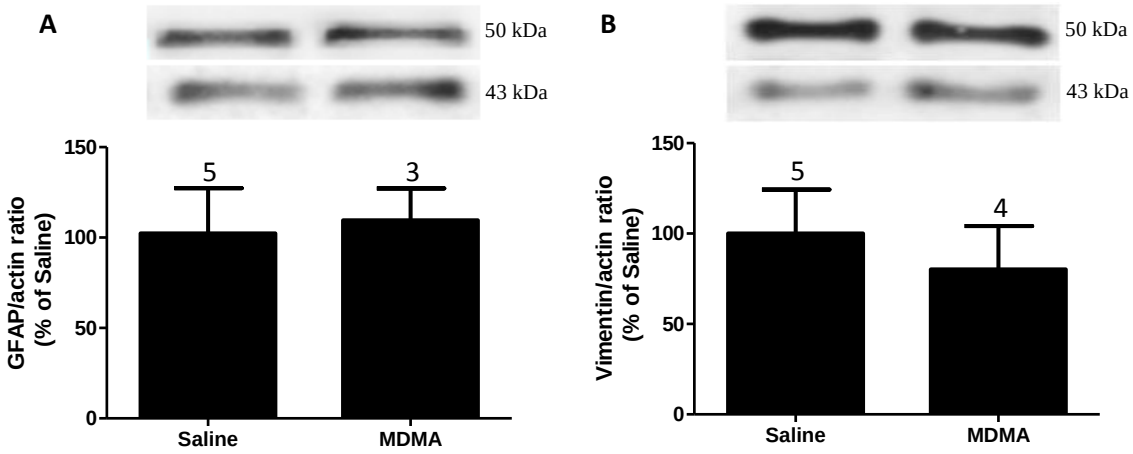


**Figure 37** – Effect of repeated MDMA administration on GFAP **(A)** and vimentin **(B)** immunoreactivity, as assessed by Western blotting. The densitometric measurements of the bands were performed and the ratio between GFAP or vimentin and β-actin immunoreactivities was calculated. Statistical analysis was performed using *Mann Whitney test*. Total retinal extracts of each group is presented above each graphic bar. Data is presented as mean±SEM.

The effects of MDMA on Cd11-b immunoreactivity was assessed in whole-mounted retinas and in retinal slices. No significant differences were observed between MDMA and Saline groups neither with a qualitative analysis (Figures 38E and 39) nor with a quantitative analysis (Figure 38F).

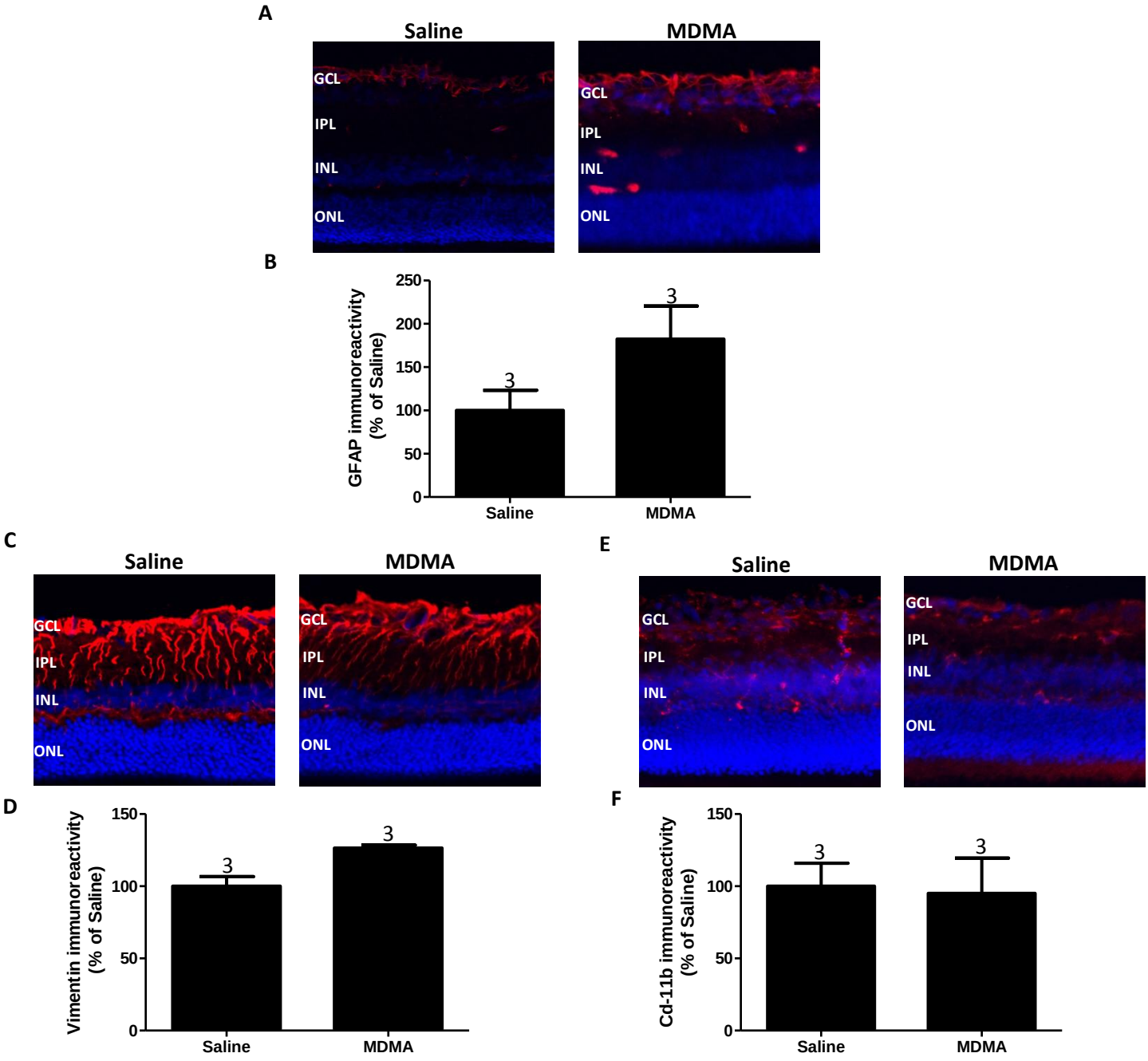


**Figure 38** – Effect of repeated MDMA administration on GFAP, vimentin and Cd11-b immunoreactivity in retinal slices. A densitometry analysis was performed and data was analyzed using *Mann Whitney test*. Above each graphical bar is represented the total number of animals used. **(A, C, E)** – Representative images of GFAP, vimentin and Cd11-b immunoreactivity, respectively, for both MDMA and Saline groups. **(B, D, F)** – Quantification of GFAP, vimentin and Cd11-b immunoreactivity, respectively. Data is presented as mean±SEM. GCL, ganglion cell layer; IPL, inner plexiform layer; INL, inner nuclear layer; ONL, outer nuclear layer.

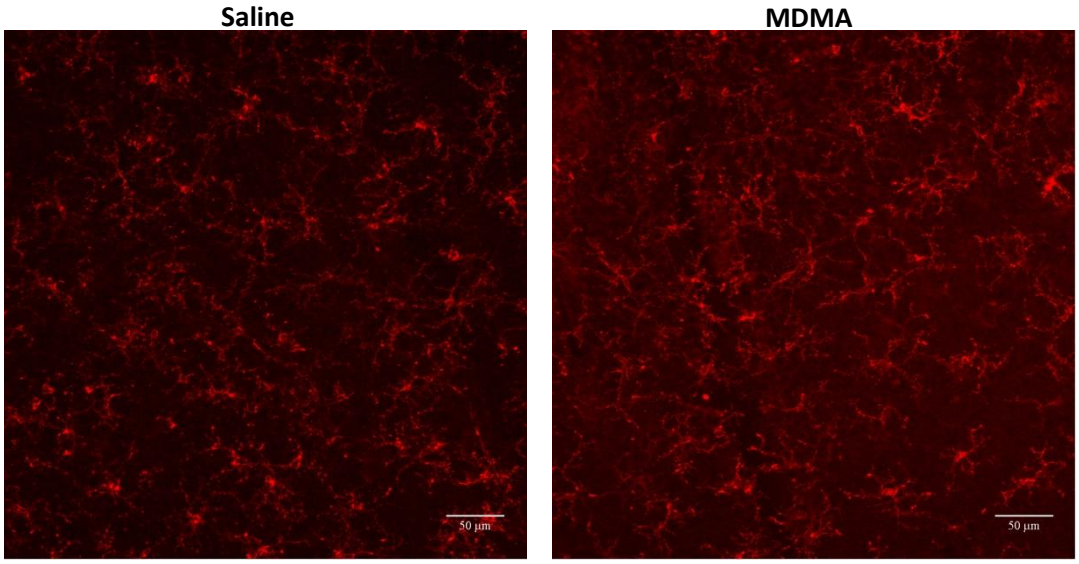


**Figure 39** – Effect of repeated MDMA administration on Cd11-b immunoreactivity in whole-mount retinas. For each retina from Saline- (n=4) or MDMA-injected (n=4) animals, five random pictures were acquired.

### *3.3. Protocol 3*

In Protocol 3, animals received an intraperitoneal injection of MDMA (5 mg/kg) or Saline, once a day, twice a week, at two consecutive days, during four weeks (in a total of 10 injections). ERGs were performed in 8 animals (4 per group, which had been selected randomly), 7 days before starting treatment (baseline recording), and 24 h and 7 days after the last Saline or MDMA administration. Statistical analysis was performed as described in Protocol 2. The effects of MDMA administration on glial reactivity were also analyzed.

#### *3.3.1. Effect of sporadic MDMA administration on rat scotopic ERG*

Scotopic ERGs were elicited by light stimuli with intensities ranging from 0.0095 to 9.49 cd-s/$m^2$ (Figure 40). For a-wave amplitude, significant differences were found overtime in Saline group ($p < 0.01$). A significant increase was noticed at 7 days time point when compared to baseline ($p < 0.05$) and 24 h ($p < 0.01$) time point. Comparing the time points in pairs of two, in MDMA group there was a significant increase at 7 days time point ($p < 0.01$) when compared to baseline (Figure 41A). Despite a-wave implicit time did not present significant differences between the three time points, for both groups, in MDMA group there was a significant decrease at 7 days time point ($p < 0.05$) when compared to baseline (Figure 41B). Regarding b-wave amplitude,

significant differences were found in Saline group between the three time points ($p < 0.01$). The amplitude at 7 days time point was significantly higher than at 24 h time point ($p < 0.001$). In MDMA group, a significant decrease was observed between baseline and 24 h time point ($p < 0.01$) (Figure 41C). For b-wave implicit time, only Saline group showed significant differences overtime ($p < 0.01$). However, in both groups the implicit time was significant lower at 24 h and 7 days time points than in baseline ($p < 0.01$ and $p < 0.05$ for Saline and MDMA group, respectively) (Figure 41D).

For this protocol, a small number of animals was tested, resulting in a high data variability. Due to this variability, almost all data obtained from OPs was eliminated, after exclusion of the values that were not included in the interval mean ± 3 standard deviations, thus not allowing the statistical analysis of these parameters to be performed.

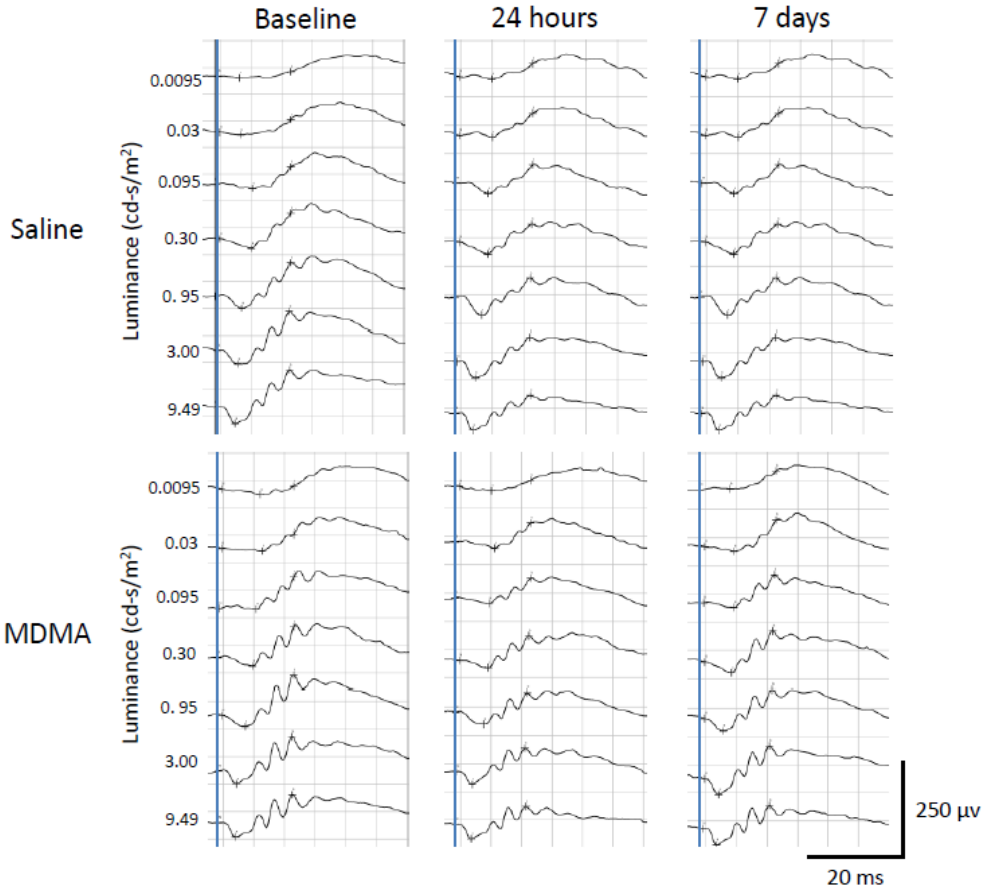


**Figure 40** – Representative recordings of rat scotopic ERGs. ERGs were recorded 7 days before (baseline), and 24 h and 7 days after the last Saline or MDMA intraperitoneal injection. Waveforms were elicited by light stimuli with intensities ranging from 0.0095 to 9.49 cd-s/$m^2$. Each trace represents the average of three responses to light stimulus of the same intensity. Solid blue vertical line indicates the light stimulus onset. Four animals were used for each group.

As in the previous protocols, the ratio between b-wave and a-wave amplitude was calculated (Table 7) to determine the MDMA effect on b-wave amplitude relatively to a-wave amplitude. No significant changes were observed for both MDMA and Saline groups.

**Table 7 –** b/a ratio for Saline and MDMA.

| | **Group** | *Saline* | | | *MDMA* | | |
|---|---|---|---|---|---|---|---|
| | **Time Point** | *Baseline* | *24 h* | *7 days* | *Baseline* | *24 h* | *7 days* |
| **Ratio b/a** | *Mean* | 13.86 | 12.86 | 7.86 | 11.38 | 13.25 | 12.50 |
| | *SEM* | 5.63 | 6.82 | 2.47 | 4.40 | 5.44 | 6.15 |

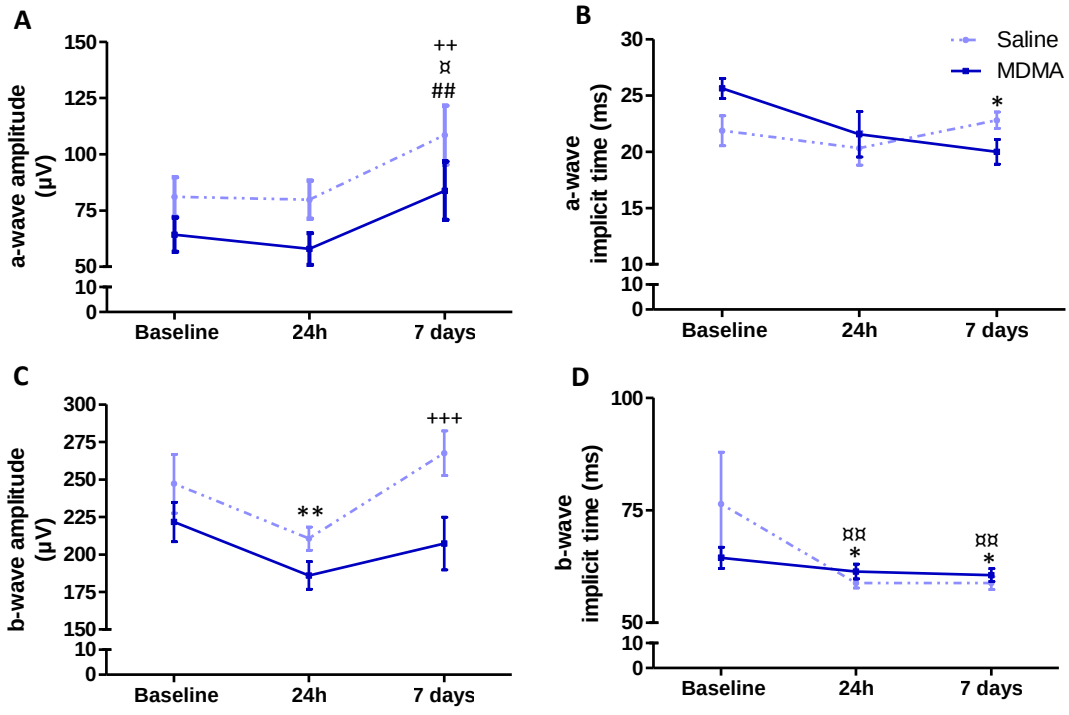


**Figure 41** – Effect of MDMA administration on rat scotopic a-wave and b-wave. The ERGs were elicited by seven different light intensities ranging from 0.0095 to 9.49 cd-s/m$^2$ and were recorded 7 days before (baseline recording), and 24 h and 7 days after the last Saline or MDMA intraperitoneal injection. Data was analyzed using *Friedman test* followed by *Wilcoxon test*. **(A, C)** – Scotopic a-wave amplitude and implicit time, respectively. **(B, C)** – Scotopic b-wave amplitude and implicit time, respectively. Data is presented as mean±SEM (n = 4 for each group). * $\rho<0.05$, ** $\rho<0.01$ – Comparing with baseline for MDMA group; ## $\rho<0.01$ – Comparing with 24 h time point for MDMA group; ¤ $\rho<0.05$, ¤¤ $\rho<0.01$ – Comparing with baseline for Saline group; ++ $\rho<0.01$, +++ $\rho<0.001$ – Comparing with 24 h time point for Saline group.

### *3.3.2. Effect of sporadic MDMA administration on rat photopic ERG*

#### *3.3.2.1. Light adaptation*

Animals were light adapted in order to evaluate MDMA effects on photopic ERG. During light adaptation period, ERGs were recorded and b-wave was analyzed (Figure 42).

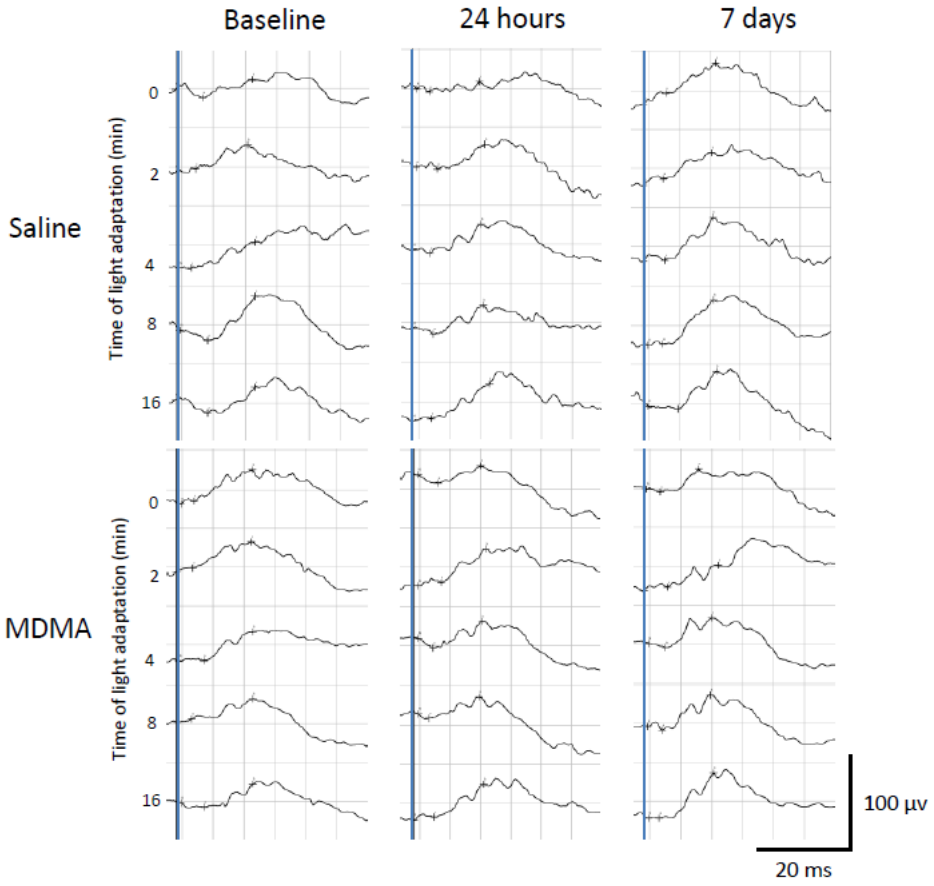


**Figure 42** – Representative recordings of light adaptation ERGs performed 7 days before treatment (baseline), and 24 h and 7 days after the last Saline or MDMA administration. ERGs were elicited by bright white flashes (9.49 cd-s/m$^2$) delivered at 0 min (onset), 2, 4, 8 and 16 min with a white background light (25 cd/m$^2$). An average of three responses to light stimuli of the same intensity is represented in each trace. Solid blue vertical lines indicate the light stimulus onset. Four animals were used in each group.

From light adaptation ERGs, b-wave was extracted and the mean value of all times of adaptation was analyzed. In the Saline group, the b-wave amplitude was significantly increased at 7 days time point compared to 24 h time point ($p < 0.01$). In the MDMA group, the amplitude of b-wave was significantly higher at 7 days time point compared

to baseline ($p < 0.05$) and 24 h time point ($p < 0.01$) (Figure 43A). For b-wave implicit time no significant differences were observed (Figure 43B).

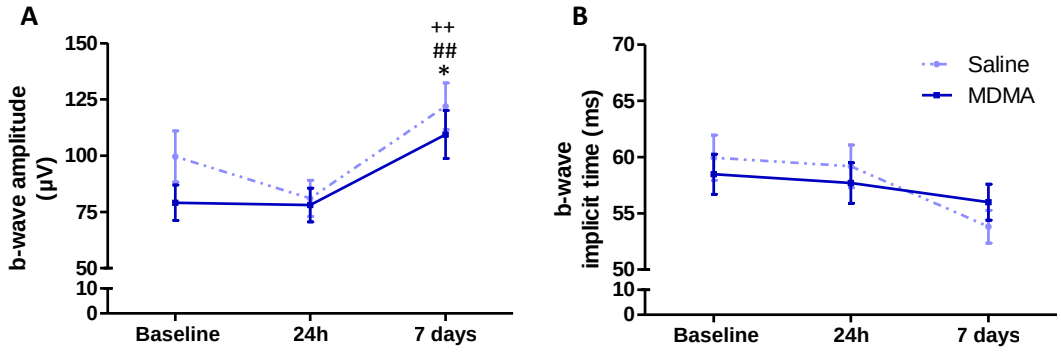


**Figure 43**– Effect of sporadic MDMA administration on light adaptation b-wave amplitude (**A**) and implicit time (**B**). ERGs were recorded during light adaptation, 7 days before (baseline record), and 24 h and 7 days after treatment, and were elicited by bright white flashes (9.49 cd-s/m$^2$) delivered at 0 min (onset), 2, 4, 8 and 16 min with a white background (25 cd/m$^2$). Data were analyzed using *Friedman test* followed by *Wilcoxon test*. Data is presented as mean±SEM (n = 4 per group). * $\rho<0.05$ – Comparing with baseline for MDMA group; ## $\rho<0.01$ – Comparing with 24 h time point for MDMA group; ++ $\rho<0.01$ – Comparing with 24 h time point for Saline group.

### *3.3.2.2. Photopic b-wave*

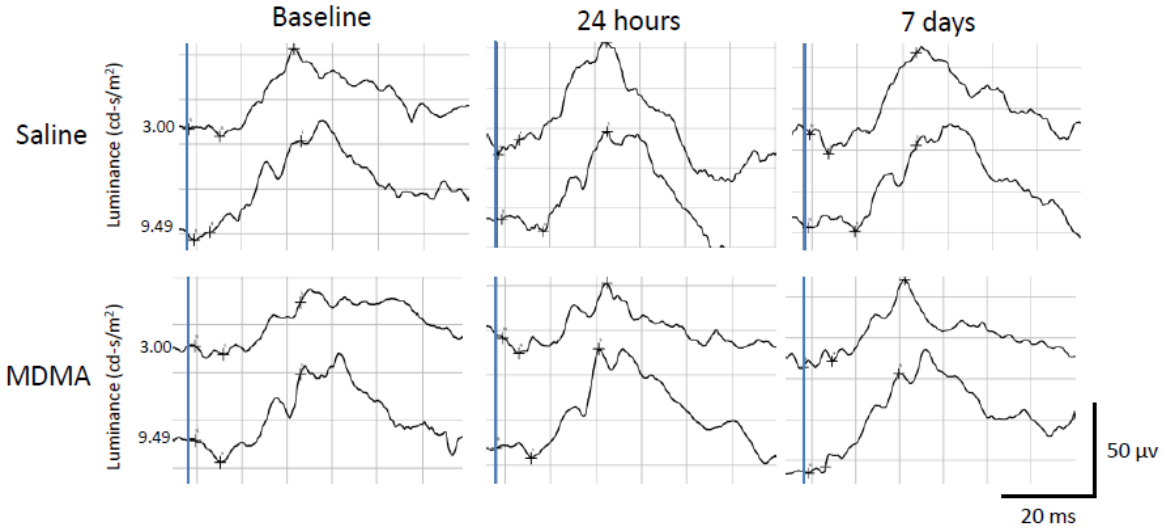


**Figure 44** – Representative recordings of rat photopic ERGs. ERGs were performed 7 days before (baseline recording), and 24 h and 7 days after sporadic MDMA or Saline administration and were elicited by seven different light intensities (0.0095 to 9.49 cd-s/m$^2$) with a white background. The responses to bright light flashes (3.00 and 9.49 cd-s/m$^2$) are presented. Each trace represents an average of three responses to light stimuli with the same intensity. Solid blue vertical lines represent the onset of light stimulus. (n = 4 for each group).

Photopic ERGs were performed after light adaptation and were elicited by seven different light intensities (0.0095 to 9.49 cd-s/$m^2$) with a white background (Figure 44). The b-wave amplitude was only observed for the bright light stimuli with luminances of 3.00 and 9.49 cd-s/$m^2$. For b-wave amplitude, no significant differences were observed overtime. However, in MDMA group, at 24 h time point, the amplitude was significantly decreased when compared to baseline ($p < 0.05$) (Figure 45A). Both MDMA and Saline groups did not show significant differences in b-wave implicit time (Figure 45B).

For the same reason presented before, regarding the scotopic OPs analysis, the analysis of the amplitude and implicit times of photopic oscillatory potentials was not performed.

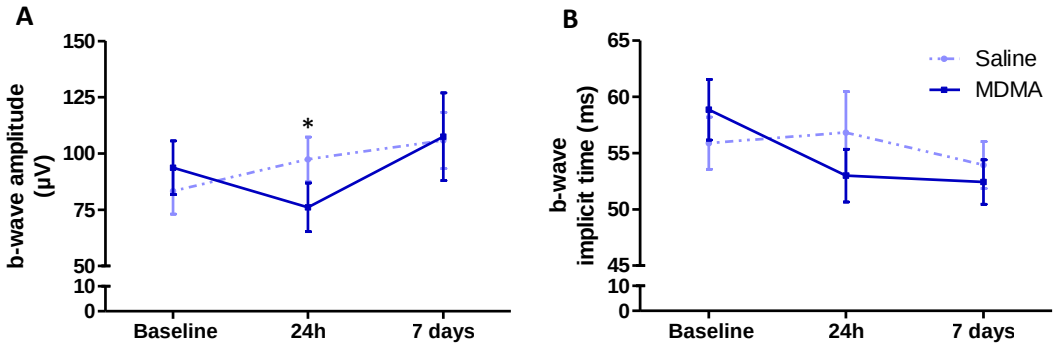


**Figure 45** – Effect of sporadic MDMA administration on photopic b-wave amplitude **(A)** and implicit time **(B)**. ERGs were recorded 7 days before (baseline recording), and 24 h and 7 days after the last MDMA or Saline intraperitoneal injection, and were elicited by different light intensities ranging from 0.0095 to 9.49 cd-s/$m^2$ with a white background. Data were analyzed using *Friedman test* followed by *Wilcoxon test*. Data is presented as mean±SEM (n = 4 in each group). * $\rho<0.05$ – Comparing with baseline for MDMA group.

### *3.3.3. Effect of sporadic MDMA administration on rat photopic flicker ERG*

Pure cone response was obtained with photopic flicker ERG, which was elicited by two different light intensities (3.00 and 9.49 cd-s/m$^2$) with a white background (Figure 46).

From the waveforms, FFT first harmonic and second harmonic amplitude and implicit time values were obtained. For first harmonic amplitude no significant differences were observed between the three time points. However, in MDMA group, the amplitude at 7 days time point was significantly increased when compared to baseline and 24 h time point values ($p < 0.05$ for both time points) (Figure 47A). First harmonic implicit time did not show significant differences for both groups (Figure 47B). Regarding the second harmonic amplitude, significant differences were found in MDMA group. At 7 days time point the amplitude was higher than in baseline ($p < 0.05$) and 24 h time point ($p < 0.01$) (Figure 47C). For second harmonic implicit time no significant changes were observed in both groups. However, analyzing the time points in pairs of two, baseline values were significantly higher comparing to 24 h ($p < 0.05$) and 7 days time point ($p < 0.05$) values (Figure 47D).

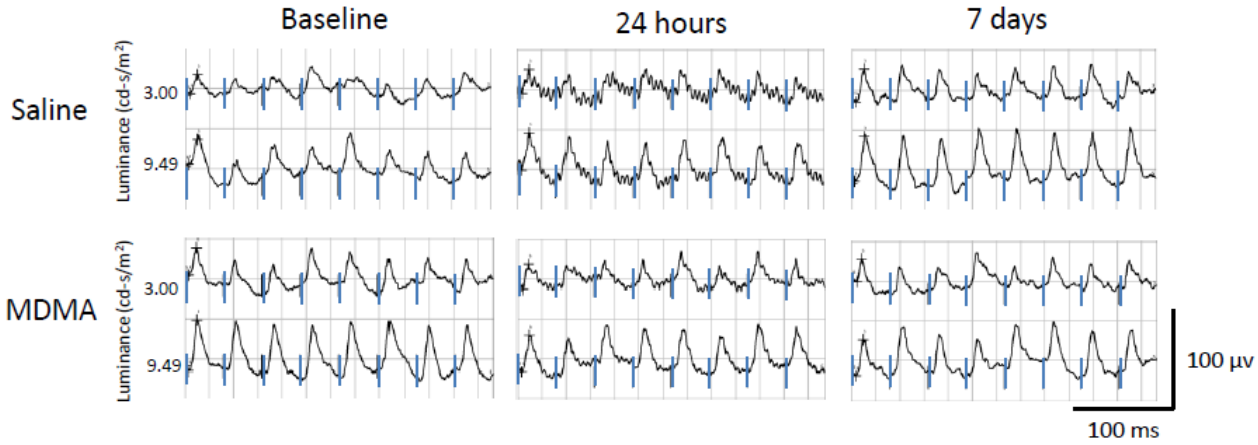


**Figure 46** – Representative recordings of rat photopic flicker ERGs. ERGs were elicited by two different light intensities (3.00 and 9.49 cd-s/m$^2$) with a white background and were performed 7 days before treatment (baseline), and 24 h and 7 days after the last Saline or MDMA administration. An average of ten responses to light stimulus with the same intensity is represented in each trace. Small solid blue vertical lines indicate the onset of light stimulus.

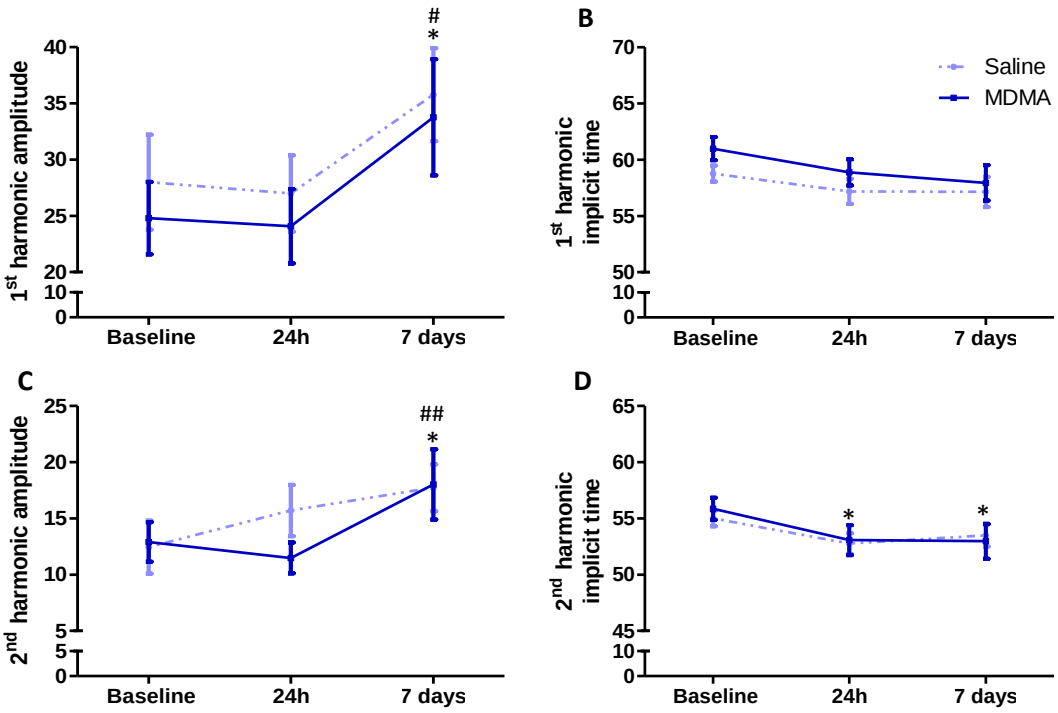


**Figure 47** – Effect of MDMA administration on rat photopic flicker ERG. ERGs were performed 7 days before (baseline recording), and 24 h and 7 days after the last Saline or MDMA intraperitoneal injection. Animals were exposed to two different light intensities, 3.00 and 9.49 cd-s/$m^2$, with a white background. Data was analyzed using *Friedman test* followed by *Wilcoxon test*. **(A, C)** – First harmonic amplitude and implicit time, respectively. **(B, D)** – Second harmonic amplitude and implicit time, respectively. Data is presented as mean±SEM. Four animals were tested for each group. * $\rho<0.05$ – Comparing with baseline for MDMA group; # $\rho<0.05$, ## $\rho<0.01$ – Comparing with 24 h time point for MDMA group.

### *3.3.4. Effect of sporadic MDMA administration on glial reactivity*

The immunoreactivity of GFAP and Vimentin was analyzed by Western blot in total retinal extracts to evaluate the effect of MDMA administration in retinal glial cells, 7 days after the last MDMA or Saline administration. No significant differences were observed between Saline- and MDMA-injected animals (Figures 48A and 48B).

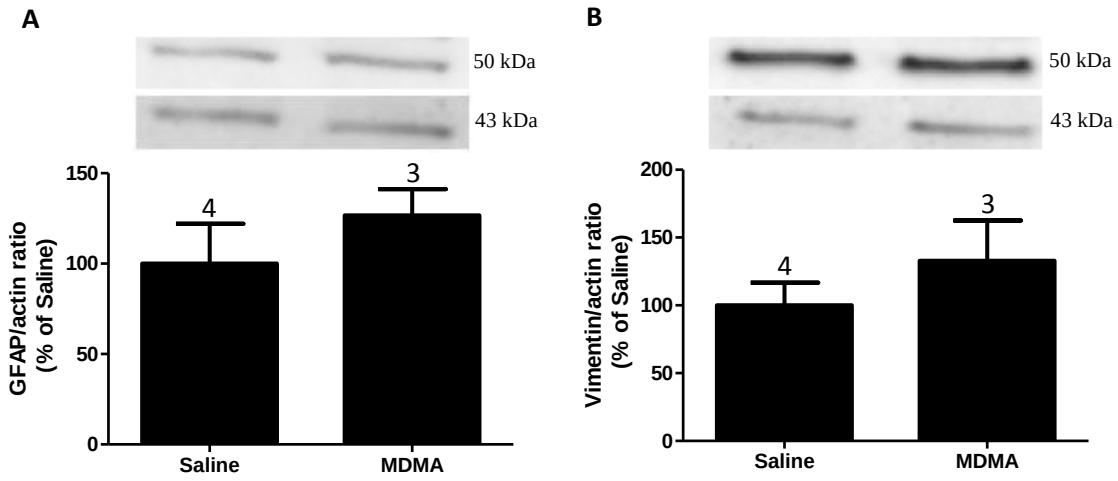


**Figure 48** – Effect of MDMA on the immunoreactivity of GFAP **(A)** and vimentin **(B),** as assessed by Western blotting. The total number of Saline- and MDMA-injected animals used to prepare retinal extracts is indicated above each graphic bar. The densitometric measurements were performed and the ratio between GFAP or vimentin and β-actin immunoreactivities was analyzed. Statistical analysis was performed using *Mann Whitney test*. Data is presented as mean±SEM.

## *4. Discussion*

MDMA is a ring substituted amphetamine derivative (Kay *et al*, 2010) that exhibits stimulant and hallucinogenic properties (Green *et al*, 2003; Kay *et al*, 2010). This drug is known to cause feelings of relaxation and tranquility (Green *et al*, 2003, Valentine, 2002), but it is also known to induce hyperthermia, hyponatremia, multiorganic failure, rabdomiolisis, disseminated intravascular coagulation, and can ultimately lead to death (Farré *et al*, 2004). The effects of MDMA administration in several brain regions are well characterized. It increases the extracellular concentrations of monoamine neurotransmitters, such as 5-HT, DA and NE (Bogena *et al*, 2003; Green *et al*, 2003; Gudelsky *et al*, 2008; Xavier *et al*, 2008). In rats, as in humans, the long-term effect of this drug is mainly the depletion of 5-HT from nerve endings (Colado *et al*, 1997; Green *et al*, 2003; O'Shea *et al*, 2006; Gudelsky *et al*, 2008). Although a few evidences indicate that MDMA can cause toxic damage in the retina, few were the attempts performed in order to assess its effects in this CNS structure. It was reported that repeated MDMA consumption can induce changes in light perception (Farré *et al*, 2004). The analysis of toxic reports after MDMA fatal overdose showed the presence of this drug, as well as of its metabolite MDA, in the humor vitreous (De Letter *et al*, 2002). MDMA was also demonstrated to decrease the cell viability in retinal cell cultures (Álvaro *et al*, 2008) and to induce retinal cell apoptosis, especially in GCL and INL (Miranda *et al*, 2007). Based on these evidences, recently a study was initiated by this group to analyze MDMA effects on retinal physiology using ERG recordings. A significant decrease in the implicit time of all parameters evaluated was observed 3 h after a single MDMA administration (15mg/kg) in both scotopic and photopic conditions. A significant increase in the amplitude of a-wave, photopic b-wave and photopic OP4 was also observed at this time point; however, 24 h after MDMA treatment, only a-wave amplitude was elevated.

The main aim of this study was to further evaluate whether MDMA affects retinal function. For that, three MDMA administration protocols were used. The first one allowed determining the long-term effects of a single MDMA (15 mg/kg) administration on retinal physiology. In the others, two routines of MDMA users consumption were mimicked to evaluate its acute (24 h after the last administration) and

long-term (7 days after the last administration) effects on retinal physiology, after repeated (Protocol 2) and sporadic (Protocol 3) administration.

To determine the MDMA effects on retinal physiology we used electroretinography, which is a non-invasive technique that has clinical value diagnosing and assessing visual diseases (Wali & Leguire, 1991; Rosolen *et al*, 2005). It is also commonly used to determine the toxicity of chemical agents to the retina (Rosolen *et al*, 2005). Unlike humans, rats need to be anesthetized during ERG record. Since anesthesia influence ERG signal (Rosolen *et al*, 2005), the same anesthetic was used during the entire study.

The effects of MDMA on glial reactivity was another issue that we tried to clarify in this study. Since glial reactivity is generally accepted as an indicator of neural damage (Green *et al*, 2003; Fantegrossi *et al*, 2008), we used this parameter as a way to indirectly detect neural damage induced to the retina by this drug. We assessed the expression of the three proteins expressed by glial cells in the retina: GFAP, the major protein of intermediate filaments in astrocytes, which can be used as a marker of astrocytes and Müller cells; vimentin, which is a marker of Müller cells; and Cd11-b that labels microglial cells.

The effects of a single MDMA intraperitoneal injection were analyzed 7 days after treatment. A-wave amplitude and both scotopic and photopic b-wave and OPs amplitudes did not present significant differences; however, significant differences were observed in scotopic OPs. Previously, our group showed that 3 h after MDMA administration there was an increase in the amplitude and a decrease in the implicit time of the majority of parameters evaluated, but 24 h after MDMA administration only a-wave amplitude was elevated. These results may explain the lack of effect observed in the majority of the parameters evaluated 7 days after MDMA administration and also indicate that the effects of a single MDMA administration in the retina are essentially acute effects. Regarding the significant differences observed in scotopic OPs, similar changes were observed in the Saline group, especially in implicit time values, suggesting that MDMA-induced changes cannot be considered so relevant. OPs are believed to reflect the inhibitory feedback circuits in the inner part of the retina initiated by amacrine cells (Wanger & Persson, 1984; Li *et al*, 1991; Creel, 2010). So, the decrease observed in OPs amplitude and the increase observed in their implicit time may be due to changes in the activity of amacrine cells.

In the second experimental protocol (Protocol 2), the effects of repeated MDMA administration on retinal physiology were analyzed. In this protocol, unexpected results were obtained. The majority of the parameters, in both scotopic and photopic conditions, showed a similar pattern in both MDMA and Saline group. For instance, both groups presented a significant decrease in both scotopic a-wave and b-wave amplitudes at 24 h time point ERG, followed by an increase at 7 days time point ERG. Some amplitudes of scotopic OPs were also decreased at 24 h time point for both groups. Taking into consideration the physiological meaning of a-wave amplitude, which is the reflex of the amount of photoreceptors activated by light, it would be expected that a reduction in the number of photoreceptors induced by MDMA injury could cause a decrease in the overall response. However, no evidences exist that under these conditions photoreceptors die, although their function might be compromised. In addition, in scotopic conditions, 7 days time point values were increased when compared to 24 h time point values; however, this increase was not enough to reach the baseline values, indicating that the effects of MDMA in the retina may last for long periods or even become permanent, but to clarify this issue more experiments should be carried out at longer periods after drug administration.

We hypothesized that the existence of similar results in Saline and MDMA groups might be due to stress. Repeated and regular (animals were injected always in the morning to avoid cycle circadian rhythm influences) injections is a source of stress. It is known that ERG responses can be influenced by several factors, as the intensity and duration of the stimulus, or by the wavelength and pattern of the stimulus (Forrester *et al*, 2002; Barraco *et al*, 2006). The anesthetic is another source of influence (Rosolen *et al*, 2005), and it has also been reported that physical effort can significantly change ERG responses in humans (Zwierko *et al*, 2010). However, no evidences exist that stress can significantly modify ERG responses. It has been reported that stress induced by escapable foot shock in rats influences neuronal cell death in the retina (O'Shea *et al*, 2006). So, assuming that regular IP injections can induce stress, modifications in ERG responses can be expected. Further studies will be necessary to confirm this hypothesis.

The consequences of sporadic MDMA administration in retinal physiology were assessed in Protocol 3. In this case, and unexpectedly, the majority of statistical differences were observed in Saline group; however, these experiments were performed in a small number of animals, and so we cannot draw any conclusion. As mentioned

before, four animals were used for each condition (Saline and MDMA-treated animals) resulting in a huge data variability which influenced the statistical analysis. For the same reason, it was not possible to analyze data of both scotopic and photopic oscillatory potentials amplitude and implicit time. The number of animals tested in this protocol must be increased in the future to ensure a correct analysis of the data.

Regarding the potential glial reactivity induced by MDMA, a slight increase in GFAP immunoreactivity was noticed in the MDMA group in the three experimental protocols, but no statistical significance was reached. These results are correlated with findings in brain after MDMA administration. In animals, the increase in GFAP expression after MDMA administration has been reported. For instance, an increase in GFAP immunoreactivity was observed in mouse (Thomas *et al*, 2004) and in rat (Baumann *et al*, 2006) after high and repeated MDMA administrations. Moreover, GFAP protein expression increments in the mice retina were observed after administration single and repeated doses of methamphetamine (Meth), which is another amphetamine derivative known to induce an acute release of monoamine neurotransmitters.

In Protocol 1, immunohistochemistry analysis showed a significant increase in vimentin expression for MDMA group. This increase indicates an increase in Müller cells reactivity, which can be considered as an indicator of toxic damage induced by MDMA; however, this result was not confirmed by Western blot analysis, where no significant differences were observed. After multiple MDMA intraperitoneal injections (Protocol 2 and 3) no significant differences were observed between MDMA and Saline group in vimentin expression.

Cd11-b protein expression was assessed for protocols 1 and 2 by immunohistochemistry in whole-mounted retinas. A qualitative analysis was performed and no evident differences were detected between the two groups in both protocols. Microglial cells were reported as sensible to toxic effects induced by MDMA in retinal cell cultures, even with low doses (Álvaro *et al*, 2008). Studies conducted in mice also showed microglial activation after MDMA administration; however the dose was higher (20 mg/kg) as well as the periodicity (4 injections, 2 h apart from each other) than the ones used in Protocols 1 and 2 (Thomas *et al*, 2004). Although some evidences suggest that MDMA induce an activation of microglia, opposite results have also been demonstrated. Fantegrossi and collegues demonstrated that administration of repeated

high doses of MDMA in mice was not consistently accompanied by an activation of microglia (Fantegrossi *et al*, 2008).

Taking into account all results obtained on glial cell reactivity, it seems that, at least for the protocols used in this study, no significant glial reactivity occurs in the retina. It is likely that with high doses of MDMA and more repeated administrations, glial reactivity could become more evident.

In conclusion, the potential harmful effects of MDMA in the retina is an important issue, and studies regarding this topic must be continued to clarify the actions of MDMA, as well as other related drugs.

# *5. Conclusions and Future Directions*

With this work, we demonstrated that a single MDMA administration (15 mg/kg; Protocol 1) did not cause significant long-term effects in retinal physiology, since most of the ERG parameters were not altered.

Regarding the effects of repeated MDMA administration (Protocol 2) on ERG recordings, in scotopic conditions several parameters (a-wave, b-wave, OP2, OP3 and OP4 amplitudes) showed a significant decrease between baseline and 24 h time point and an increase between 24 h time point and 7 days time point. These differences were also observed for Saline group, suggesting that another factor, for example stress, due to regular and repeated injections, may be contributing to ERG response modifications, disguising MDMA effects. Further tests will be necessary to confirm this hypothesis.

The number of animals tested for Protocol 3 was small, which did not allow conclusive findings. Most of the ERG parameters showed significant differences for Saline group, and almost no significant changes were observed for MDMA group. Further studies will be necessary to determine the precise acute and long-term effects of sporadic MDMA administration in retinal physiology.

The glial reactivity was assessed after single and multiple MDMA administrations and an increase in GFAP expression was reported for all three Protocols, but no significant differences were reached. Regarding vimentin immunoreactivity, immunohistochemistry analysis showed an increase in vimentin expression after a single MDMA; however this result was not confirmed by Western blotting analysis.

Taking into account the results obtained, it is clear that more studies must be performed to a better understanding of MDMA effects on the retinal physiology. In particular, protocol 3 must be repeated to determine the correct effects of sporadic MDMA administration in the retina. Moreover, the reason why saline administration by intraperitoneal injection equally affects scotopic and photopic ERG parameters should be also clarified.

## 6. References


| *Reference* | *Publication* |
|---|---|
| Alexander *et al*, 2006 | Alexander, K.R., Raghuram, A., Rajagopalan, A.S. (2006). Cone phototransduction and growth of the ERG b-wave during light adaptation. Vision Research. 46: 3941–3948 |
| Álvaro *et al*, 2008 | Álvaro, A.R., Martins, J., Costa, A.C., Fernandes, E., Carvalho, F., Ambrósio A.F., Cavadas C. (2008). Neuropeptide Y protects retinal neural cells against cell death induced by ecstasy. Neuroscience. 152: 97–105 |
| Barraco *et al*, 2006 | Barraco, R., Bellomonte, L., Brai, M., Anastasi, M. (2006). Analysis of the human a-wave ERG component. Physiol. Meas. 27: 881–899 |
| Barthel & Raymond, 1990 | Barthel, L.K., Raymond, P.A. (1990). Improved Method for Obtaining 3-µm Cryosections for Immunocytochemistry. The Journal of Histochemistry and Cytochemistry. 58(9): 1383-1388 |
| Baumann *et al*, 2006 | Baumann, M.H., Wang, X., Rothman, R.B. (2006). 3,4-Methylenedioxymethamphetamine (MDMA) neurotoxicity in rats: a reappraisal of past and present findings. Psychopharmacology. 189: 407–424 |
| Bogena *et al*, 2003 | Bogena, I.L., Huse Hauga, K., Myhrea, O., Fonnuma, F. (2003). Short- and long-term effects of MDMA ("ecstasy") on synaptosomal and vesicular uptake of neurotransmitters in vitro and ex vivo. Neurochemistry International. 43: 393–400 |
| Bringman *et al*, 2006 | Bringmann, A., Pannicke, T., Grosche, J., Francke, M., Wiedemann, P., Skatchkovc, S.N., Osborne, N.N., Reichenbach, A. (2006). Progress in Retinal and Eye Research. 25: 397–424 |
| Che *et al*, 1995 | Che, S., Johnson, M., Hanson, G.R., Gibb, J.W. (1995). Body temperature effect on methylenedioxymethamphetamine-induced acute decrease in tryptophan hydroxylase activity. Environmental Toxicology and Pharmacology Section. 293: 447-453 |
| Colado & Green, 1995 | Colado, M.I., Green, A.R. (1995). The spin trap reagent alpha-phenyl-N-tert-butyl nitrone prevents 'ecstasy'-induced neurodegeneration of 5-hydroxytryptamine neurones. Eur J Pharmacol. 280(3): 343-346 |
| Colado *et al*, 1997 | Colado, M.I., O'Shea, E., Granados, R., Murray, T.K., Green A.R. In vivo evidence for free radical involvement in the degeneration of rat brain 5-HT following administration of MDMA ('ecstasy') and *p*-chloroamphetamine but not the degeneration following fenfluramine. (1997). British Journal of Pharmacology. 121: 889–900 |
| Colado *et al*, 1999 | Colado, M.I., O'Shea, E., Esteban, B., Granados, R., Green, A.R. (1999). In vivo evidence against clomethiazole being neuroprotective against MDMA ('ecstasy')-induced degeneration of rat brain 5-HT nerve terminals by a free radical scavenging mechanism. Neuropharmacology. 38: 307–314 |

| | |
|---|---|
| Colado *et al, 2001* | Colado, M.I., Camarero, J., Mechan, A.O., Sanchez, V., Esteban, B., Elliott, J.M., Green, A.R. (2001). A study of the mechanisms involved in the neurotoxic action of 3,4-methylenedioxymethamphetamine (MDMA, 'ecstasy') on dopamine neurones in mouse brain. British Journal of Pharmacology. 134: 1711–1723 |
| Colado *et al*, 2004 | Colado, M.I., O'Shea, E., Green, A.R. (2004). Acute and long-term effects of MDMA on cerebral dopamine biochemistry and function. Psychopharmacology. 173: 49–263 |
| Cole & Sumnall, 2003 | Cole, J.C., Sumnall, H.R. (2003). Altered states: the clinical effects of Ecstasy. Pharmacology & Therapeutics. 98: 35– 58 |
| Creel, 2010 | Creel, D. The Electroretinogram: Clinical Applications. Retrieved July 17, 2010 from http://webvision.med.uthad.edu/ClinicalERG.html |
| De Letter *et al*, 2002 | De Letter, E.A., Clauwaert, K.M., Lambert, W.E., Van Bocxlaer, J.F., De Leenheer, A.P., Piette M.H.A. (2002). Distribution Study of 3,4-Methylenedioxymethamphetamine and 3,4-Methylenedioxyamphetamine in a Fatal Overdose. Journal of Analytical Toxicology. 26: 114-118 |
| Diller *et al*, 2007 | Diller, A.J., Rocha A., Cardon, A.L., Valles, R., Wellman, P.J., Nation J.R. (2007). The effects of concurrent administration of (±)3,4-Methylenedioxymethamphetamine and cocaine on conditioned place preference in the adult male rat. Pharmacology, Biochemistry and Behavior. 88: 165–170 |
| Fantegrossi *et al*, 2008 | Fantegrossi, W E., Ciullo, J.R., Wakabayashi, K.T., Garza, R., Traynor, J.R., Woods, J.H. (2008). A Comparison of the Physiological, Behavioral, Neurochemical and Microglial Effects of Methanphetamine and 3,4-Methylenedioxymethamphetamine in the Mouse. Neuroscience. 151: 533–543 |
| Farré *et al*, 2004 | Farré, M., Torre, R., Ó Mathúna, B., Roset, P.N., Peiró, A.M., Torrens, M., Ortuño, J., Pujadas, M., Camí, J. (2004). Repeated doses administration of MDMA in humans: pharmacological effects and pharmacokinetics. Psychopharmacology. 173: 364–375 |
| Forrester *et al*, 2002 | Forrester, J.V., Dick, A.D., McMenamin, P.G., Lee, W.R. (2002). The Eye: Basic Sciences Practice. 2nd edition, Elsevier. |
| Franze *et al*, 2007 | Franze, K., Grosche, J., Skatchkov, S.N., Schinkinger, S., Foja, C., Schild, D., Uckermann, O., Travis, K., Reichenbach, A., Guck, J. (2007). Müller cells are living optical fibers in the vertebrate retina. PNAS. 104(20): 8287-8292 |
| Freudenmann *et al*, 2006 | Freudenmann, R.W., Öxler F., Bernschneider-Reif S. (2006). The origin of MDMA (ecstasy) revisited: the true story reconstructed from the original documents. Addiction. 101(9):1241-1245. |
| Green *et al*, 2003 | Green, A.R, Mechan A.O., Elliott J.M., O'Shea E., Colado M.I. (2003). The Pharmacology and Clinical Pharmacology of 3,4-Methylenedioxymethamphetamine (MDMA, "Ecstasy"). Pharmacol Rev. 55: 463–508 |

| | |
|---|---|
| Gudelsky *et al*, 2008 | Gudelsky, G.A., Yamamoto, B.K. (2008). Actions of 3,4-Methylenedioxymethamphetamine (MDMA) on cerebral dopamineric, seroroneric and cholinergic neurons. Pharmacol Biochem Behav. 90(2): 198–207 |
| Gyongyosi *et al*, 2010 | Gyongyosi, N., Balogh, B., Katai, Z., Molnar E., Laufer, R., Tekes, K., Bagdy, G. (2010). Activation of 5-HT3 receptors leads to altered responses 6 months after MDMA treatment. J Neural Transm. 117: 285–292 |
| Johnson *et al*, 1992 | Johnson, M., Mitros, K., Stone, D.M., Zobrist, R., Hanson, G.R., Gibb, J.W. (1992). Effect of flunarizine and nimodipine on the decrease in tryptophan hydroxylase activity induced by methamphetamine and 3,4-methylenedioxymethamphetamine. J Pharmacol Exp Ther. 261(2):586-591. |
| Kay *et al*, 2010 | Kay, C., Harper, D.N., Hunt, M. (2010). Differential effects of MDMA and scopolamine on working versus reference memory in the radial arm maze task. Neurobiology of Learning and Memory. 93: 151–156 |
| Koch *et al*, 1997 | Koch, S., Galloway, M.P. (1997). MDMA induced dopamine release in vivo: role of endogenous serotonin. J Neural Transm. 104: 135-146 |
| Kolb *et al*, 1994 | Kolb, H., Fernandez, E., Schouten, J., Ahnelt, P., Linberg, K.A., Fisher, S.K. (1994). Are there three types of horizontal cell in the human retina? J Comp Neurol. 343(3): 370-386 |
| Kolb, 2003 | Kolb, H. (2003). How the retina works. Am Scientist. 91: 28-35 |
| Lai *et al*, 2009 | Lai, H., Zeng, H., Zhang, C., Wang, L., Tso, M.O.M., Lai, S. (2009). Toxic Effect of Methamphetamine on the Retina of CD1 Mice. Curr Eye Res. 34(9): 785–790 |
| Langmann, 2007 | Langmann, T. (2007). Microglia activation in retinal degeneration. Journal of Leukocyte Biology. 81: 1345-1351 |
| Leonardi *et al*, 1994 | Leonardi, E.T.K., Azrnitia, E.C. (1994). MDMA (Ecstasy) Inhibition of MAO Type Aand Type B: Comparisons with Fenfluramine and Fluoxetine(prozac). Neuropsychopharmacology. 10(4): 231-238 |
| Li *et al*, 1991 | Li, X.X., Yaun, N., Hong, J., Song, P. (1991). The influence of adaptation on the oscillatory potentials of human electroretinogram. Documenta Ophthalmologica. 76: 389-394 |
| Liechti *et al*, 2000 | Liechti, M.E., Baumann, C., Gamma, A., Vollenweider, F.X. (2000). Acute Psychological Effects of 3,4-Methylenedioxymethamphetamine (MDMA, "Ecstasy") are Attenuated by the Serotonin Uptake Inhibitor Citalopram. Neuropsychopharmacology. 22(5): 513-521 |
| Manookin *et al*, 2010 | Manookin, M.B., Weick, M., Stafford, B.K., Demb, J.B. (2010). NMDA Receptor Contributions to Visual Contrast Coding. Neuron. 67: 280-293 |
| Marmor *et al*, 2004 | Marmor, M.F., Holder, G.E., Seeliger, M.W., Yamamoto, S. (2004). Standard for clinical electroretinography (2004 update). Documenta Ophthalmologica. 108: 107–114 |

| | |
|---|---|
| Michael *et al*, 2003 | Michael, J.C., Pak, J., Pulido, J., Venecia, G. (2003). Central Serous Chorioretinopathy Associated With Administration of Sympathomimetic Agents. Am J Ophthalmol. 135: 170-180 |
| Miranda *et al*, 2007 | Miranda, M., Bosch-Morell, F., Johnsen-Soriano, S., Barcia, J., Almansa, I., Asensio, S., Araiz, J., Messeguer, A., Romero, F.J. (2007). Oxidative Stress in Rat Retina and Hippocampus after Chronic MDMA ('ecstasy') Administration. Neurochem Res. 32: 1156–1162 |
| Nair *et al*, 2004 | Nair, S.G., Gudelsky, G.A. (2004). Protein kinase C inhibition differentially affects 3,4-methylenedioxymethamphetamine-induced dopamine release in the striatum and prefrontal cortex of the rat. Brain Research. 1013: 168–173 |
| Newman & Reichenbach, 1996 | Newman, E., Reichenbach, A. (1996). The Müller cell: a functional element of the retina. TrendsNeurosci. 19: 307-312 |
| Nixon *et al*, 2001 | Nixon, P.J., Bui, B.V., Armitage, J.A., Vingrys A.J. (2001). The contribution of cone responses to rat electroretinograms. Clinical and Experimental Ophthalmology. 29: 193-196 |
| O'Shea *et al*, 2006 | O'Shea, E., Orio, L., Escobedo, I., Sanchez, V., Camarero, J., Green, A.R., Colado, M.I. (2006). MDMA-induced neurotoxicity: long-term effects on 5-HT biosynthesis and the influence of ambient temperature. British Journal of Pharmacology. 148: 778–785 |
| Perlman, 2010 | Perlman, I. The Electroretinogram: ERG. Retrieved July 18, 2010 from http://webvision.med.uthad.edu/ERG.html |
| Pootanakit & Brunken, 2000 | Pootanakit, K., Brunken, W.J. (2000). 5-HT1A and 5-HT7 receptor expression in the mammalian retina. Brain Research. 875: 152–156 |
| Purves *et al*, 2004 | Purves, D., Augustine, G.J., Fitzpatrick, D., Hall, W.C., LaMantia, A.S., McNamara, J., Williams, S.M. (2004). Neuroscience. 3rd edition, Sunderland, Massachusetts U.S.A |
| Rosolen *et al*, 2005 | Rosolen, S.G., Rigaudière, F., Gargasson, J.F., Brigell, M.G. (2005). Recommendations for a toxicological screening ERG procedure in laboratory animals. Documenta Ophthalmologica. 110: 57-66 |
| Schwartz *et al*, 1997 | Schwartz, R.H., Miller, N.S. (1997). MDMA (ecstasy) and the rave: A review. Pediatrics. 100 (4): 705-708 |
| Shankaran *et al*, 1998 | Shankaran, M., Gudelsky, G.A. (1998). Effect of 3,4-Methylenedioxymethamphetamine (MDMA) on Hippocampal Dopamine and Serotonin. Pharmacology Biochemistry and Behavior. 61: 361–366 |
| Shankaran et al, 1999 | Shankaran, M., Yamamoto, B.K., Gudelsky, G.A. (1999). Mazindol Attenuates the 3,4-Methylenedioxymethamphetamine-Induced Formation of Hydroxyl Radicals and Long-Term Depletion of Serotonin in the Striatum. Journal of Neurochemistry. 72(6): 2516-2522 |
| Siegel *et al*, 2006 | Siegel, G., Albers, R.W., Brady, S., Price, D. Basic Neurochemistry: Molecular, Cellular, and Medical Aspects. (2006). 7th edition, Elsevier. |

| | |
|---|---|
| Sprague & Nichols, 1995 | Sprague, J.E., Nichols, D.E. (1995). The monoamine oxidase-B inhibitor L-deprenyl protects against 3,4-methylenedioxymethamphetamine-induced lipid peroxidation and long-term serotonergic deficits. J Pharmacol Exp Ther. 273(2): 667-673 |
| Stockton & Slaughter, 1989 | Stockton, R.A., Slaughter, M.M. (1989). B-Wave of the Electroretinogram: A Reflection of ON Bipolar Cell Activity. J. Gen. Physiol. 93: 101-122 |
| Thomas *et al*, 2004 | Thomas, D.M., Dowgiert, J., Geddes, T.J., Francescutti-Verbeem, D., Liu, X., Kuhn, D.M. (2004). Microglial activation is a pharmacologically specific marker for the neurotoxic amphetamines. Neuroscience Letters. 367: 349–354 |
| Valentine, 2002 | Valentine, G. (2002). MDMA and Ecstasy. Phychiatric Times. XIX(2). |
| Wali & Leguire, 1991 | Wali, N., Leguire, L.E. (1991). Dark-adapted luminance-response functions with skin and corneal electrodes. Documenta Ophthalmologica. 76: 367-375 |
| Wanger & Persson, 1984 | Wanger, P., Persson, H.E. (1984). Oscillatory Potentials, Flash and Pattern-Revesal Electroretinograms in Amblyopia. Acta Ophthalmologica. 62: 643-650 |
| Wen & Oakley, 1990 | Wen, R., Oakley, B. (1990). K+-evoked Muller cell depolarization generates b-wave of electroretinogram in toad retina. Proc. Natl. Acad. Sci. USA. 87: 2117-2121 |
| Xavier *et al*, 2008 | Xavier, C.A.C., Lobo, P.L.D., Fonteles, M.M.F., Vasconcelos, S.M.M., Viana G.S.B., Sousa F.C.F. (2008). Ecstasy (MDMA): pharmacological and toxic effects, mechanism of action and clinical management. Rev. Psiq. Clín. 35(3): 96-103 |
| Zhang & Stone, 1997 | Zhang, Y., Stone, J. (1997). Role of Astrocytes in the Control of Developing Retinal Vessels. Investigative Ophthalmology & Visual Science. 38(9): 1653-1666 |
| Zwierko *et al*, 2010 | Zwierko, T., Czepita, D., Lubinski, W. (2010). The effect of physical effort on retinal activity in the human eye: rod and cone flicker electroretinogram studies. Graefes Arch. Clin. Exp. Ophthalmol. 248: 659-666 |